

Lecture 5

GNSS Measurements and Data Pre-processing



Professors: Dr. J. Sanz Subirana, Dr. J.M. Juan Zornoza
and Dr. Adrià Rovira García

Contents

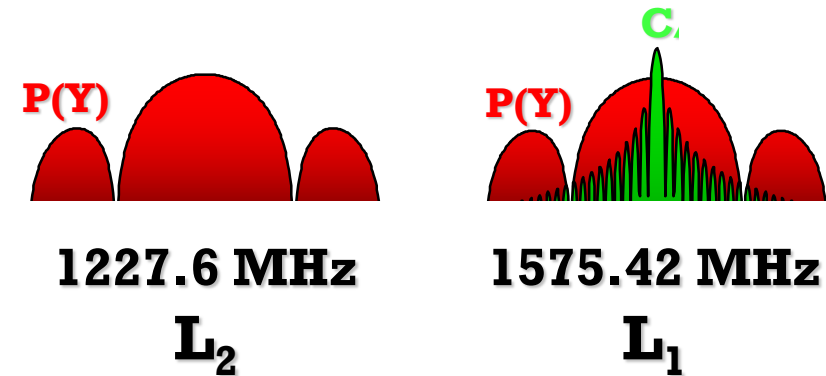
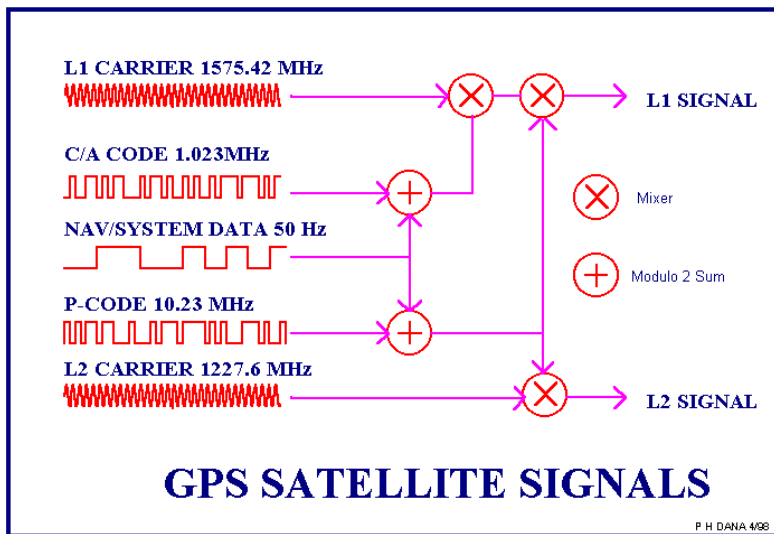
1. Review of GNSS measurements.
2. Linear combinations of measurements.
3. Carrier cycle-slips detection.
4. Carrier smoothing of code pseudorange.
5. Code Multipath.

GPS SIGNAL STRUCTURE

Two carriers in L-band:

- $L_1 = 154 \cdot f_0 = 1575.42 \text{ MHz}$
- $L_2 = 120 \cdot f_0 = 1227.60 \text{ MHz}$
where $f_0 = 10.23 \text{ MHz}$

- C/A-code for civilian users $[X_C(t)]$
- P-code only for military and authorized users $[X_P(t)]$
- Navigation message with satellite ephemeris and clock corrections $[D(t)]$



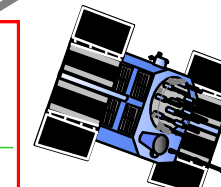
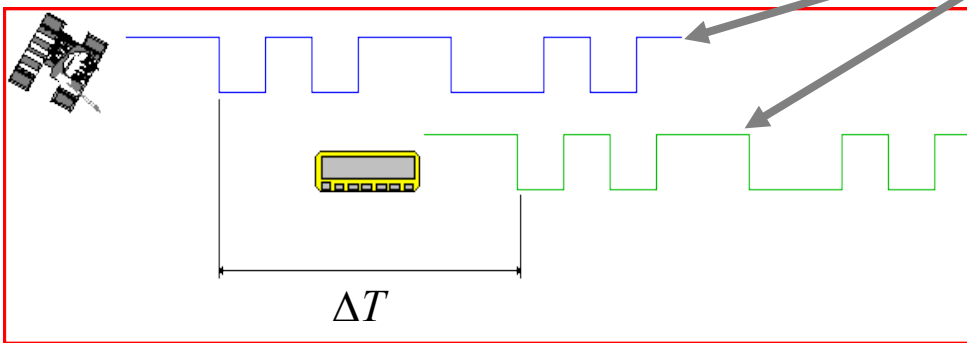
$$\begin{aligned} S_{L_1}^{(k)}(t) &= a_P X_P^{(k)}(t) D^{(k)}(t) \sin(\omega_1 t + \phi_{L_1}) + a_C X_C^{(k)}(t) D^{(k)}(t) \cos(\omega_1 t + \phi_{L_1}) \\ S_{L_2}^{(k)}(t) &= b_P X_P^{(k)}(t) D^{(k)}(t) \sin(\omega_2 t + \phi_{L_2}) \end{aligned}$$

GPS Code Pseudorange Measurements

$$S_{L_1}^{(k)}(t) = a_P X_P^{(k)}(t) D^{(k)}(t) \sin(\omega_l t + \varphi_{L_1}) + a_C X_C^{(k)}(t) D^{(k)}(t) \cos(\omega_l t + \varphi_{L_1})$$

$$S_{L_2}^{(k)}(t) = b_P X_P^{(k)}(t) D^{(k)}(t) \sin(\omega_2 t + \varphi_{L_2})$$

binary code $X_P(t)$



C_1, P_1, P_2



$$P(T) = c \Delta T = c [t_{rec}(T) - t^{sat}(T - \Delta T)]$$

From hereafter we will call:

- C_1 pseudorange computed from $X_C(t)$ binary code (on frequency 1)
- P_1 pseudorange computed from $X_P(t)$ binary code (on frequency 1)
- P_2 pseudorange computed from $X_P(t)$ binary code (on frequency 2)

GPS Carrier Phase Measurements

$$S_{L_1}^{(k)}(t) = a_P X_P^{(k)}(t) D^{(k)}(t) \sin(\omega_1 t + \varphi_{L_1}) + a_C X_C^{(k)}(t) D^{(k)}(t) \cos(\omega_1 t + \varphi_{L_1})$$

$$S_{L_2}^{(k)}(t) = b_P X_P^{(k)}(t) D^{(k)}(t) \sin(\omega_2 t + \varphi_{L_2})$$

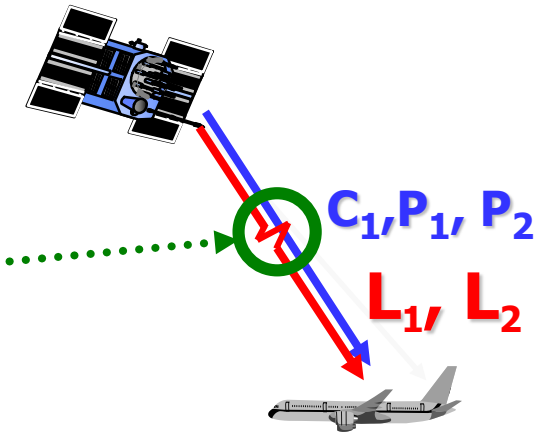
Carrier phase

Carrier beat phase:

$$\phi_L(T) = \phi_{L\text{ rec}}(T) - \phi_{L\text{ sat}}^{sat}(T - \Delta\bar{T})$$

$$= \frac{c}{\lambda} \Delta\bar{T} + N$$

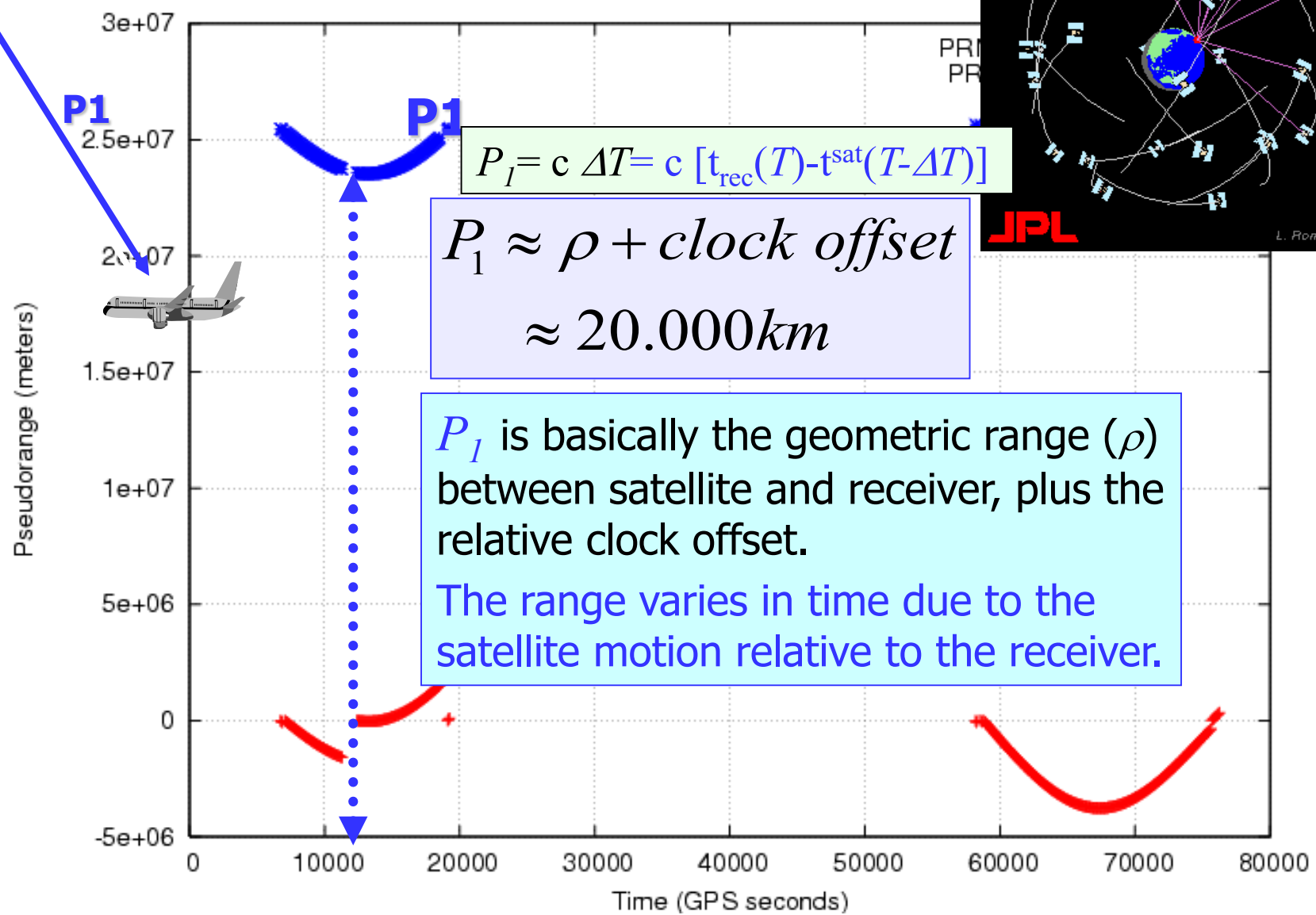
Unknown ambiguity



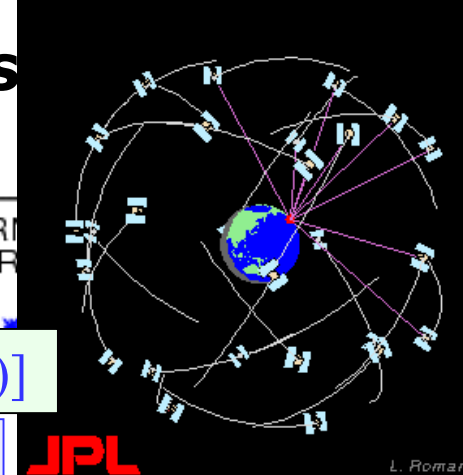
From hereafter we will call:

- $L_1 = \lambda_1 \phi_{L1}$ measur. computed from the carrier phase on frequency 1
- $L_2 = \lambda_2 \phi_{L2}$ measur. computed from the carrier phase on frequency 2
- C_1 pseudorange computed from $X_C(t)$ binary code (on frequency 1)
- P_1 pseudorange computed from $X_P(t)$ binary code (on frequency 1)
- P_2 pseudorange computed from $X_P(t)$ binary code (on frequency 2)

Carrier and Code pseudorange meas

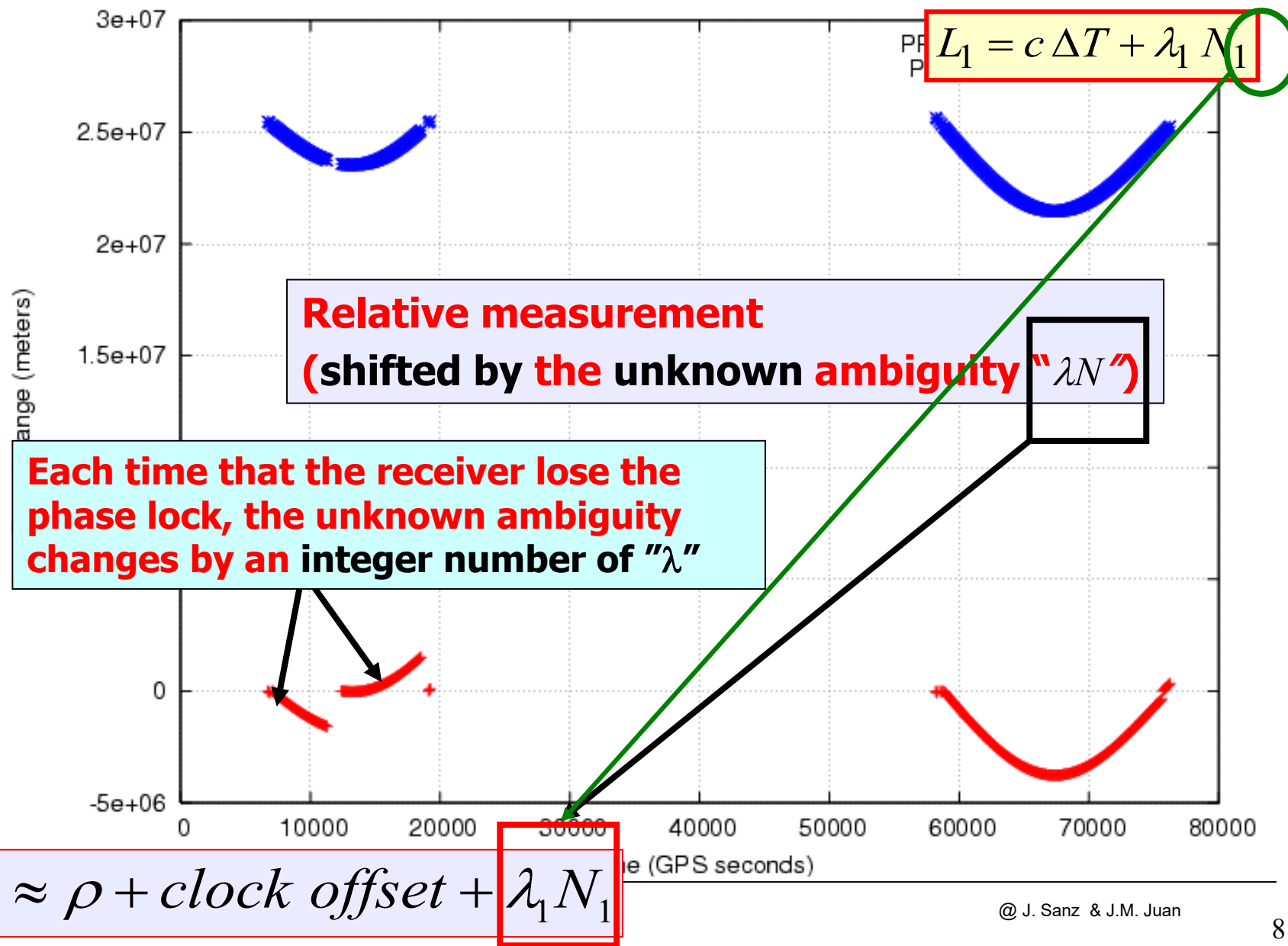


P_I is an **absolute** measurement (**unambiguous**)

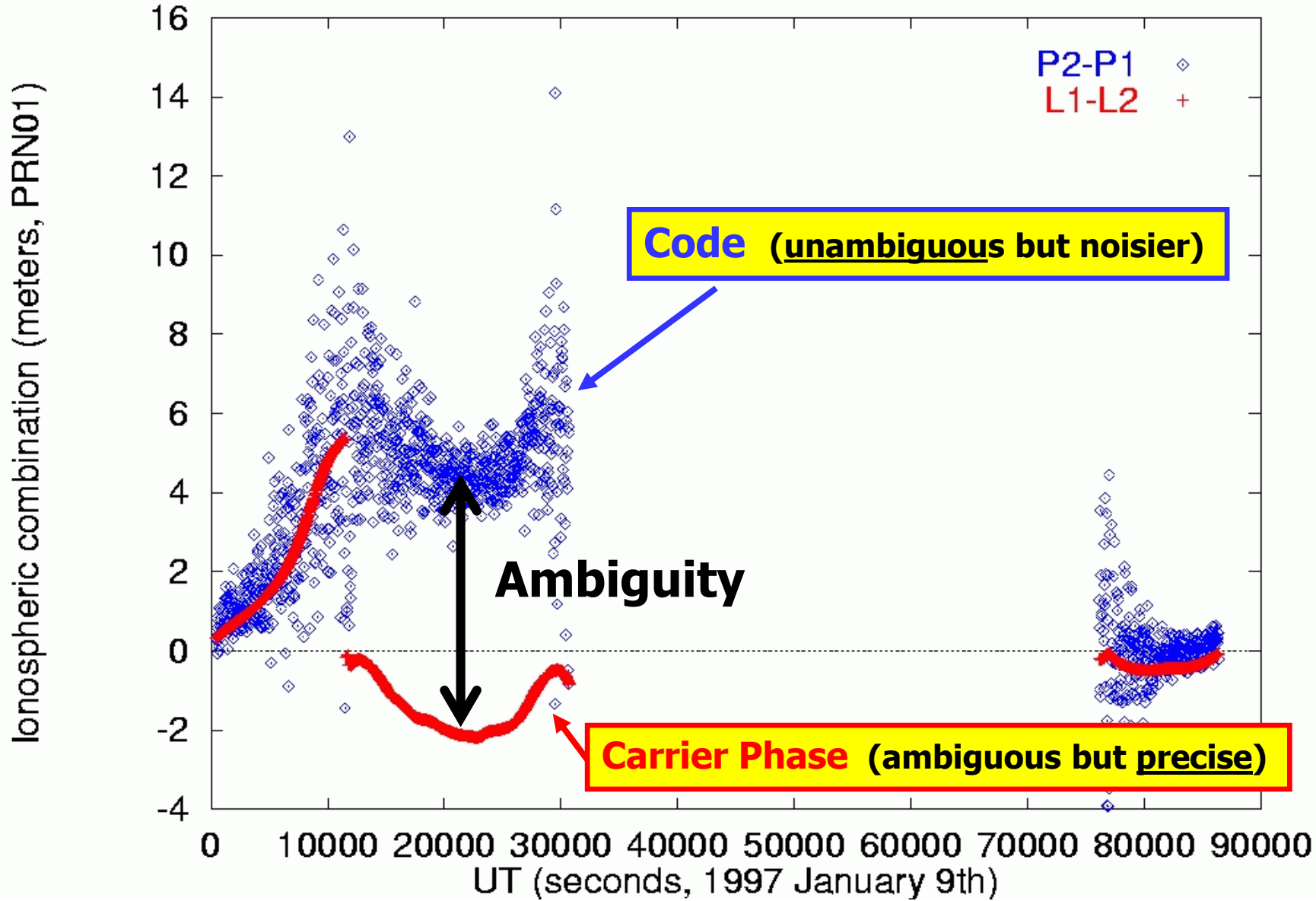


L. Romans

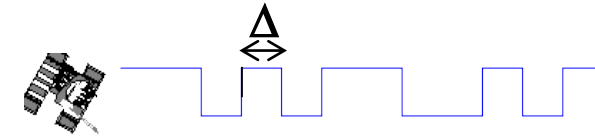
Phase and Code pseudorange measurements



Code and Carrier Phase measurements



GPS measurements: Code and Carrier Phase



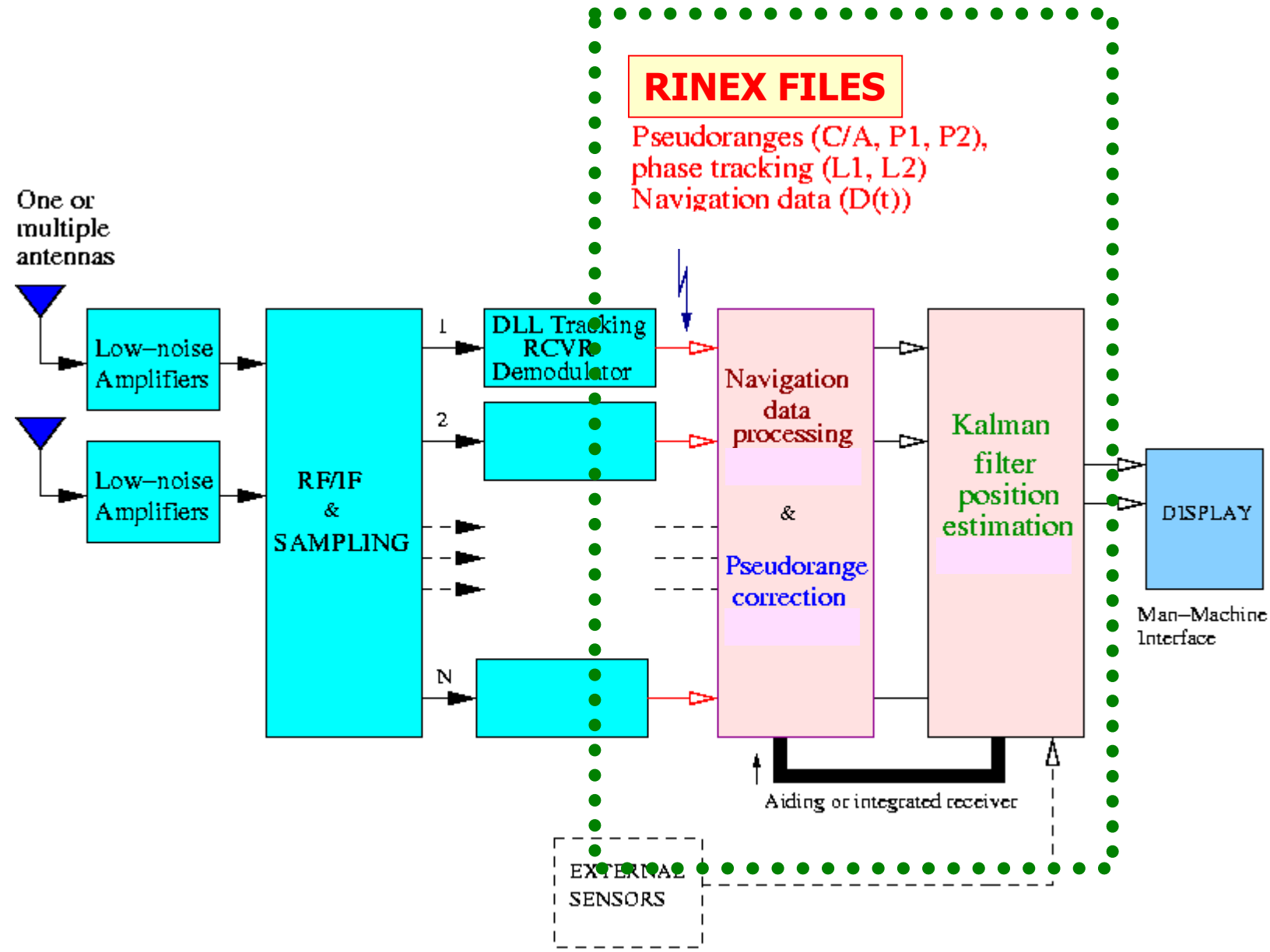
Antispoofing (A/S):

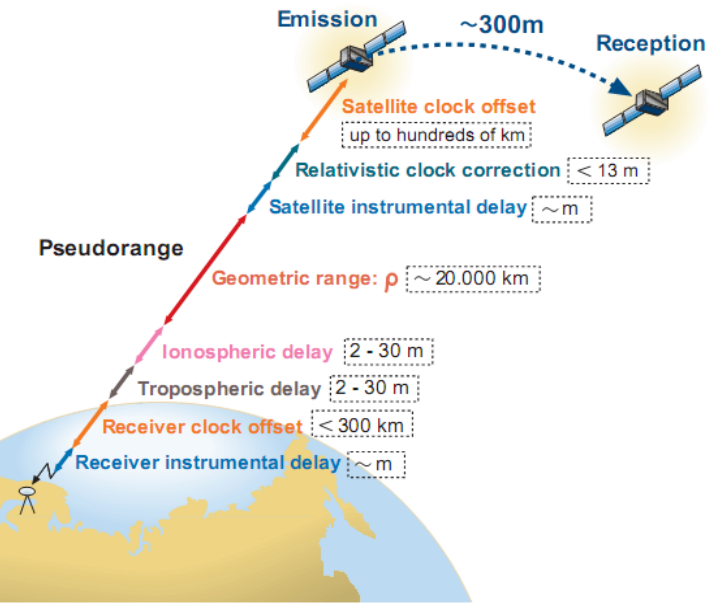
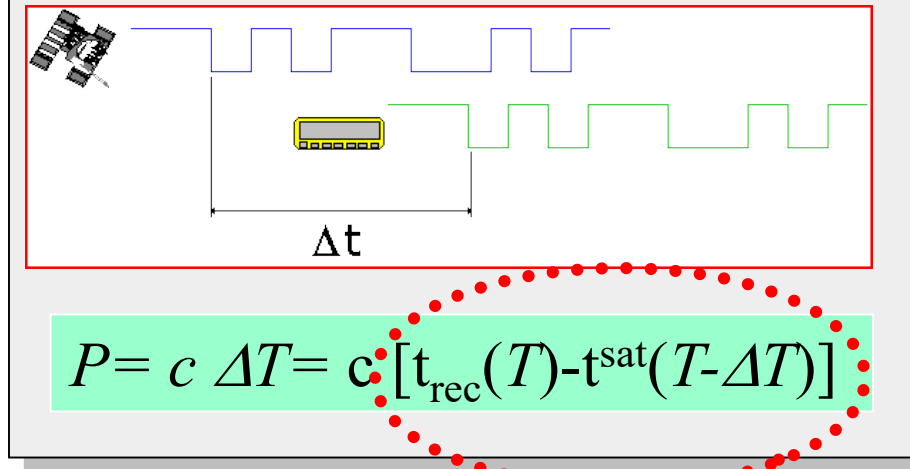
The code P is encrypted to Y.

→ Only the code C at frequency L1 is available.

	Wavelength (chip-length)	σ noise (1% of λ) [*]	Main characteristics
Code measurements			
C_1	300 m	3 m	<u>Unambiguous</u> but noisier
$P_1 (Y1)$: encrypted	30 m	30 cm	
$P_2 (Y2)$: encrypted	30 m	30 cm	
Phase measurements			
L_1	19.05 cm	2 mm	<u>Precise</u> but ambiguous
L_2	24.45 cm	2 mm	

[*] the codes can be smoothed with the phases in order to reduce noise
(i.e., C_1 smoothed with L_1 → 50 cm noise)





$$P_{rec}^{sat} = \rho_{rec}^{sat} + c \cdot (dt_{rec} - dt^{sat}) + \sum \delta$$

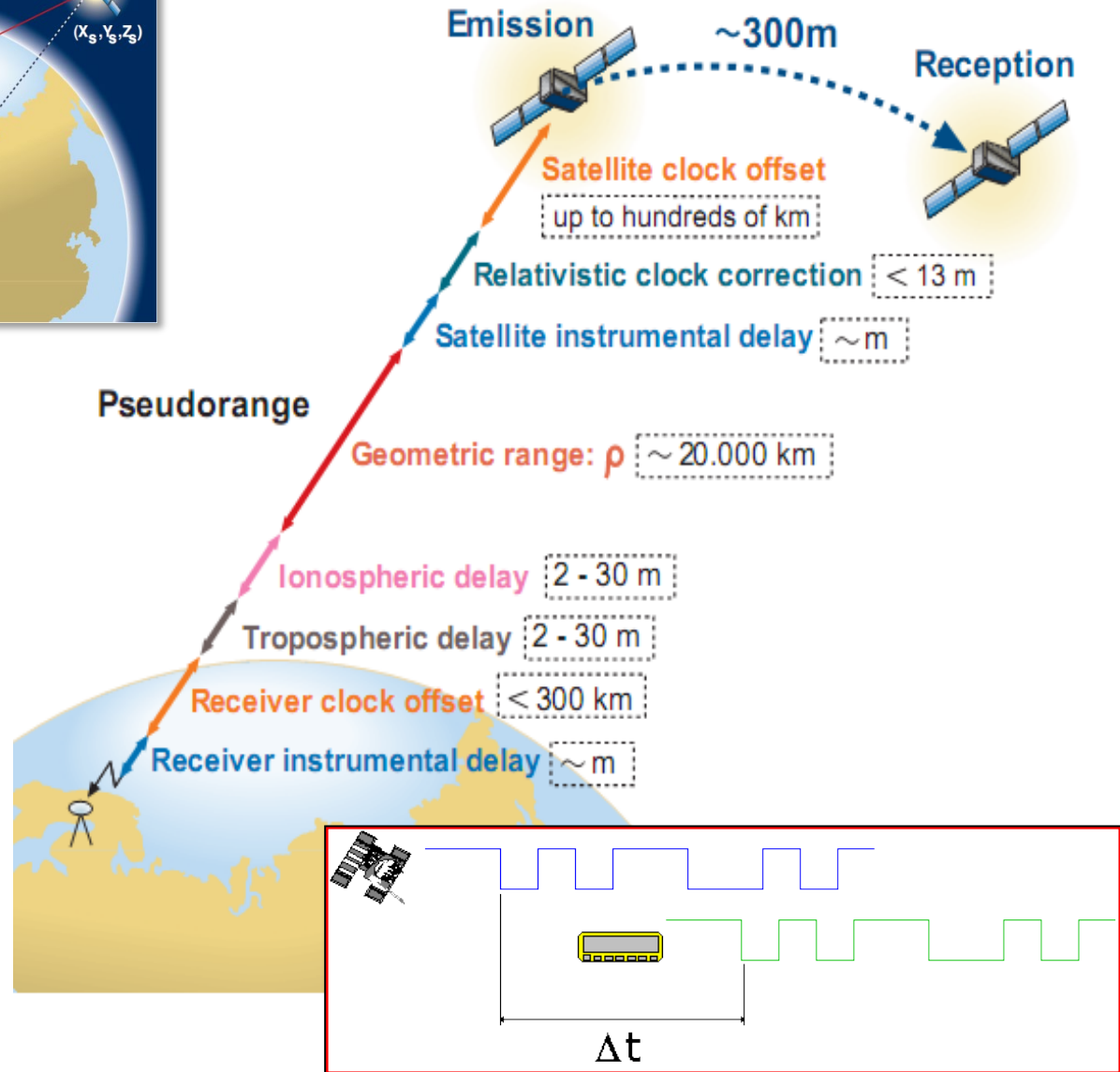
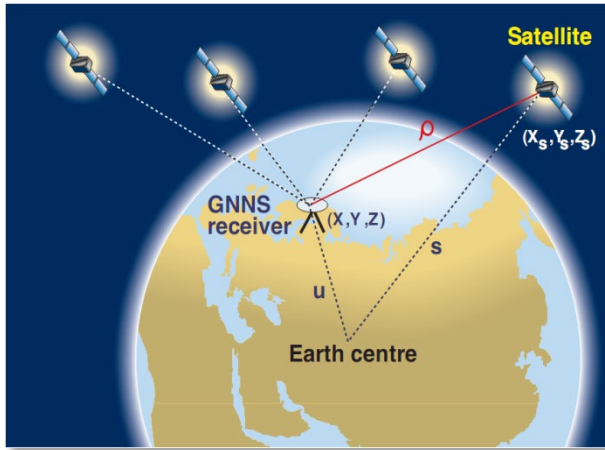
The equation shows the total pseudorange P_{rec}^{sat} as the sum of the geometric range ρ_{rec}^{sat} , the product of the speed of light c and the time difference $(dt_{rec} - dt^{sat})$, and the sum of various error terms $\sum \delta$.

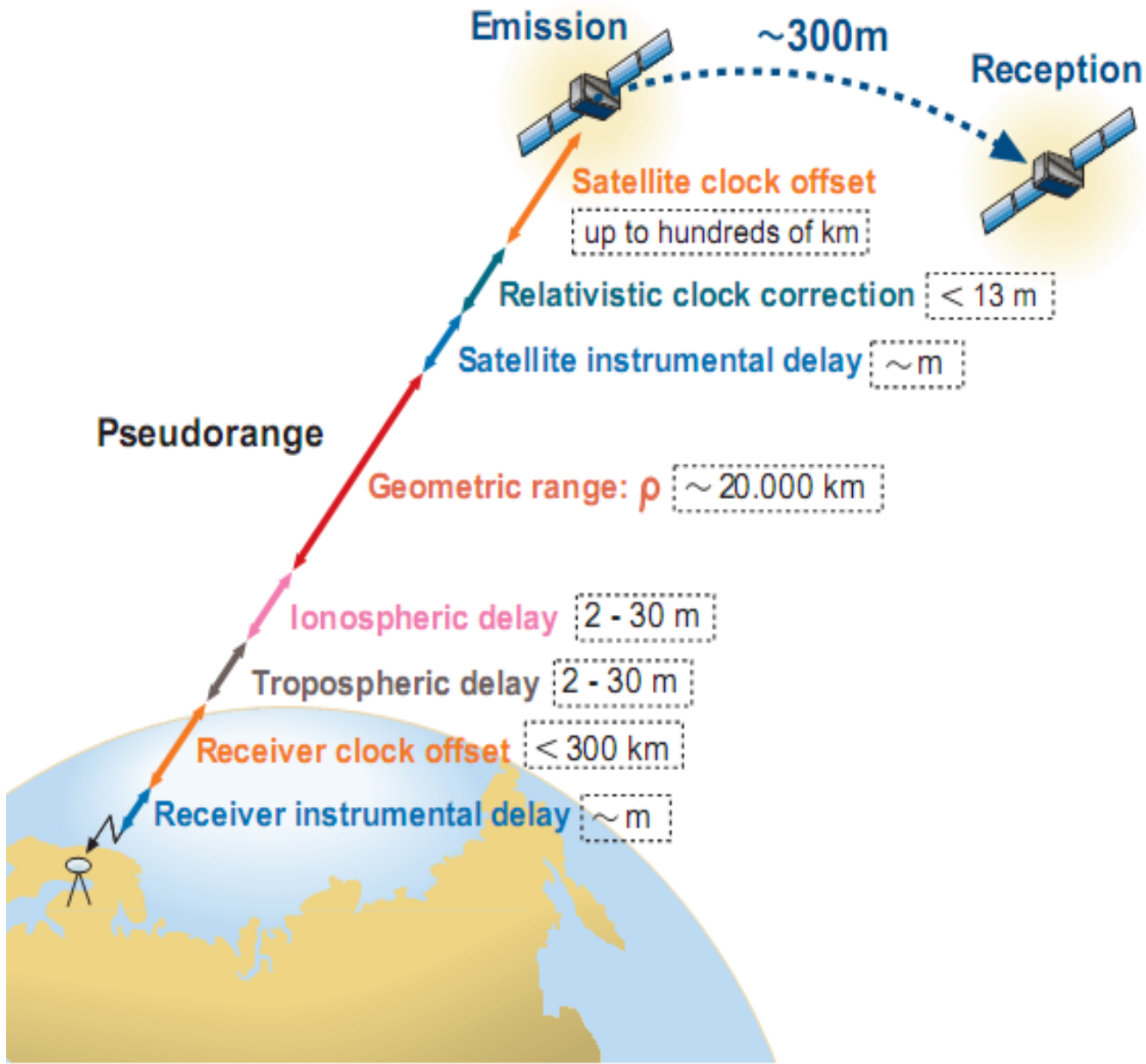
Annotations point to specific terms:

- Geometric range:** Points to ρ_{rec}^{sat}
- Clock offsets:** Points to $(dt_{rec} - dt^{sat})$

$$\sum \delta = Trop_{rec}^{sat} + Ion_{rec}^{sat} + K_{rec} + K^{sat} + \varepsilon$$

The error term $\sum \delta$ is decomposed into four components: Tropospheric delay, Ionospheric delay, Instrumental delays, and noise.





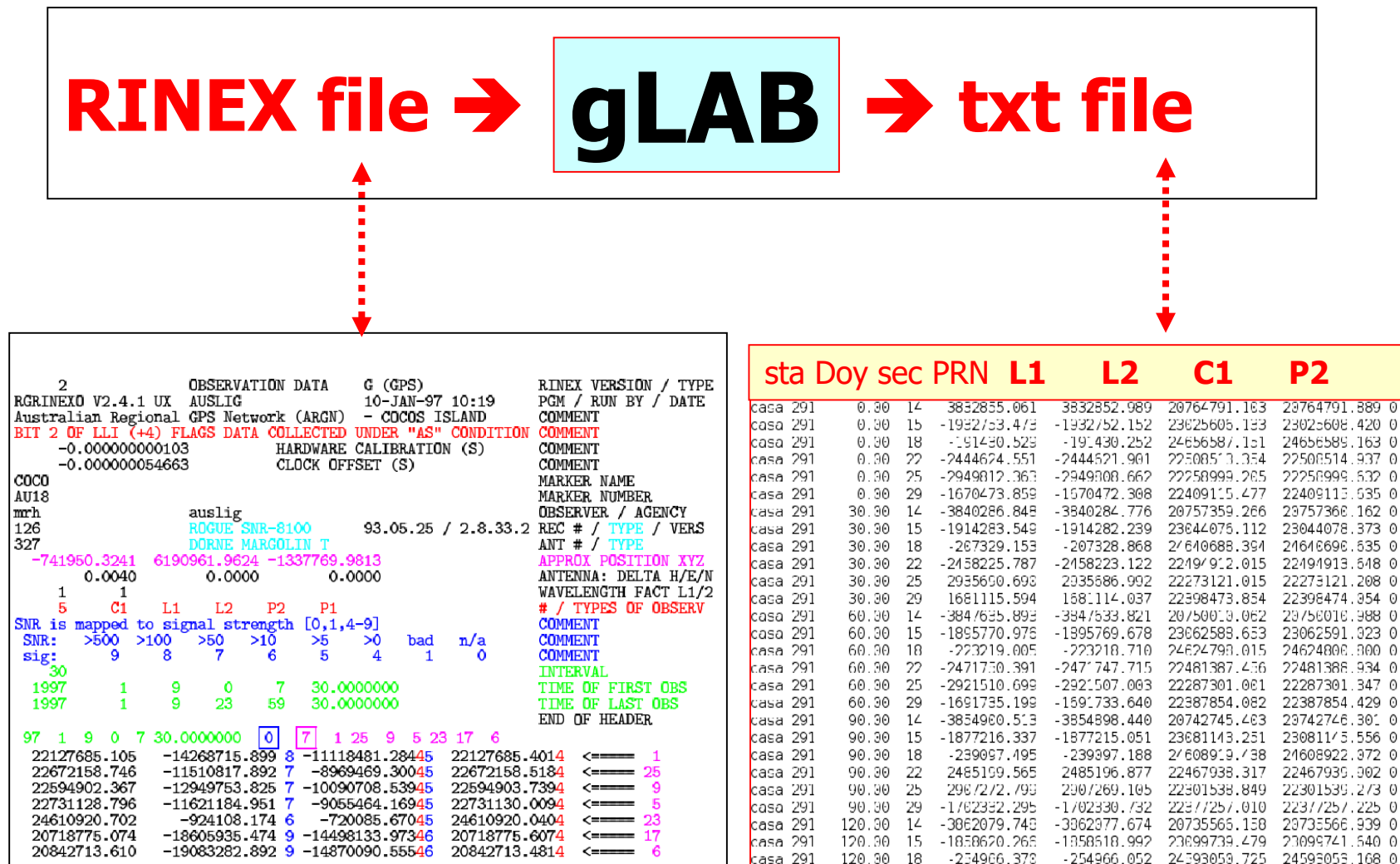
Exercise:

- a) Using the file coco0090.97o, generate the “txt” file 95oct18casa.a (with data ordered in columns).
- b) Plot code and phase measurements for satellite PRN28 and discuss the results.

Resolution:

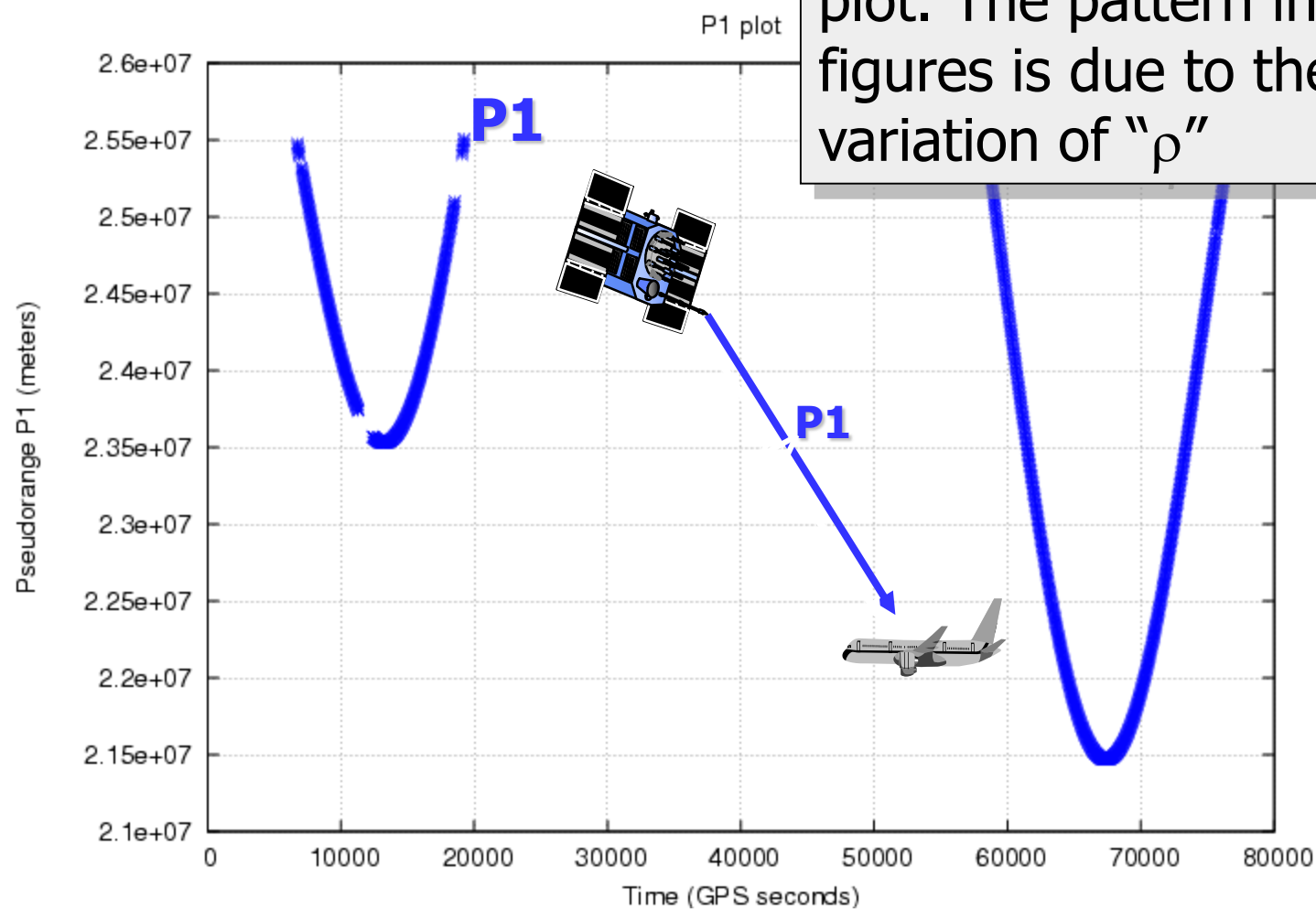
- a) **gLAb_linux -input:cfg `meas.cfg` -input:obs `coco0090.97o`**
- b) See next plots:

An example of program to read the RINEX: gLAB



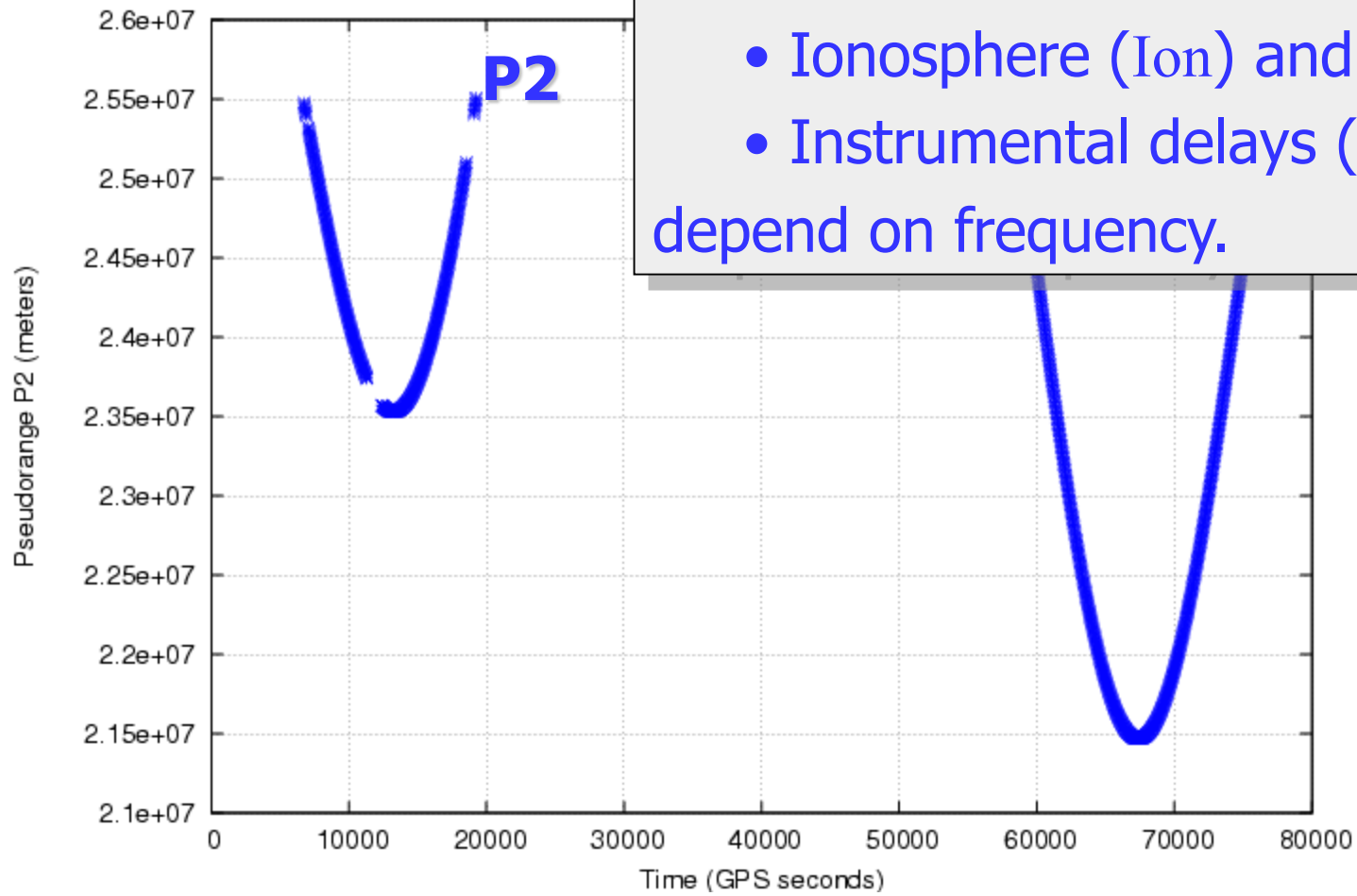
The RINEX file is converted to a “columnar format” to easily plot its content and to analyze the measurements (the public domain free tool “gnuplot” is used in the book to make the plots).

Code measurements



$$P_{1sta}^{sat} = \rho_{sta}^{sat} + c \cdot (dt_{sta} - dt^{sat}) + Trop_{sta}^{sat} + Ion_{1sta}^{sat} + K_{1sta} + K_1^{sat} + \varepsilon_1$$

Code measurements



Similar plot for code measurements at f_2 .

Notice that

- Ionosphere (Ion) and
- Instrumental delays (K) depend on frequency.

$$P_{2sta}^{sat} = \rho_{sta}^{sat} + c \cdot (dt_{sta} - dt^{sat}) + Trop_{sta}^{sat} + Ion_{2sta}^{sat} + K_{2sta} + K_2^{sat} + \varepsilon_2$$

Ionosphere delays code and advances phase measurements

Phase measurements

Code measurements: C1,P1,P2

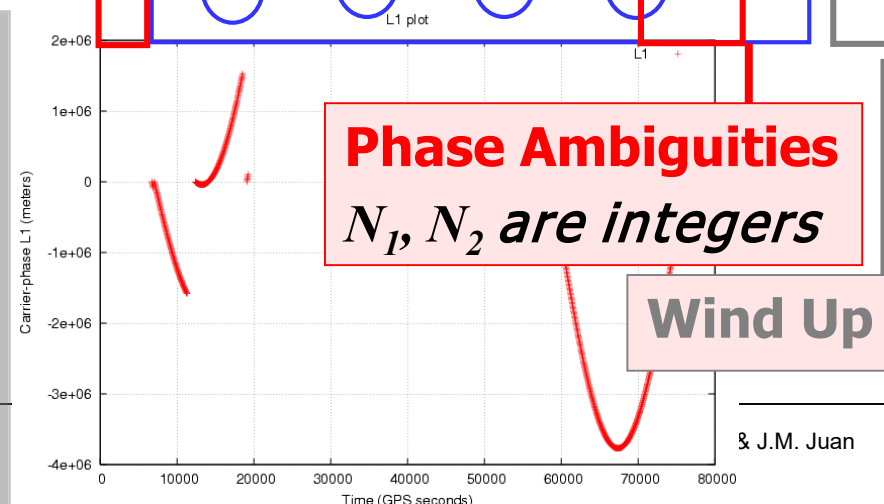
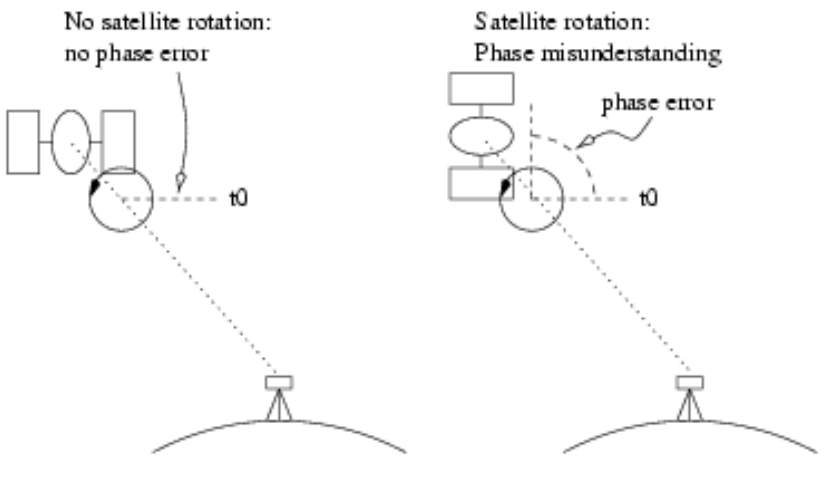
$$C_{1sta}^{sat} = \rho_{sta}^{sat} + c \cdot (dt_{sta} - dt^{sat}) + Trop_{sta}^{sat} + Ion_{1sta}^{sat} + K_{1sta} + K_1^{sat} + \varepsilon_1$$

$$P_{2sta}^{sat} = \rho_{sta}^{sat} + c \cdot (dt_{sta} - dt^{sat}) + Trop_{sta}^{sat} + Ion_{2sta}^{sat} + K_{2sta} + K_2^{sat} + \varepsilon_2$$

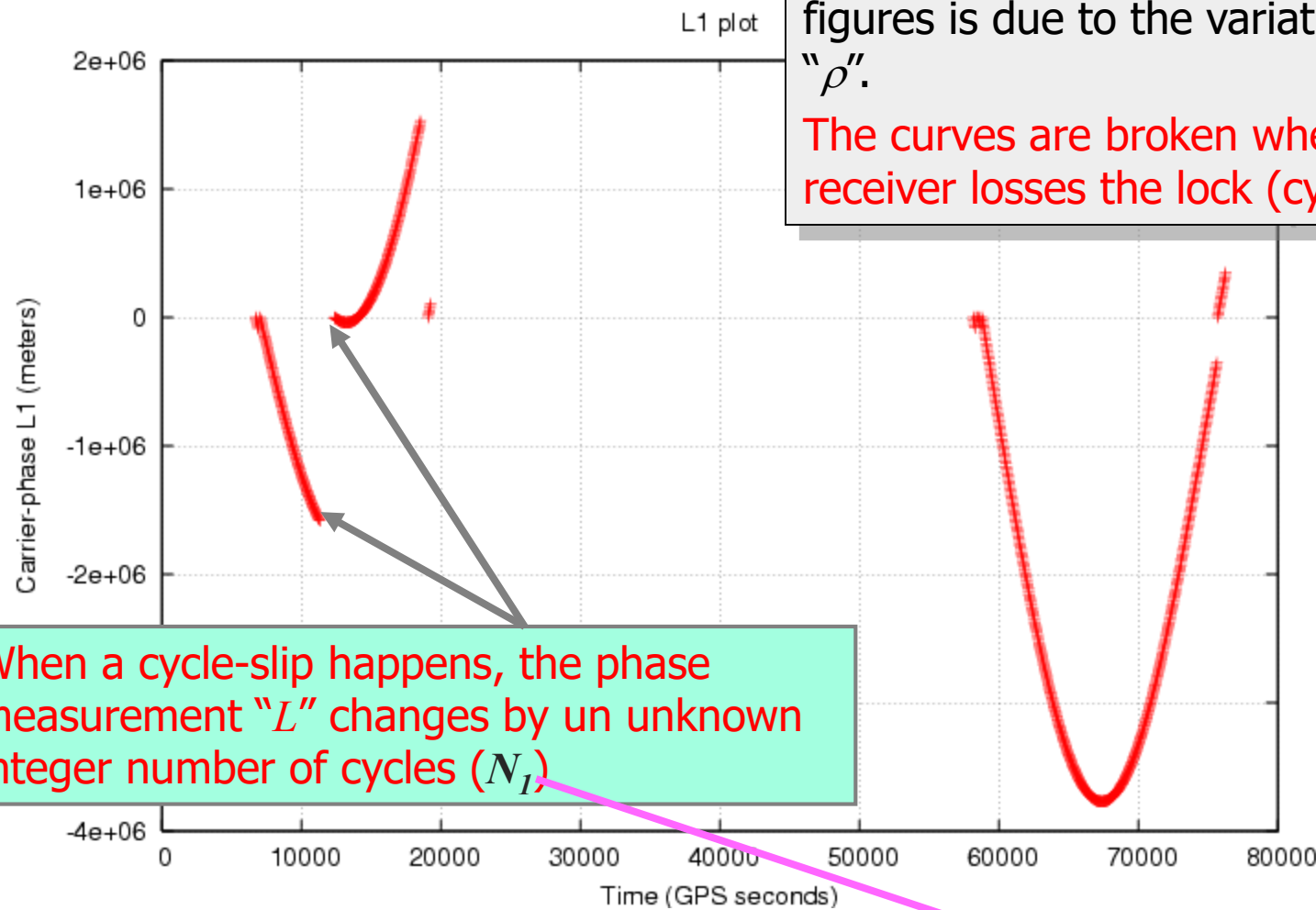
Phase measurements: L1,L2

$$L_{1sta}^{sat} = \rho_{sta}^{sat} + c \cdot (dt_{sta} - dt^{sat}) + Trop_{sta}^{sat} - Ion_{1sta}^{sat} + b_{1sta} + b_1^{sat} + \lambda_1 N_{1sta}^{sat} + \lambda_1 v_{sta}^{sat} + v_1$$

$$L_{2sta}^{sat} = \rho_{sta}^{sat} + c \cdot (dt_{sta} - dt^{sat}) + Trop_{sta}^{sat} - Ion_{2sta}^{sat} + b_{2sta} + b_2^{sat} + \lambda_2 N_{2sta}^{sat} + \lambda_2 v_{sta}^{sat} + v_2$$



Carrier Phase measurements

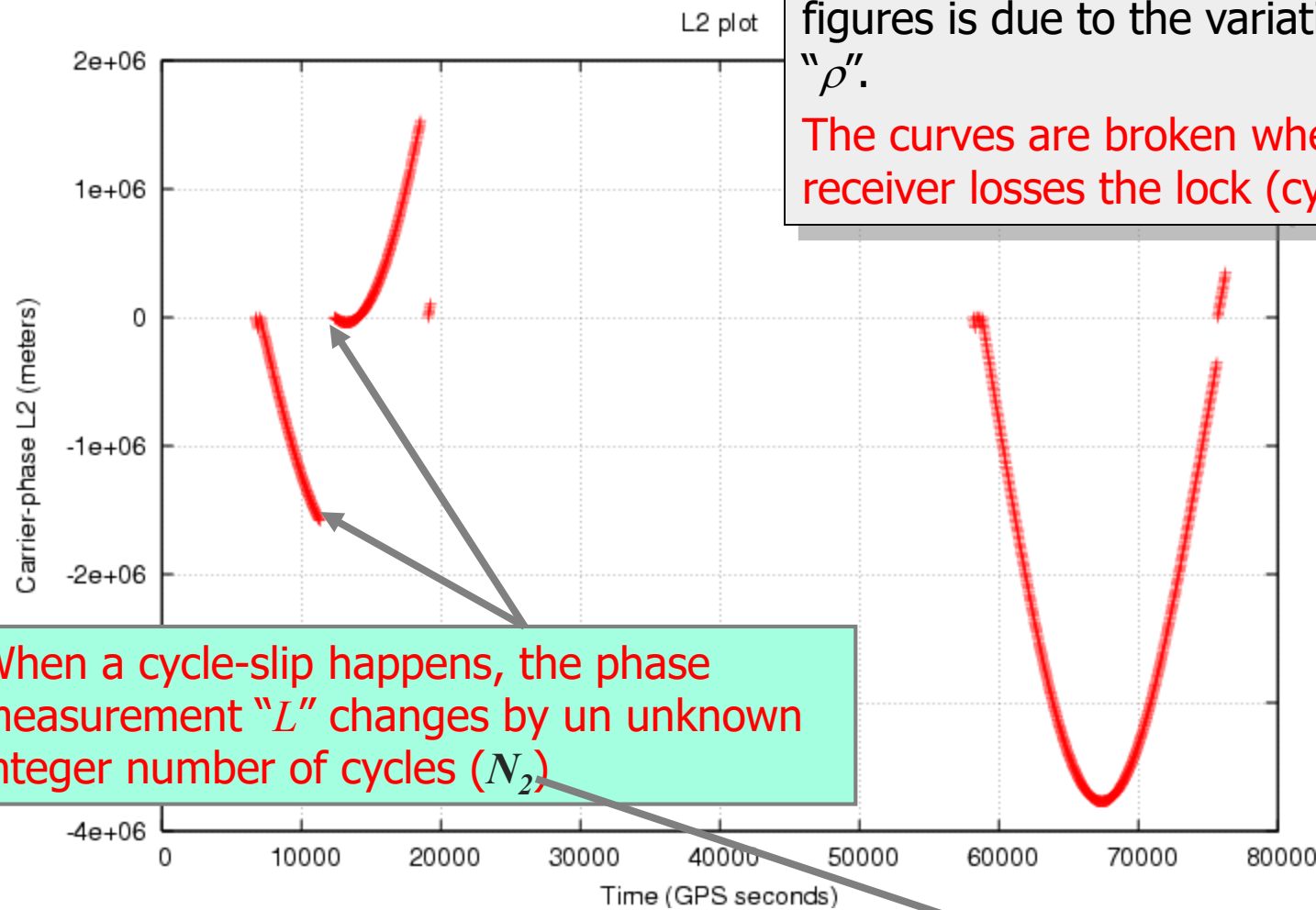


The geometry " ρ " is the dominant term in the plot. The pattern in the figures is due to the variation of " ρ ".

The curves are broken when the receiver losses the lock (cycle-slip).

$$L_{1sta}^{sat} = \rho_{sta}^{sat} + c \cdot (dt_{sta} - dt^{sat}) + Trop_{sta}^{sat} - Ion_{1sta}^{sat} + b_{1sta} + b_1^{sat} + \lambda_1 N_{1sta}^{sat} + \lambda_1 w_{sta}^{sat} + v_1$$

Carrier Phase measurements



The geometry " ρ " is the dominant term in the plot. The pattern in the figures is due to the variation of " ρ ".

The curves are broken when the receiver losses the lock (cycle-slip).

$$L_{2sta}^{sat} = \rho_{sta}^{sat} + c \cdot (dt_{sta} - dt^{sat}) + Trop_{sta}^{sat} - Ion_{2sta}^{sat} + b_{2sta} + b_2^{sat} + \lambda_2 N_{2sta}^{sat} + \lambda_2 w_{sta}^{sat} + v_2$$

Contents

1. Review of GNSS measurements.
2. Linear combinations of measurements.
3. Carrier cycle-slips detection.
4. Carrier smoothing of code pseudorange.
5. Code Multipath.

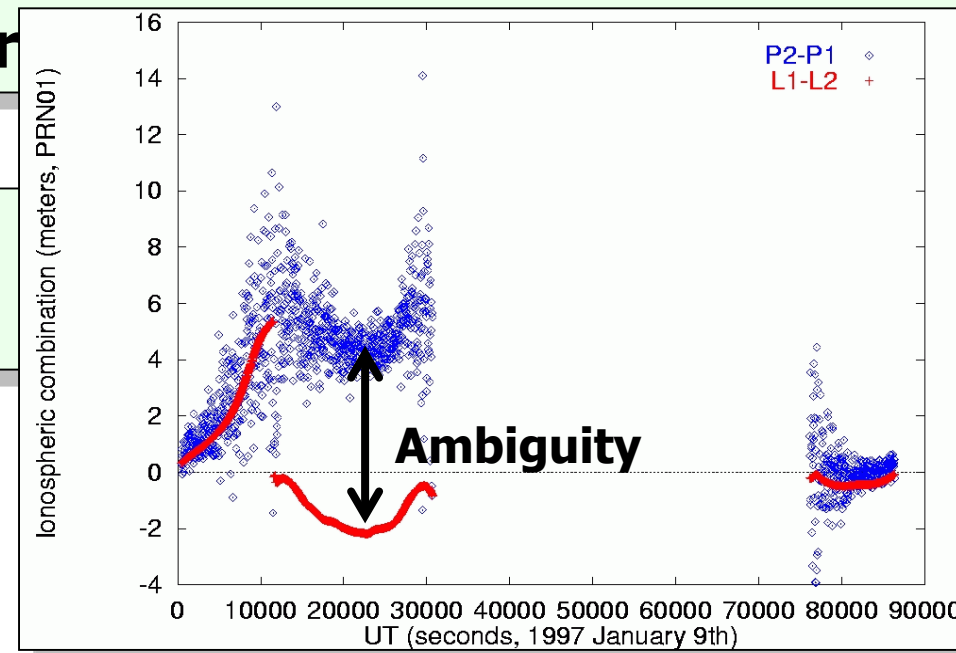
Linear Combinations of measurements:

- Geometry-free (or Ionospheric) combination.
- Ionosphere-Free combination.
- Wide-lane and Narrow-lane combinations.

1. Geometry-free (or)

$$P_I = P_2 - P_1 = \text{Iono} + \text{ctt}$$

$$L_I = L_1 - L_2 = \text{Iono} + \text{ctt} + \text{Ambig}$$



Code measurements: C, P_I, P_2

$$P_{1\text{sta}}^{\text{sat}} = \rho_{\text{sta}}^{\text{sat}} + c \cdot (dt_{\text{sta}} - dt^{\text{sat}}) + \text{Trop}_{\text{sta}}^{\text{sat}}$$

$$P_{2\text{sta}}^{\text{sat}} = \rho_{\text{sta}}^{\text{sat}} + c \cdot (dt_{\text{sta}} - dt^{\text{sat}}) + \text{Trop}_{\text{sta}}^{\text{sat}}$$

$$+ \text{Ion}_{1\text{sta}}^{\text{sat}} + K_{1\text{sta}} + K_1 + \varepsilon_1$$

$$+ \text{Ion}_{2\text{sta}}^{\text{sat}} + K_{2\text{sta}} + K_2 + \varepsilon_2$$

Carrier measurements: L1,L2

$$L_{1\text{sta}}^{\text{sat}} = \rho_{\text{sta}}^{\text{sat}} + c \cdot (dt_{\text{sta}} - dt^{\text{sat}}) + \text{Trop}_{\text{sta}}^{\text{sat}}$$

$$L_{2\text{sta}}^{\text{sat}} = \rho_{\text{sta}}^{\text{sat}} + c \cdot (dt_{\text{sta}} - dt^{\text{sat}}) + \text{Trop}_{\text{sta}}^{\text{sat}}$$

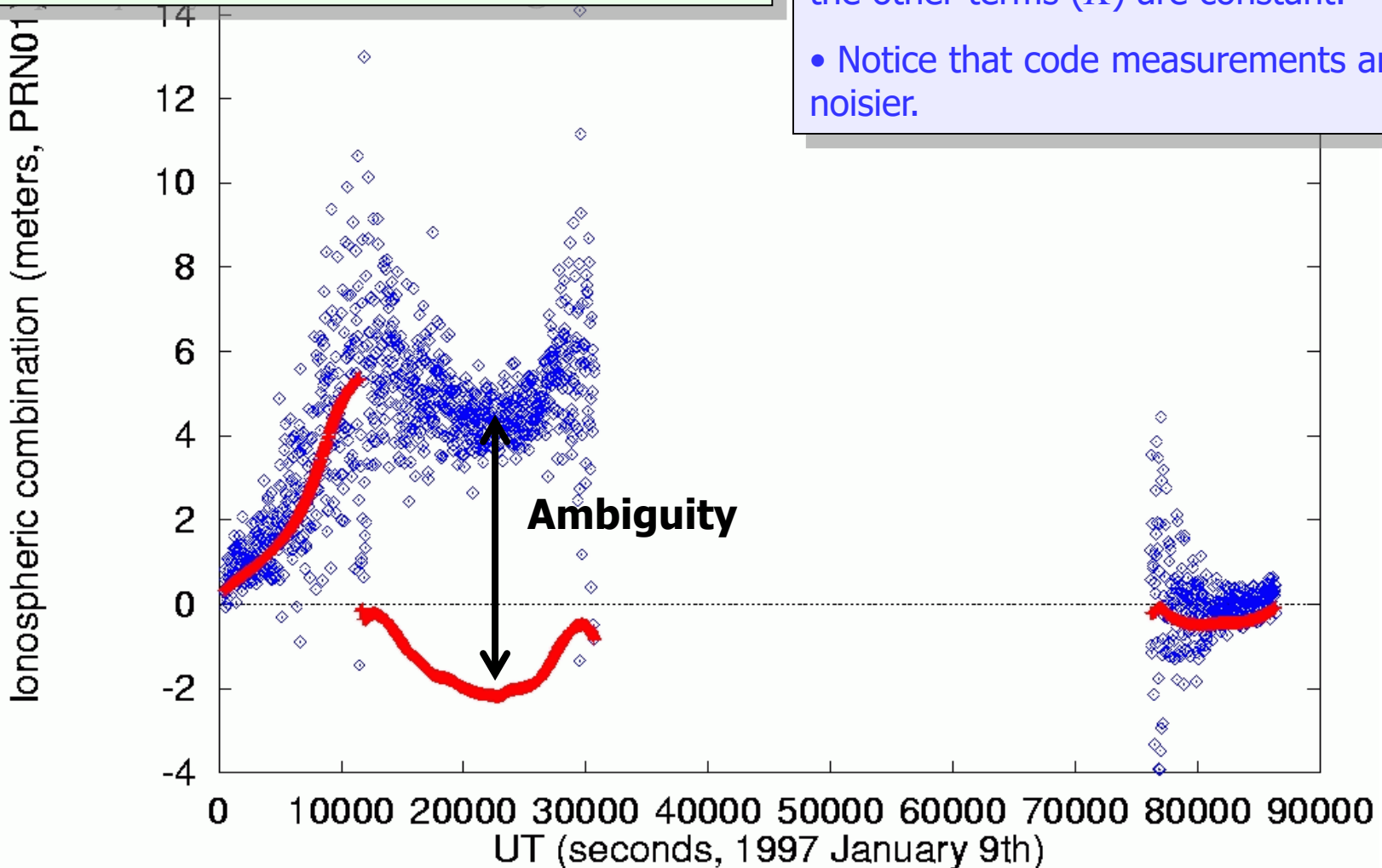
$$- \text{Ion}_{1\text{sta}}^{\text{sat}} + b_{1\text{sta}} + b_1^{\text{sat}} + \lambda_1 N_{1\text{sta}}^{\text{sat}} + \lambda_1 w_{\text{sta}}^{\text{sat}} + v_1$$

$$- \text{Ion}_{2\text{sta}}^{\text{sat}} + b_{2\text{sta}} + b_2^{\text{sat}} + \lambda_2 N_{2\text{sta}}^{\text{sat}} + \lambda_2 w_{\text{sta}}^{\text{sat}} + v_2$$

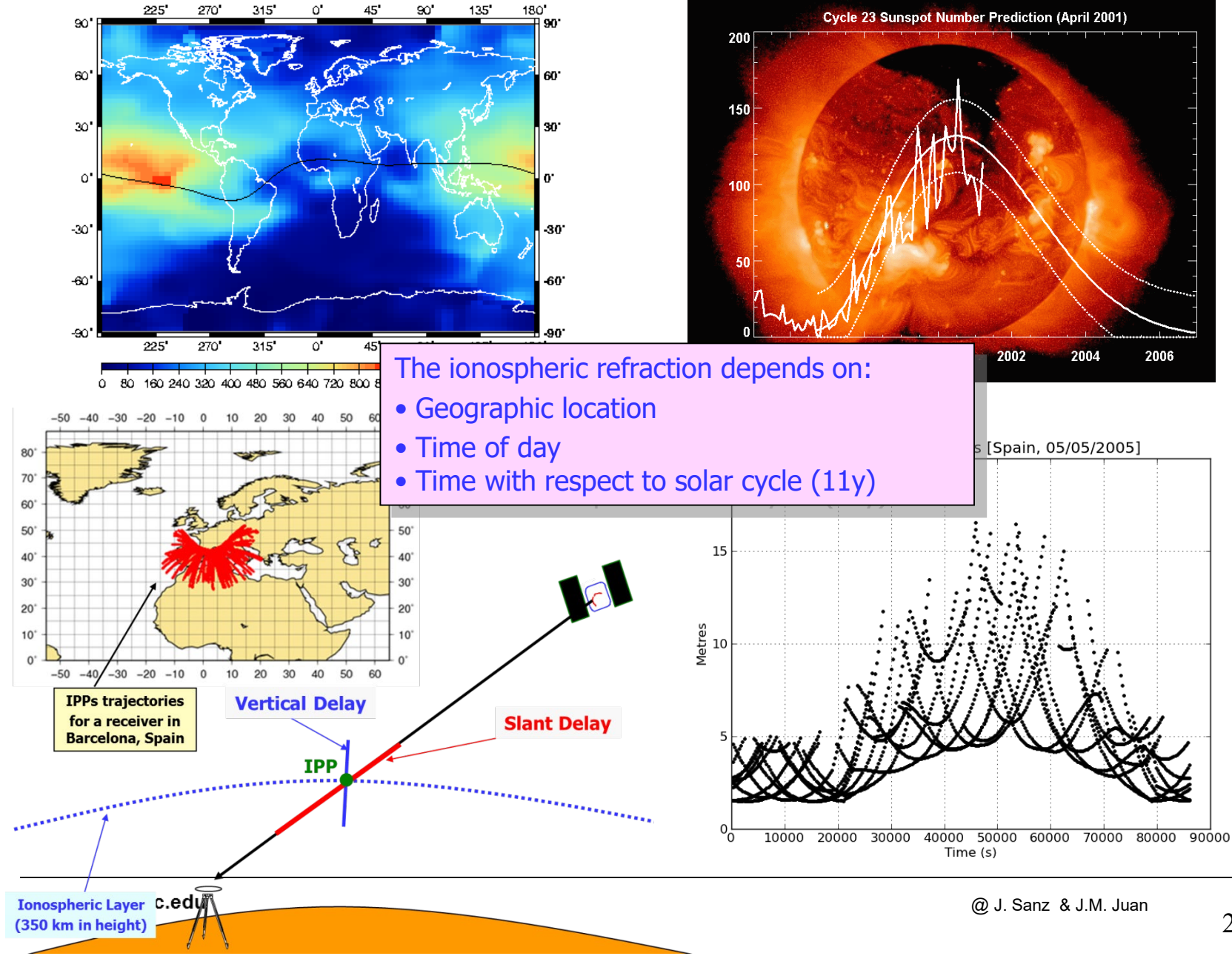
1. Geometry-free (or ionospheric) combination

$$P_I = P_2 - P_1 = \text{Iono} + \text{ctt}$$

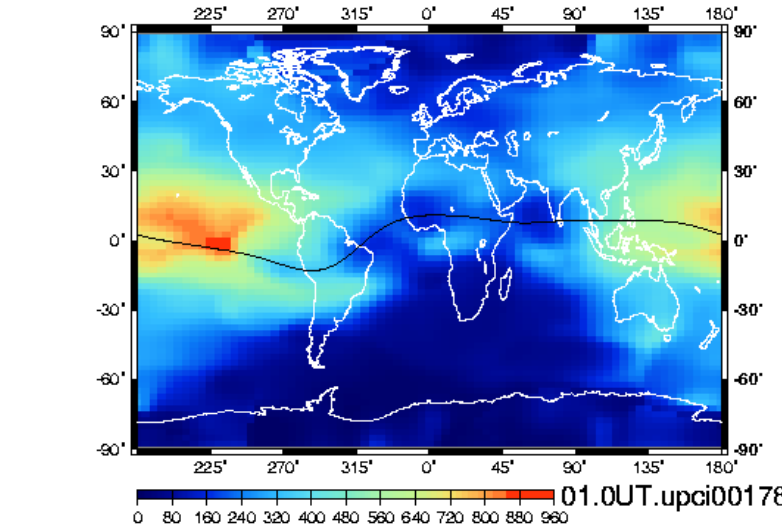
$$L_I = L_1 - L_2 = \text{Iono} + \text{ctt} + \text{Ambig}$$



Ionospheric effects



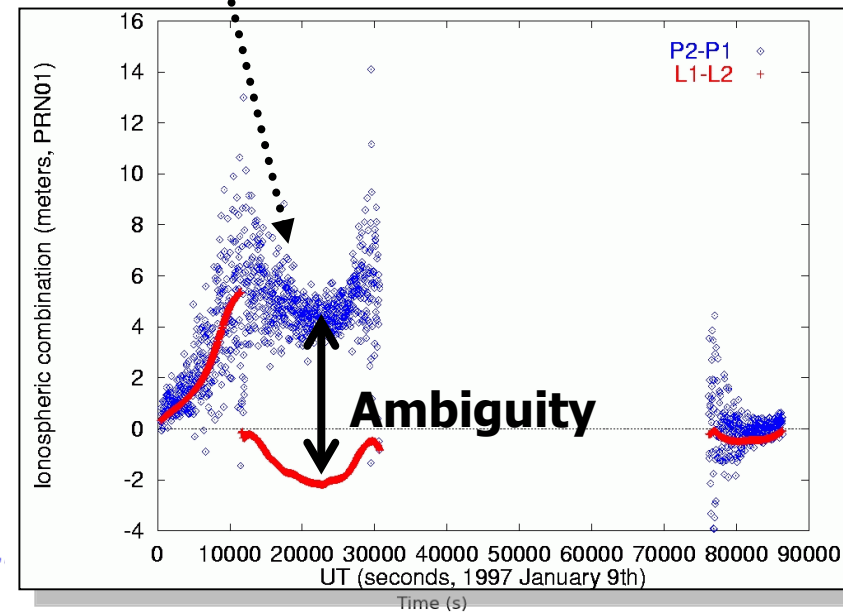
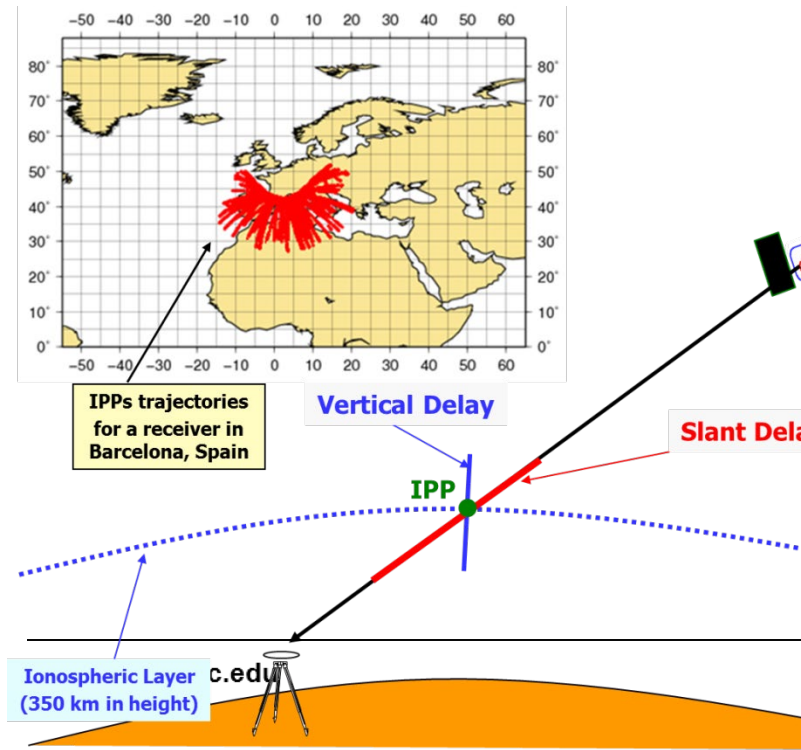
Ionospheric effects



The ionospheric delay (*Ion*) is proportional to the electron density integrated along the ray path (*STEC*)

$$Ion = \frac{40.3}{f^2} STEC$$

$$STEC = \int_{\vec{r}[\text{GPS receiver}]}^{\vec{r}[\text{GPS transmitter}]} N_e(\vec{r}, t) d\vec{r}$$



2. Ionosphere-free Combination (P_c, L_c)

The ionospheric refraction depends on the inverse of the squared frequency and can be removed up to 99.9% combining $f1$ and $f2$ signals:

$$Ion = \frac{40.3}{f^2} STEC$$

$$P_c = \frac{f_1^2 P_1 - f_2^2 P_2}{f_1^2 - f_2^2}$$

$$L_c = \frac{f_1^2 L_1 - f_2^2 L_2}{f_1^2 - f_2^2}$$

$$P_{c,sta}^{sat} = \rho_{sta}^{sat} + c \cdot (dt_{sta} - dt^{sat}) + Trop_{sta}^{sat} + \varepsilon_c$$

Note: K^{sat} cancels in P_c and K_{sta} included in dt_{sta}

$$L_{c,sta}^{sat} = \rho_{sta}^{sat} + c \cdot (dt_{sta} - dt^{sat}) + Trop_{sta}^{sat} + \lambda_N w_{sta}^{sat} + b_{c,sta} + b_c^{sat} + \lambda_N (N_{1,sta}^{sat} - \frac{\lambda_W}{\lambda_2} N_{W,sta}^{sat}) + \nu_c$$

- The ionospheric refraction has been removed in L_c and P_c

$$\lambda_N = 10.7 \text{ cm}, \lambda_W = 86.2 \text{ cm}$$

$$N_W = N_1 - N_2$$

Comments:

Two-frequency receivers are needed to apply the ionosphere-free combination.

If a single-frequency receiver is used, a ionospheric model must be applied to remove the ionospheric refraction. The GPS navigation message provides the parameters of the Klobuchar model which accounts for more than 50% (RMS) of the ionospheric delay.

3.- Narrow-lane (P_N) and Wide-lane Combination (L_W)

The wide-lane combination L_W provides a signal with a large wave-length ($\lambda_W=86.2\text{cm} \sim 4*\lambda_1$). This makes it very useful for detecting cycle-slips through the **Melbourne-Wübbena** combination: $MW=L_W-P_N$

$$P_N = \frac{f_1 P_1 + f_2 P_2}{f_1 + f_2}$$

$$L_W = \frac{f_1 L_1 - f_2 L_2}{f_1 - f_2}$$



The same iono. and sign

$$P_{Nsta}^{sat} = \rho_{sta}^{sat} + c \cdot (dt_{sta} - dt^{sat}) + Trop_{sta}^{sat} + Ion_{w,sta}^{sat} + K_{N,sta} + K_N^{sat} + \varepsilon_N$$

$$L_{Wsta}^{sat} = \rho_{sta}^{sat} + c \cdot (dt_{sta} - dt^{sat}) + Trop_{sta}^{sat} + Ion_{w,sta}^{sat} + b_{w,sta} + b_w^{sat} + \lambda_w N_{w,sta}^{sat} + \nu_w$$

No wind-up

Melbourne-Wübbena combination

$$N_W = N_1 - N_2$$

$$MW_{sta}^{sat} = L_{Wsta}^{sat} - P_{Nsta}^{sat} = b_{w,sta} + b_w^{sat} - K_{N,sta} - K_N^{sat} + \lambda_w N_{w,sta}^{sat} + \varepsilon_{MW}$$

Hardware biases

Integer Ambiguity

The ambiguities N_W are INTEGER Numbers!

Exercises:

1) Consider the wide-lane combination of carrier phase measurements

$$L_w = \frac{f_1 L_1 - f_2 L_2}{f_1 - f_2}, \text{ where } L_w \text{ is given in length units (i.e. } L_i = \lambda_i \phi_i \text{).}$$

Show that the corresponding wavelength is: $\lambda_w = \frac{c}{f_1 - f_2}$

Hint:

$$L_w = \lambda_w \phi_w; \quad \phi_w = \phi_1 - \phi_2$$

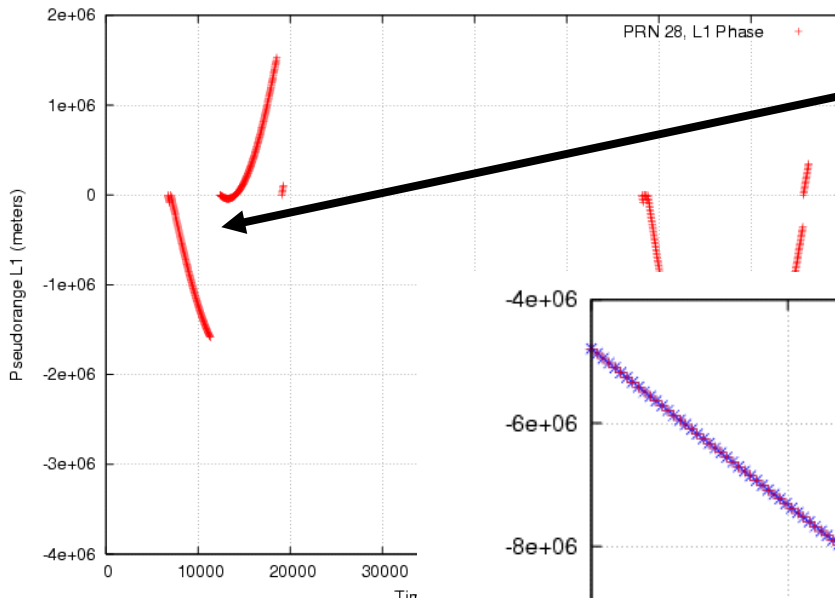
2) Assuming L_1, L_2 uncorrelated measurements with equal noise σ_L , show that:

$$\sigma_{L_w} = \frac{\sqrt{\gamma_{12} + 1}}{\sqrt{\gamma_{12} - 1}} \sigma_L \quad ; \quad \gamma_{12} = \left(\frac{f_1}{f_2} \right)^2$$

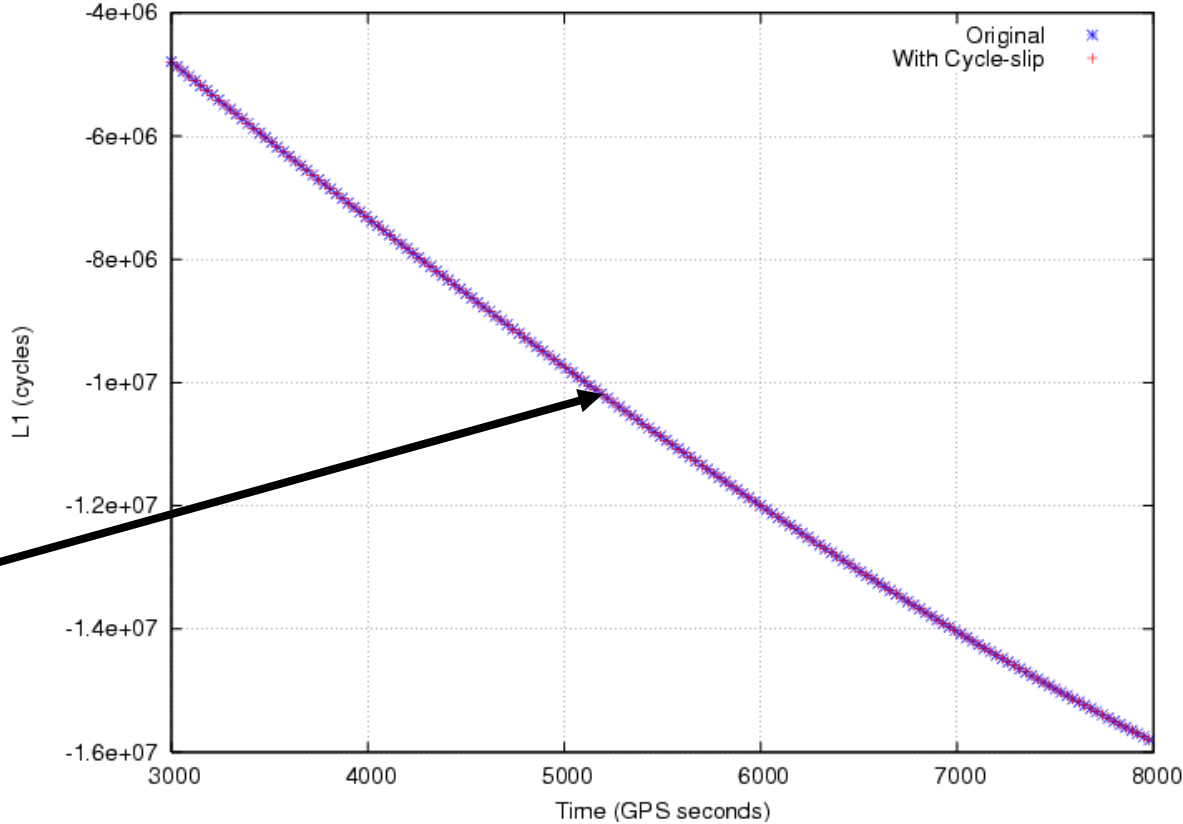
Contents

1. Review of GNSS measurements.
2. Linear combinations of measurements.
3. Carrier cycle-slips detection.
4. Carrier smoothing of code pseudorange.
5. Code Multipath.

Detecting cycle-slips



This cycle-slip involves millions of cycles → it is easy to detect!!



There is a cycle-slip of only one cycle ($\sim 20\text{cm}$) → How to detect it?

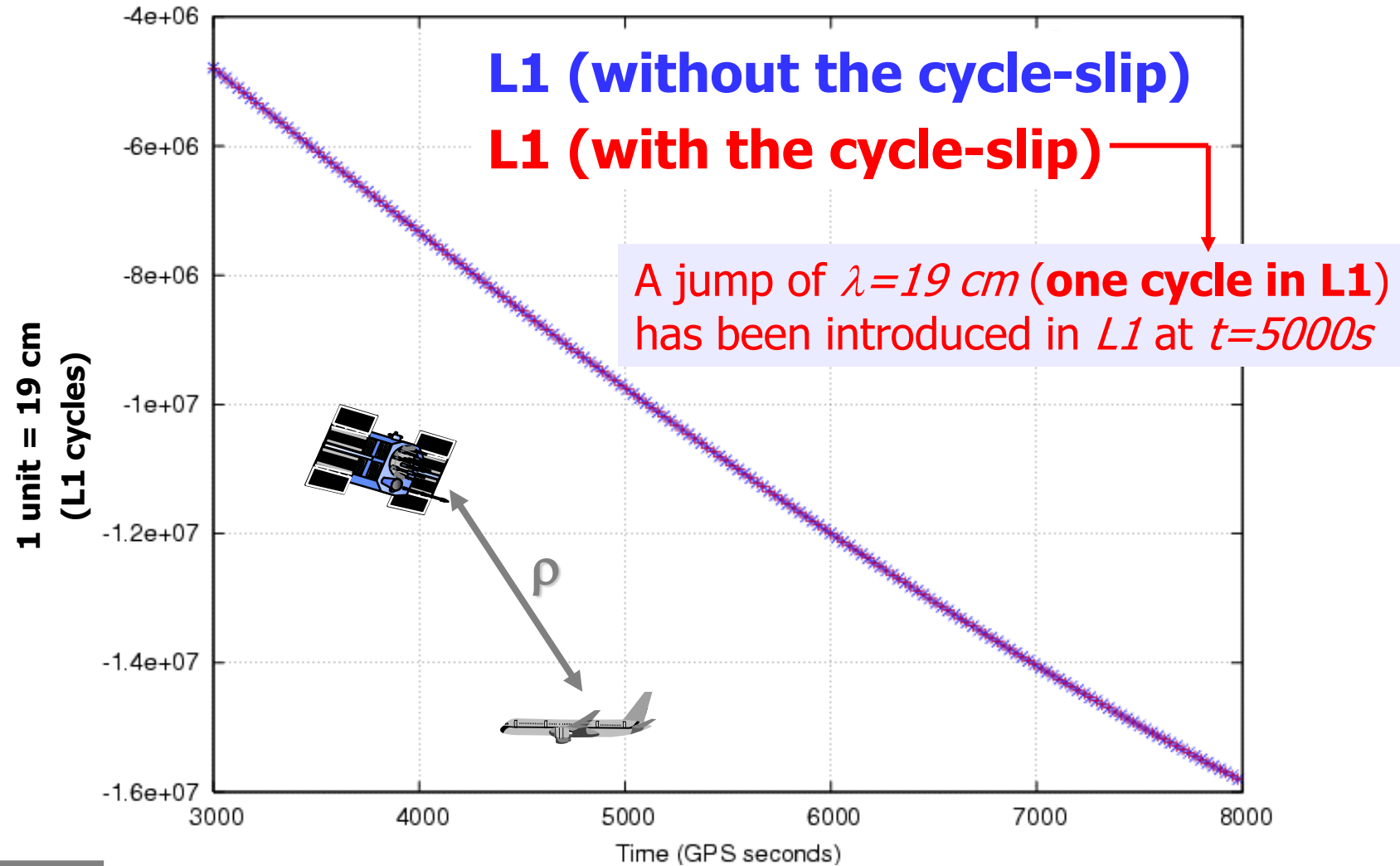
Exercise:

- Using the file 95oct18casa____r0.rnx, generate the “txt” file 95oct18casa.a (with data ordered in columns).
- Insert a **cycle-slip** of “one wavelength” (**19cm**) in **L1** measurement at t=5000 s (and no cycle-slip in L2).
- Plot the measurements “L1, L1-P1, LC-PC, Lw-P_N and L1-L2” and discuss which combination/s should be used to detect the cycle-slip.

Resolution:

- `gLAB_linux -input:cfg meas.cfg -input:obs 95oct18casa_r0.rnx`
- `cat 95oct18casa.a | gawk '{if ($4==18)
print $3,$5,$6,$7,$8}' > s18.org`
`cat s18.org | gawk '{if ($1>=5000) $2=$2+0.19;
printf "%s %f %f %f %f \n", $1,$2,$3,$4,$5}' > s18.cl`
- See next plots:

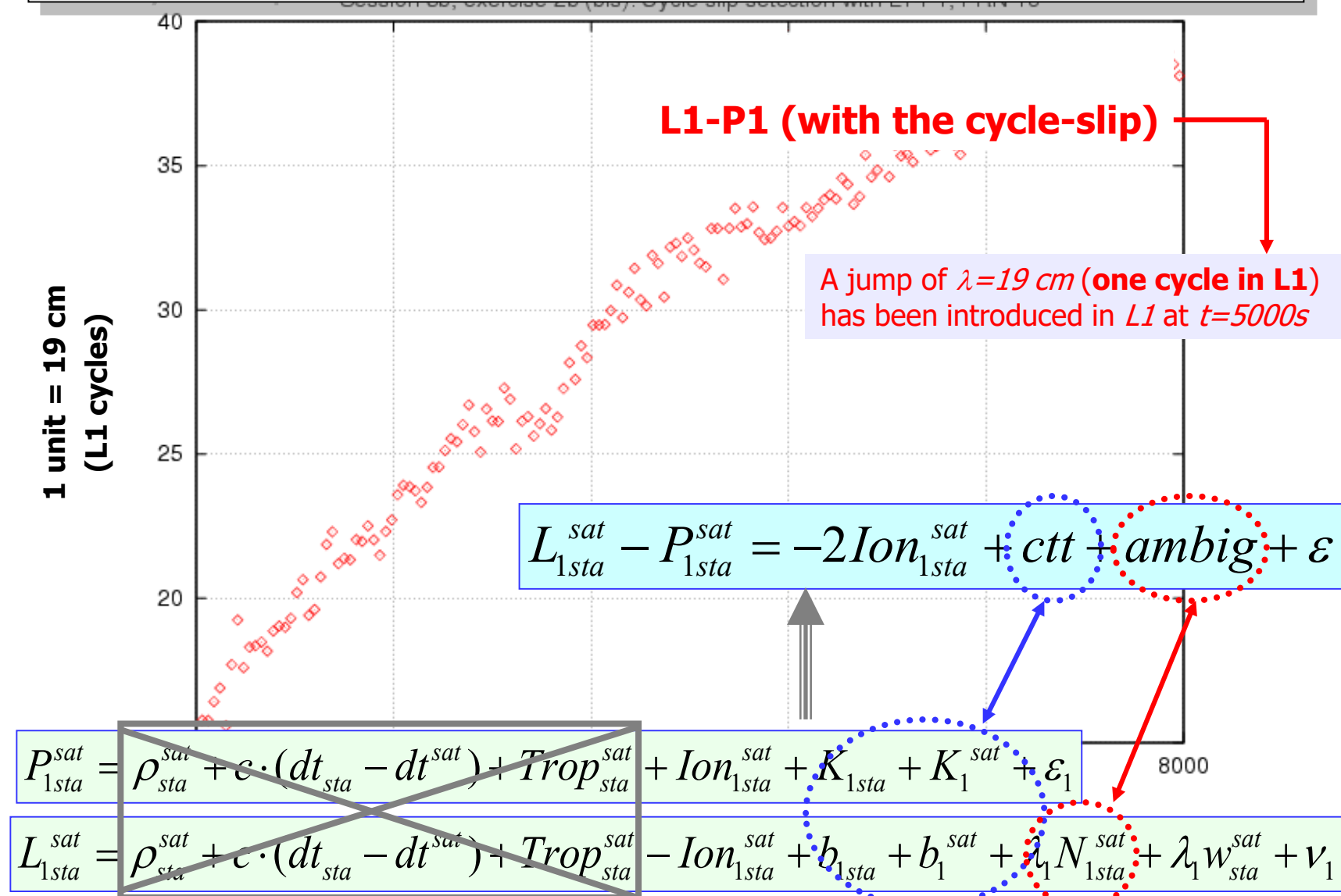
The geometry “ ρ ” is the dominant term in the plot. The variation of “ ρ ” in 1 sec may be hundreds of meters, many times greater than the cycle-slip (19 cm) → the variation of ρ shadows the cycle-slip!



$$L_{1sta}^{sat} = \rho_{sta}^{sat} + c \cdot (dt_{sta} - dt^{sat}) + Trop_{sta}^{sat} - Ion_{1sta}^{sat} + b_{1sta} + b_1^{sat} + \lambda_1 N_{1sta}^{sat} + \lambda_1 w_{sta}^{sat} + \nu_1$$

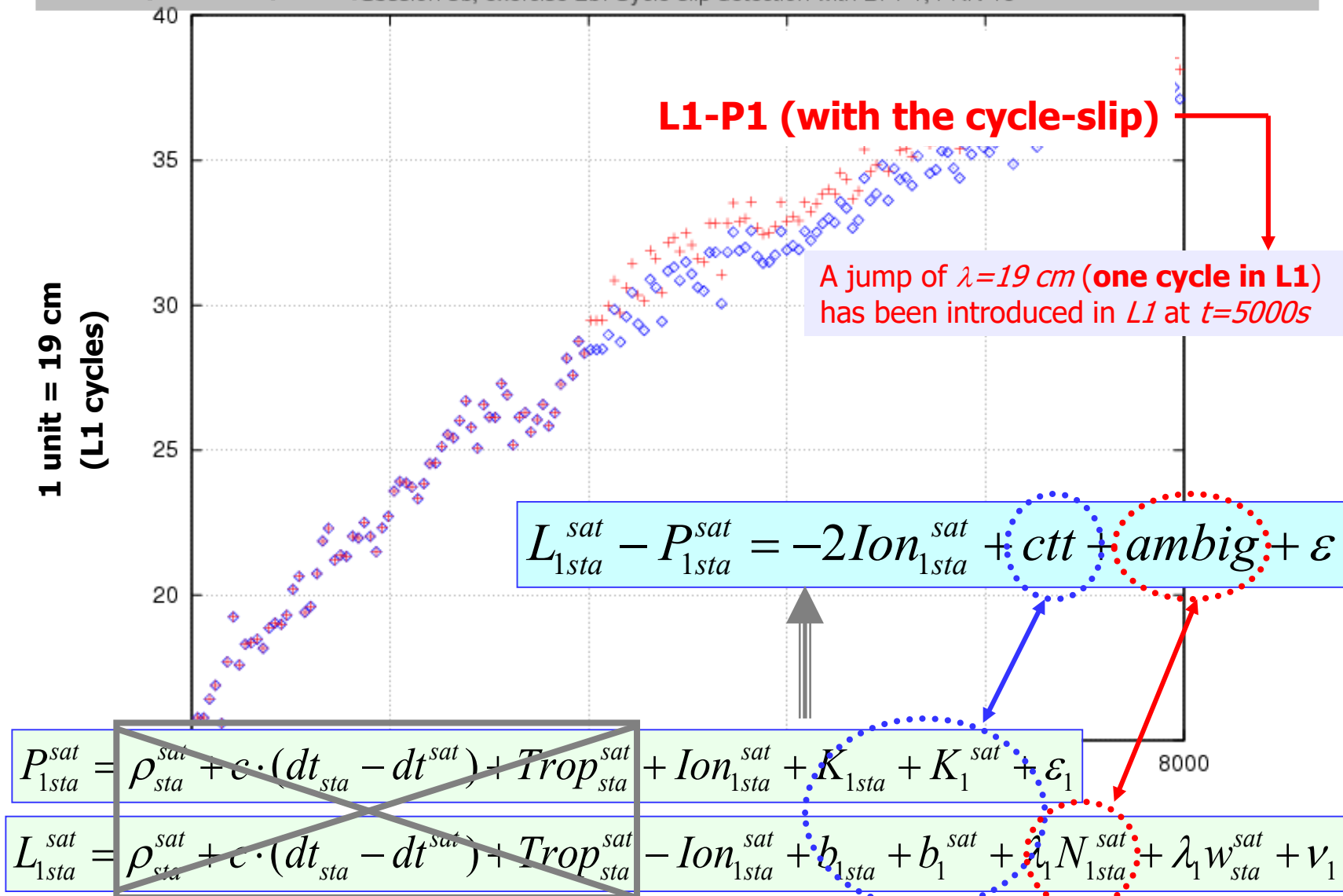
The geometry and clock offsets have been removed.

The trend is due to the Ionosphere. **The P1 code noise shadows the cycle-slip**, and without the reference (in blue), the time where the cycle-slip happens could not be identified.



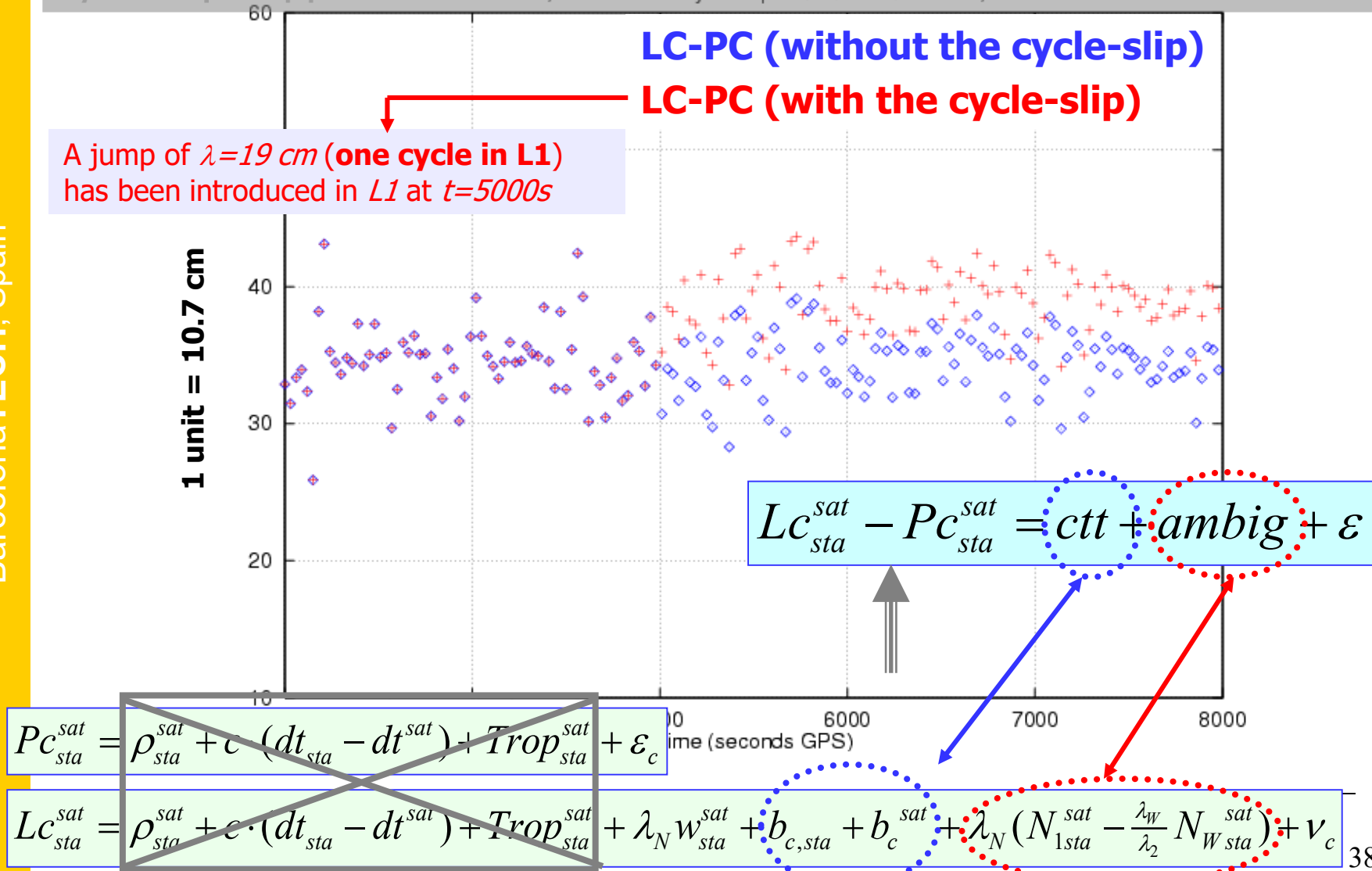
The geometry and clock offsets have been removed.

The trend is due to the Ionosphere. **The $P1$ code noise shadows the cycle-slip**, and without the reference (in blue), the time where the cycle-slip happens could not be identified.



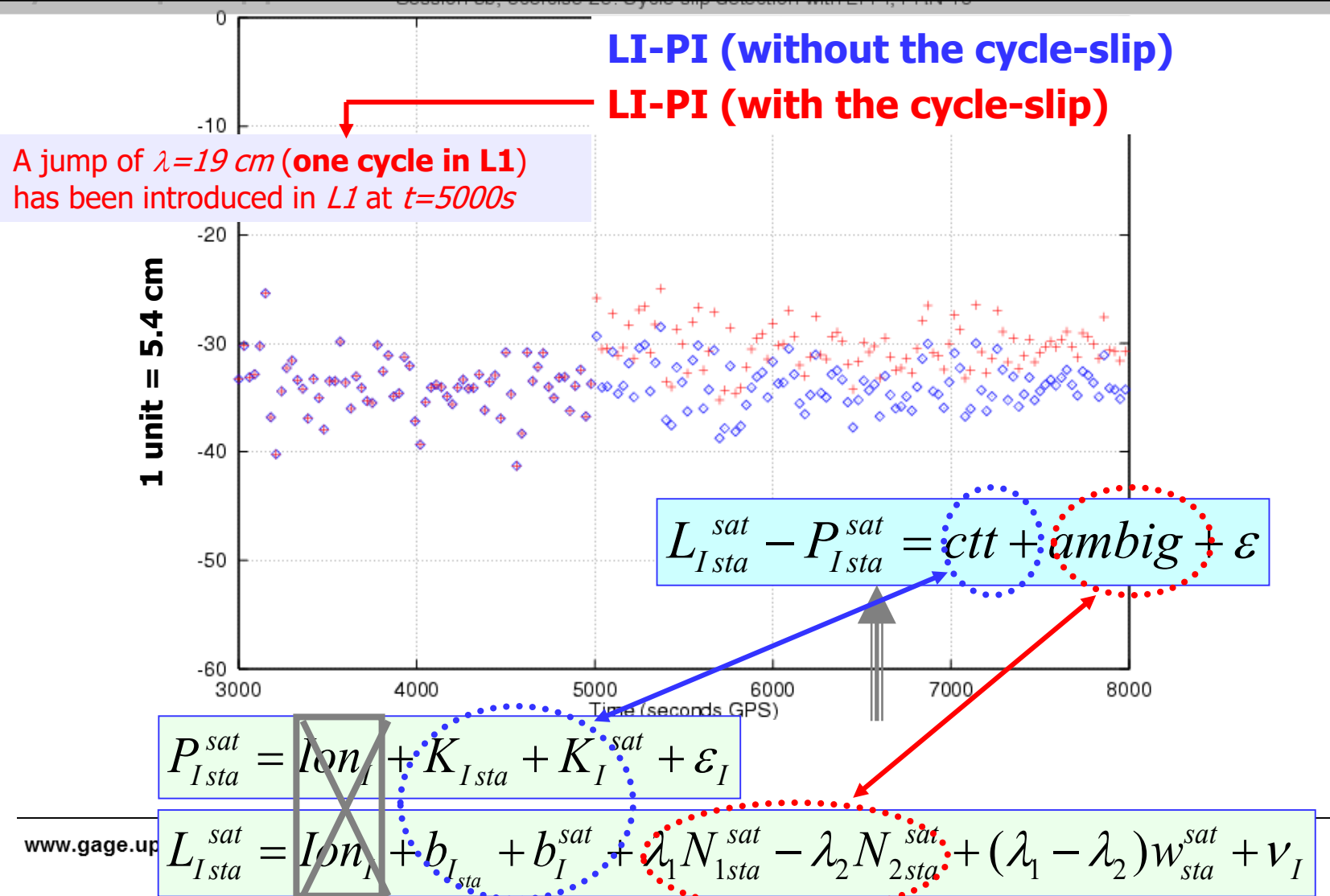
The geometry, clock offsets and iono have been removed.

There is a constant pattern plus noise. The P_C code noise also shadows the cycle-slip, and without the reference (in blue), the time where the cycle-slip happens could not be identified.



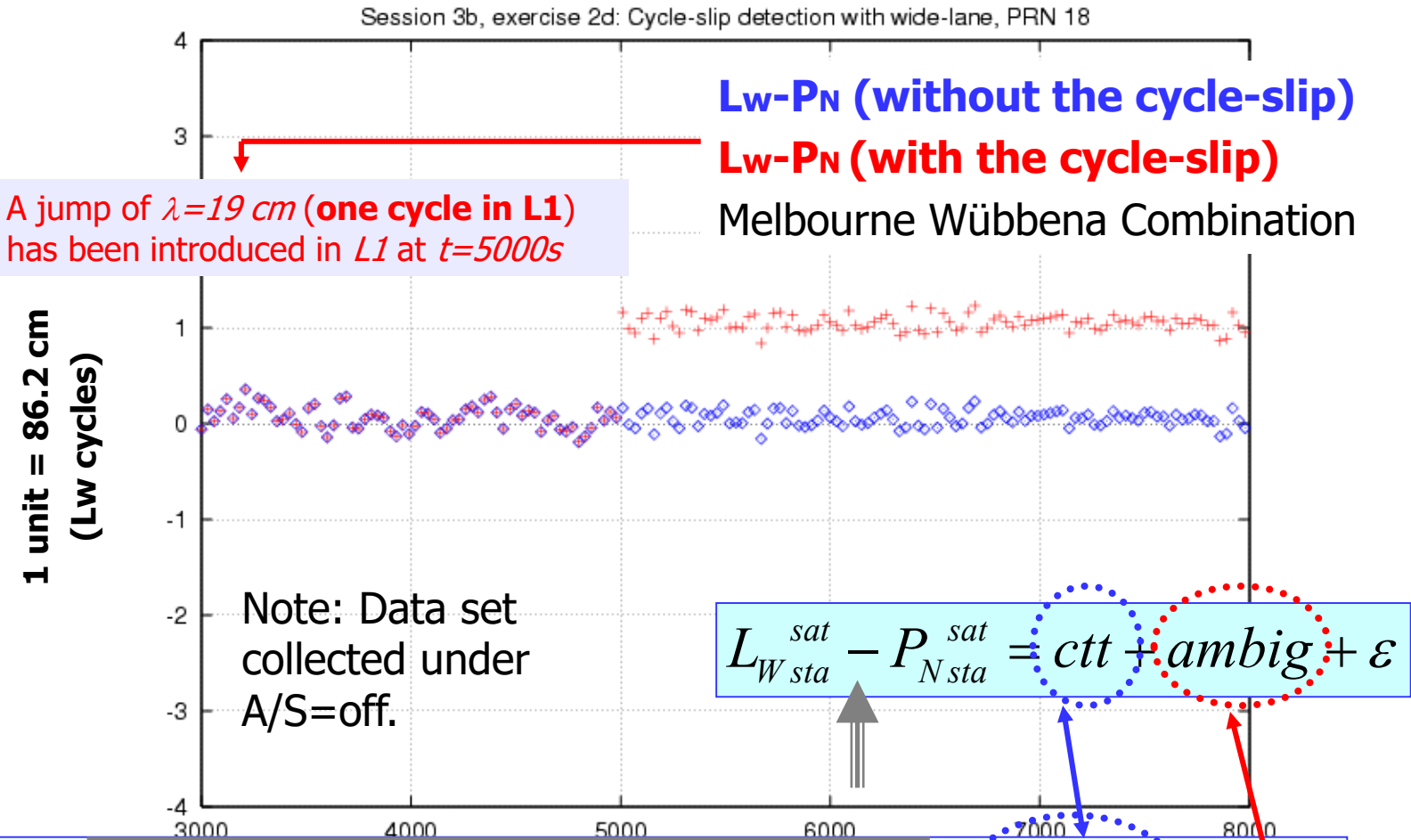
The geometry, clock offsets and iono have been removed.

There is a constant pattern plus noise. The P_I code noise also shadows the cycle-slip, and without the reference (in blue), the time where the cycle-slip happens could not be identified.



The geometry, clock offsets and iono have been removed.

There is a constant pattern plus noise. The P_N code noise is under one cycle of L_w . Thence, the cycle-slip is clearly detected

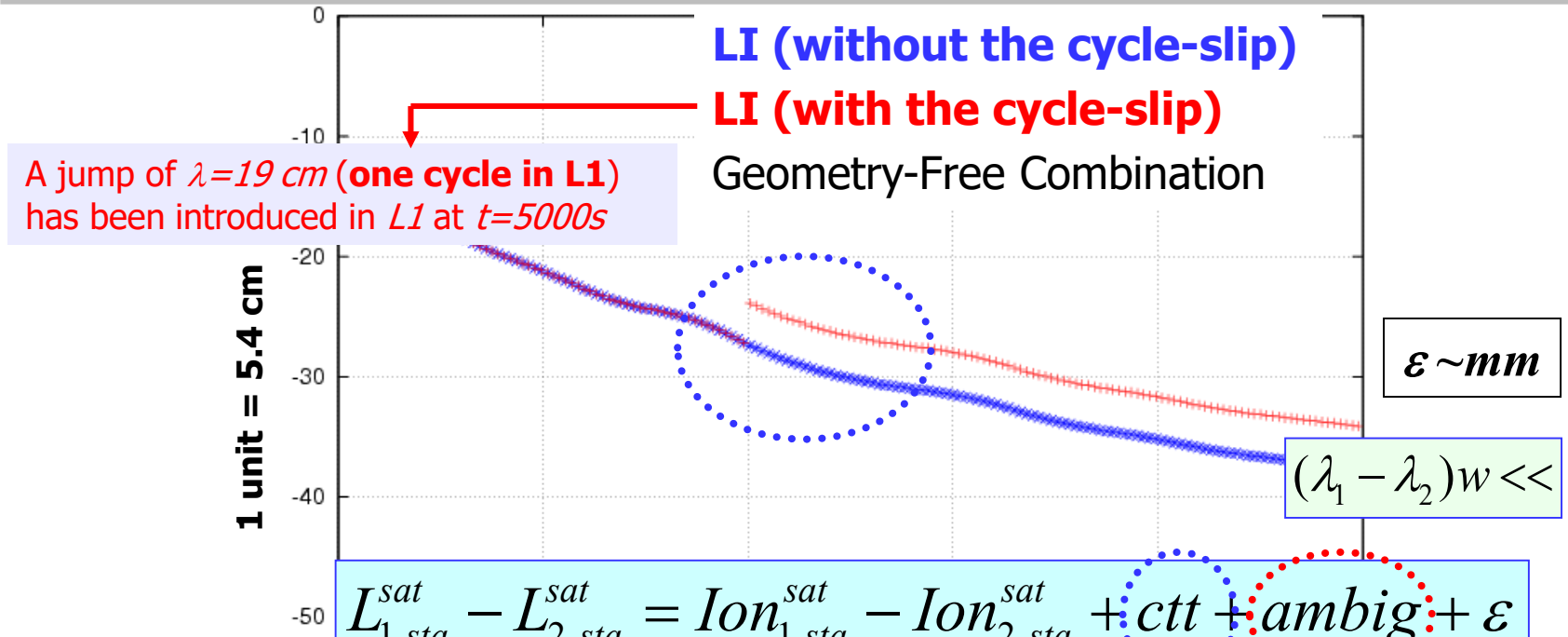


$$P_{Nsta}^{sat} = \rho_{sta}^{sat} + c \cdot (dt_{sta} - dt^{sat}) + Trop_{sta}^{sat} + Ion_{wsta}^{sat} + K_{wsta} + K_w^{sat} + \epsilon_N$$

$$L_{Wsta}^{sat} = \rho_{sta}^{sat} + c \cdot (dt_{sta} - dt^{sat}) + Trop_{sta}^{sat} + Ion_{wsta}^{sat} + b_{wsta} + b_w^{sat} + \lambda_w N_{wsta}^{sat} + v_w$$

The geometry and clock offsets have been removed.

The trend is due to the Iono. The L_I carrier noise is few mm, and the variation of the ionosphere in 1 second is lower than $\lambda_1 = 19 \text{ cm}$. Thence, the cycle-slip is detected.



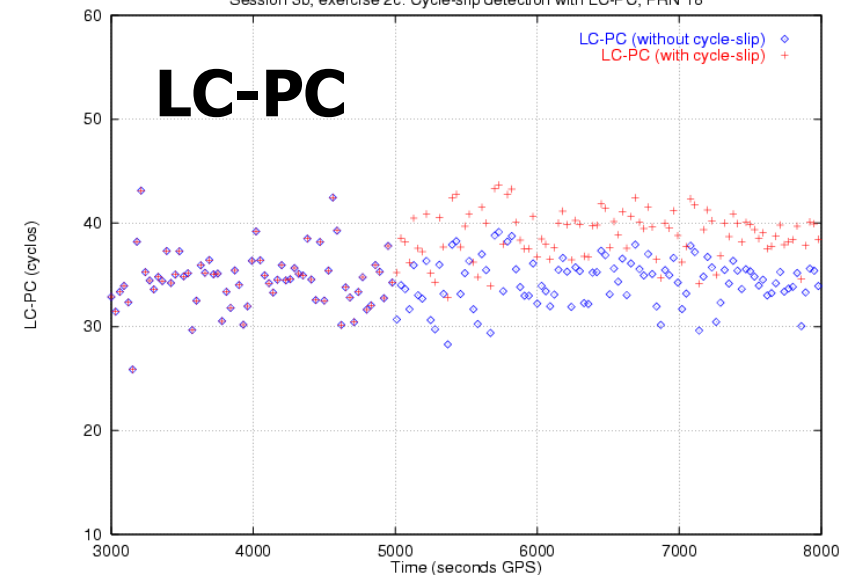
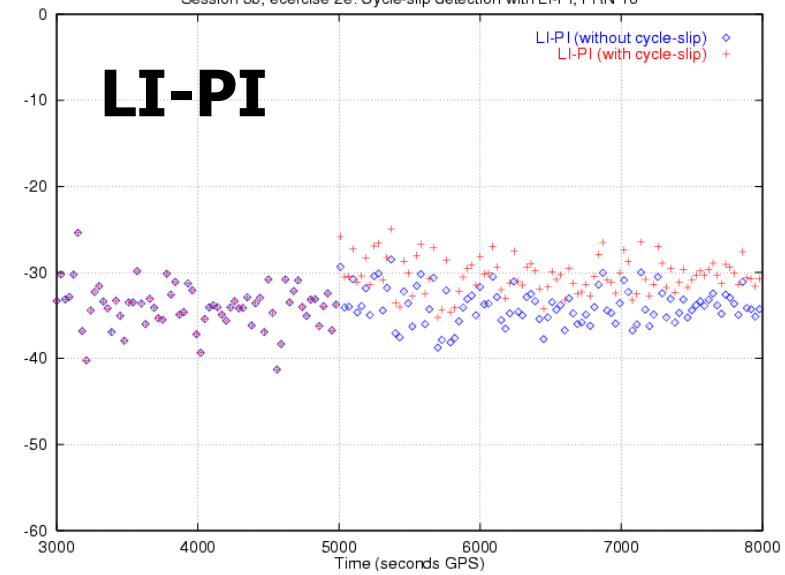
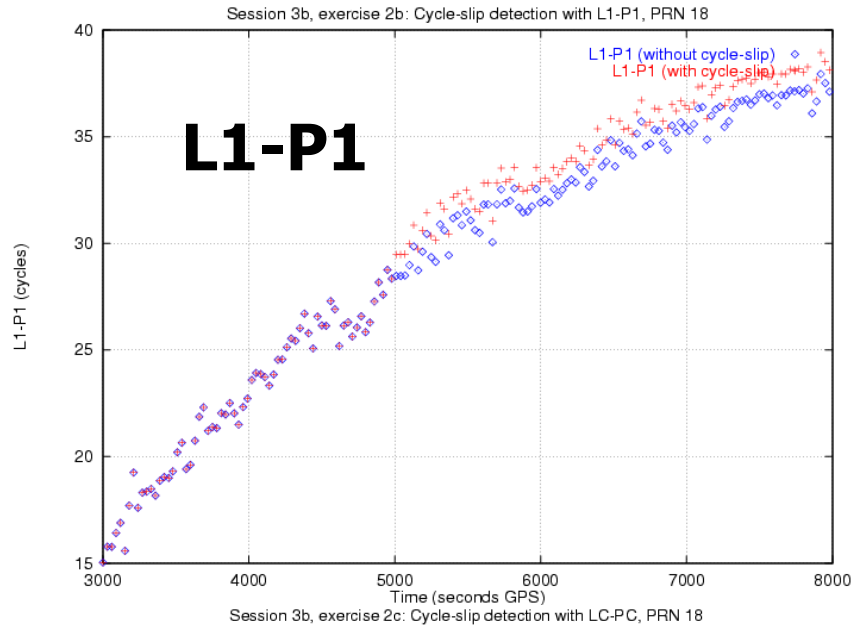
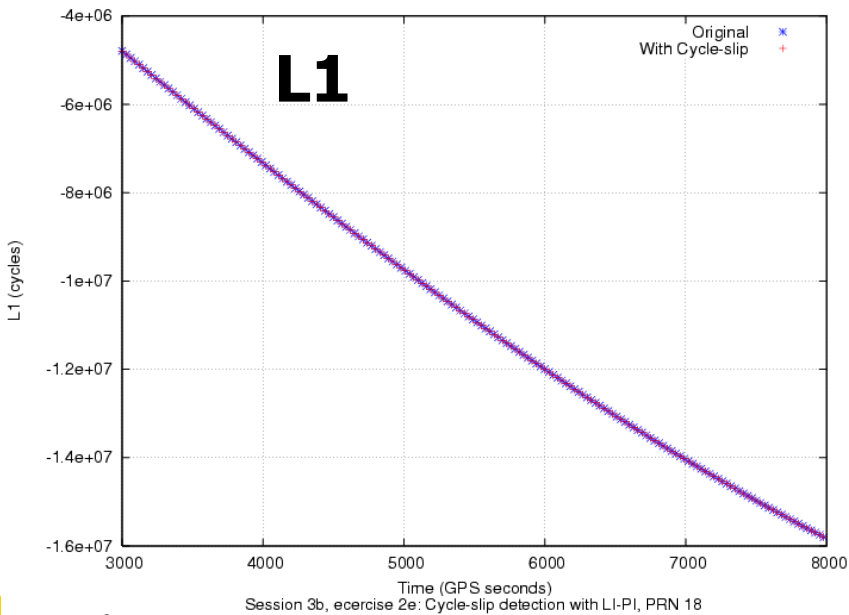
$$L_{1,\text{sta}}^{\text{sat}} = \rho_{\text{sta}}^{\text{sat}} + c \cdot (dt_{\text{sta}} - dt^{\text{sat}}) + \text{Trop}_{\text{sta}}^{\text{sat}}$$

$$L_{2,\text{sta}}^{\text{sat}} = \rho_{\text{sta}}^{\text{sat}} + c \cdot (dt_{\text{sta}} - dt^{\text{sat}}) + \text{Trop}_{\text{sta}}^{\text{sat}}$$

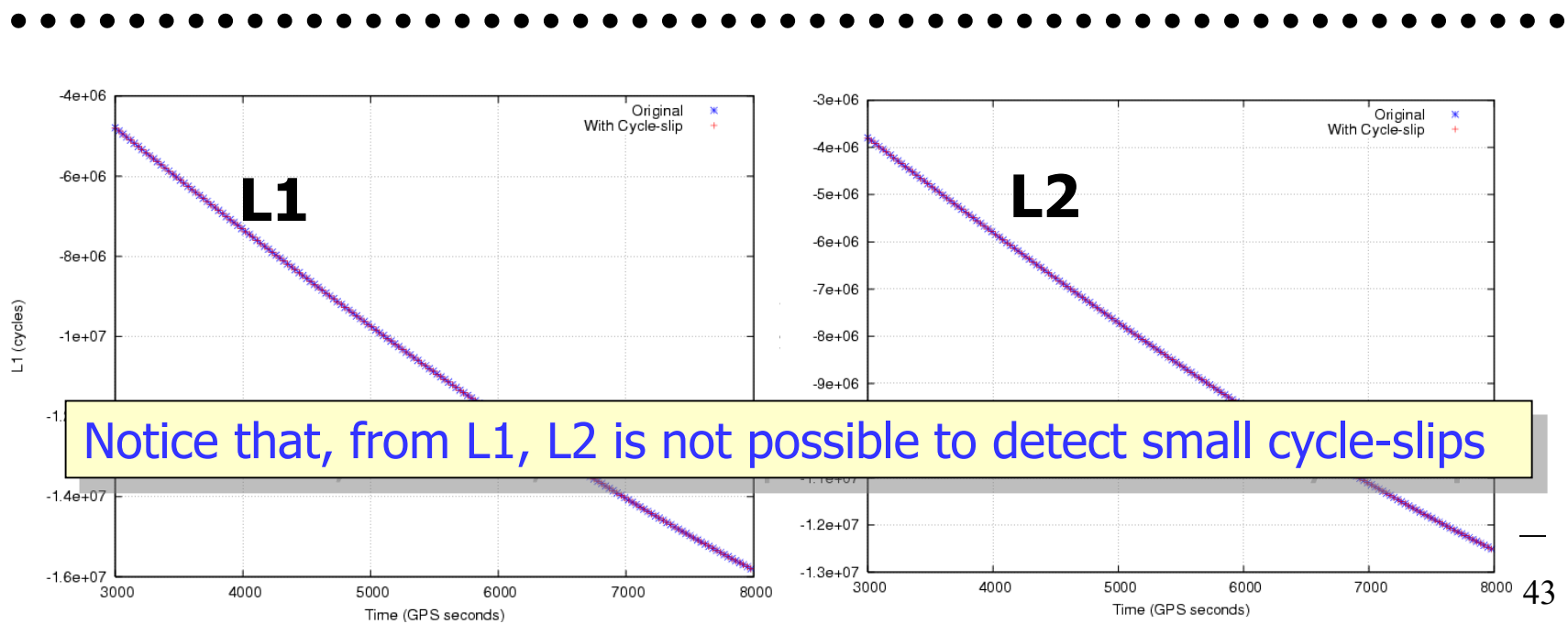
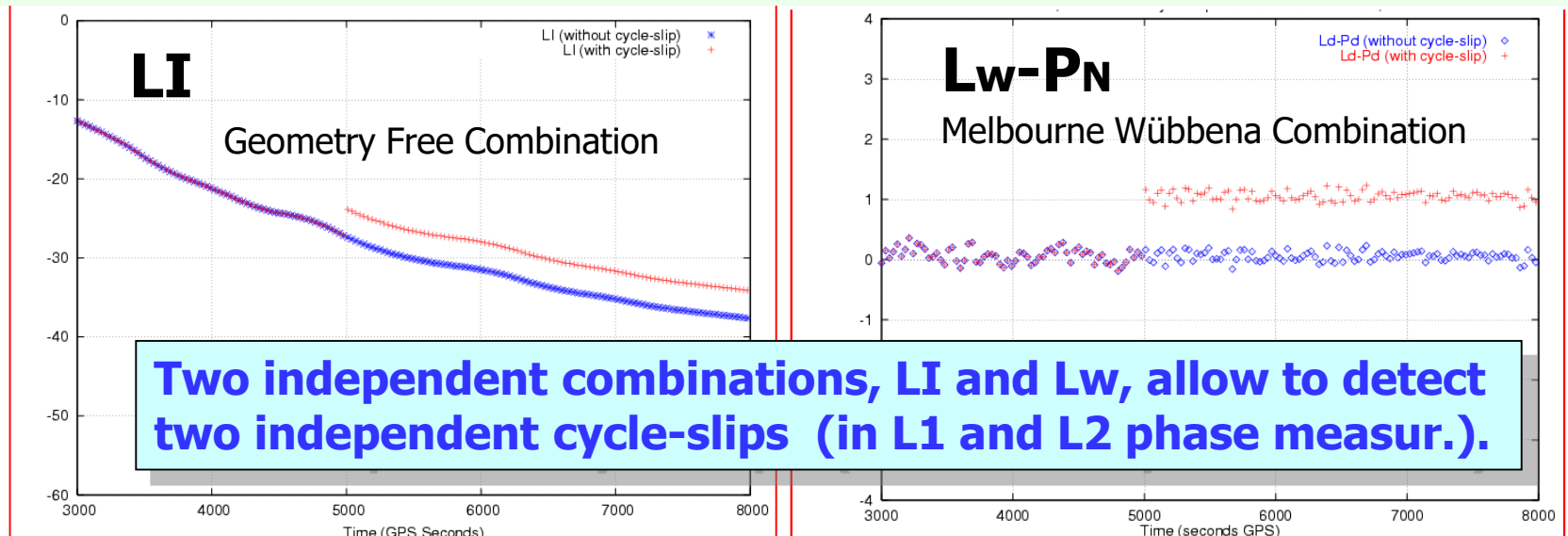
$$- \text{Ion}_{1,\text{sta}}^{\text{sat}} + b_{1,\text{sta}} + b_1^{\text{sat}} + \lambda_1 N_{1,\text{sta}}^{\text{sat}} + \lambda_1 w_{\text{sta}}^{\text{sat}} + v_1$$

$$- \text{Ion}_{2,\text{sta}}^{\text{sat}} + b_{2,\text{sta}} + b_2^{\text{sat}} + \lambda_2 N_{2,\text{sta}}^{\text{sat}} + \lambda_2 w_{\text{sta}}^{\text{sat}} + v_2$$

Summary



The cycle-slips are detected by the Ionospheric combination (LI=L1-L2) and the Melbourne Wübbena (MW=Lw-Pn)



Summary of Cycle-slip detectors

COMBINATION	MEAS	Combination Noise (σ)	λ	σ/λ
L_I-P_I	$-2 \cdot Ion + K + \lambda_I \cdot N_I$	$\sigma_{LI-PI} \approx \sigma_{PI} = 30 \text{ cm}$	$\lambda_I = 19.0 \text{ cm}$	1.58
L_c-P_c	$k_c + \lambda_N \cdot R_c$	$\sigma_{LC-PC} \approx \sigma_{PC} = 2.98 \sigma_P = 89 \text{ cm}$	$\lambda_N = 10.7 \text{ cm}$	8.32
L_I-P_I	$k_I + \lambda_I \cdot N_I - \lambda_2 \cdot N_2$	$\sigma_{LI-PI} \approx \sigma_{PI} = \sqrt{2} \sigma_P = 42 \text{ cm}$	$\lambda_2 - \lambda_I = 5.4 \text{ cm}$	7.78
L_W-P_N	$\lambda_W \cdot N_w$	$\sigma_{LW-PN} \approx \sigma_{PN} = \sigma_P / \sqrt{2} = 21 \text{ cm}$	$\lambda_W = 86.2 \text{ cm}$	0.25
L_I	$Ion + k_I + \lambda_I \cdot N_I - \lambda_2 \cdot N_2$	$\sigma_{LI} = \sqrt{2} \sigma_{PI} = 3 \text{ mm}$	$\lambda_2 - \lambda_I = 5.4 \text{ cm}$	0.06

Contents

1. Review of GNSS measurements.
2. Linear combinations of measurements.
3. Carrier cycle-slips detection.

3.1 Cycle-slip Detection Algorithms

Cycle-slip detector based on carrier phase data: The Geometry-free combination

Input data: Geometry-free combination of carrier phase measurements

$$L_I = L_1(s; k) - L_2(s; k)$$

Output: [satellite, time, cycle-slip flag].

For each epoch (k)

For each tracked satellite (s)

- Declare cycle slip when data gap greater than $tol_{\Delta t}$.¹⁶
- Fit a second-degree polynomial $p(s; k)$ to the previous values (after the last cycle-slip) $[L_I(s; k - N_I), \dots, L_I(s; k - 1)]$.
- Compare the measured $L_I(s; k)$ and the predicted value $p(s; k)$ at epoch k . If the discrepancy exceeds a given *threshold*, then declare cycle slip. That is,

if $|L_I(s; k) - p(s; k)| > threshold$ then cycle slip.

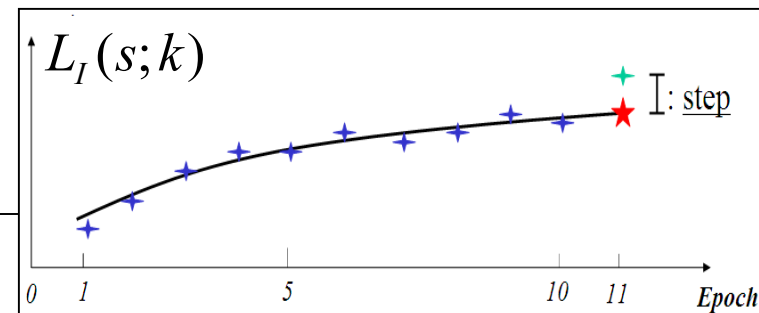
- Reset algorithm after cycle slip.

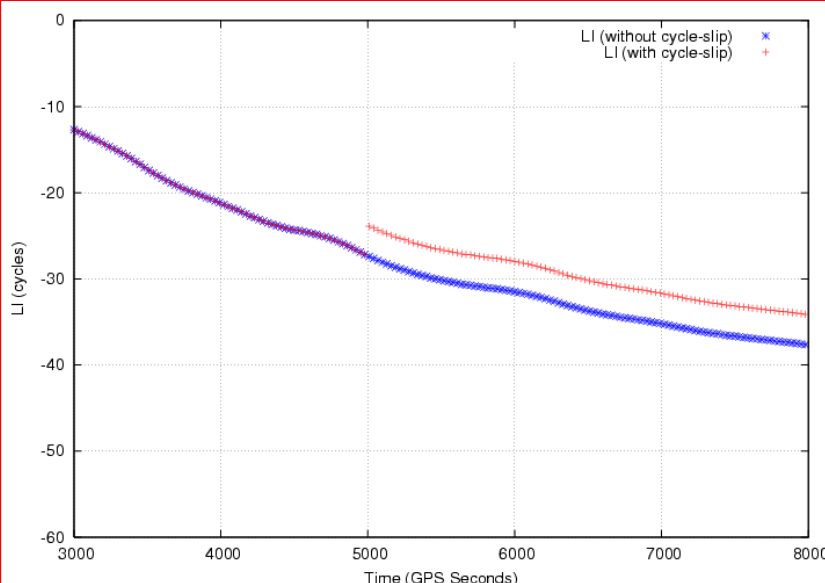
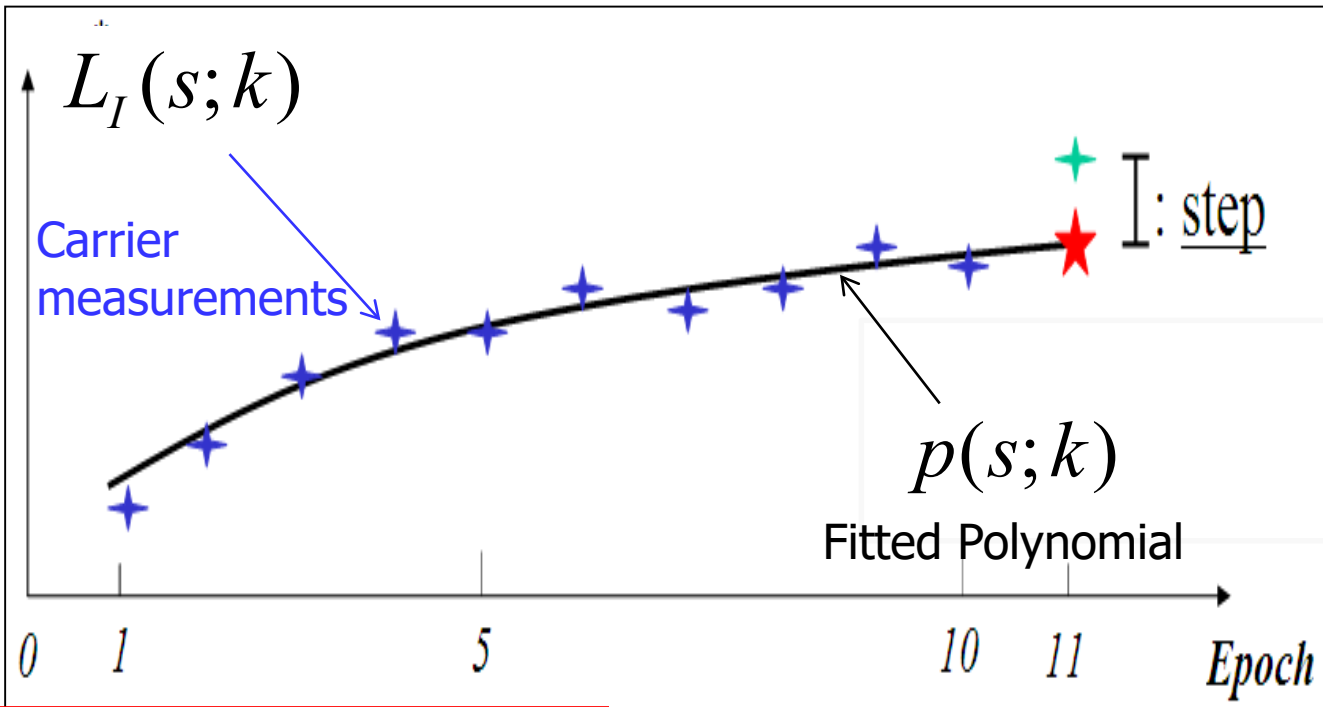
End

End

The detection is based on fitting a second order polynomial over a sliding window of N_I samples.

The predicted value is compared with the observed one to detect cycle-slip.





Under not disturbed ionospheric conditions,
**the geometry-free combination performs as a
very precise and smooth test signal,
driven by the ionospheric refraction.**

Although, for instance, the jump produced by a simultaneous one-cycle slip in both signals is smaller in this combination than in the original signals ($\lambda_2 - \lambda_1 = 5.4\text{cm}$), it can provide reliable detection even for small jumps

Cycle-slip detector based on code and carrier phase data: The Melbourne-Wübbena combination

Input data: Melbourne-Wübbena combination

$$B_W = L_W - P_N = \lambda_W N_W + \varepsilon$$

Output: [satellite (PRN), time, cycle-slip flag]

For each epoch (k)

For each tracked satellite (s)

The detection is based on real-time computation of mean (m_{BW}) and sigma (S_{BW}) values of the measurement test data B_W .

- Declare cycle-slip when data hole greater than $tol_{\Delta t}$ (e.g., 60 s).
- If no data hole larger than $tol_{\Delta t}$, thence:
- Compare the measurement $B_W(s; k)$ at the epoch k with the mean bias $m_{BW}(s; k - 1)$ computed from the previous values. If the discrepancy is over a $threshod = K_{factor} * S_{BW}$ (e.g., $K_{factor} = 4$), declare cycle-slip. That is:

If $|B_W(s; k) - m_{BW}(s; k - 1)| > K_{factor} S_{BW}(s; k - 1)$,

Thence, cycle-slip.

- Update the mean and sigma values according to the equations:

$$\begin{aligned} m_{BW}(s; k) &= \frac{k-1}{k} m_{BW}(s; k-1) + \frac{1}{k} B_W(s; k) \\ S_{BW}^2(s; k) &= \frac{k-1}{k} S_{BW}^2(s; k-1) + \frac{1}{k} (B_W(s; k) - m_{BW}(s; k-1))^2 \end{aligned} \quad (4.24)$$

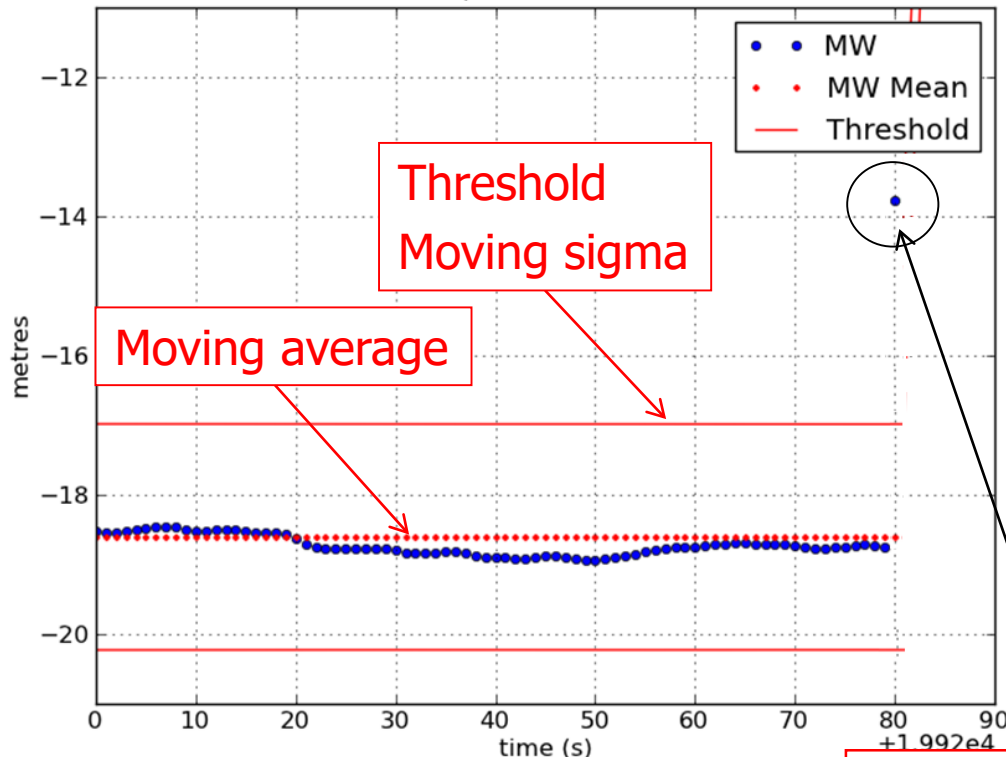
Note the S_{BW} is initialised with an a priori $S_0 = \lambda_w / 2$.

End

End

A cycle-slip is declared when the measurement differs form the mean value by a predefined number of standard deviations (S_{BW})

Session A.1, Ex10c: MW CS PRN03

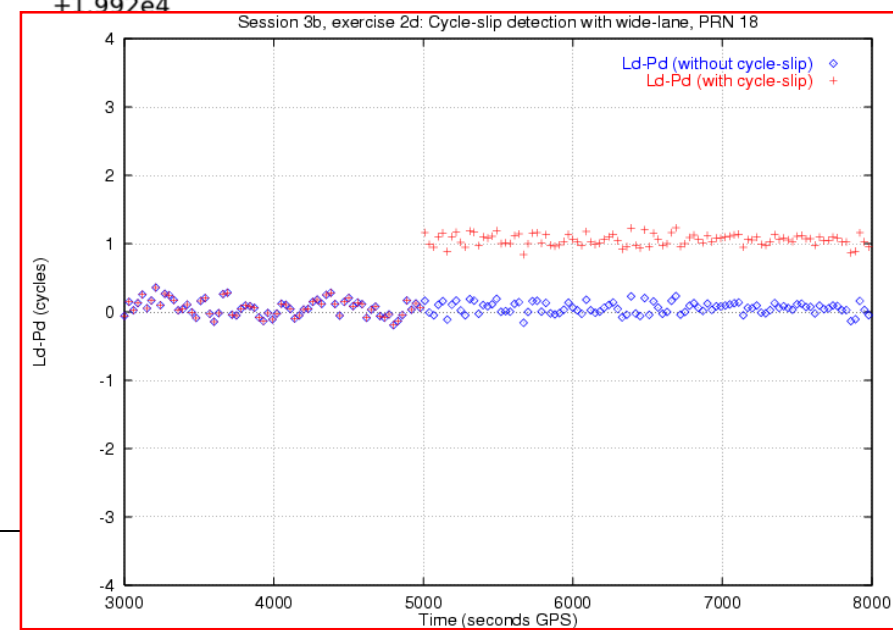


Nevertheless, in spite of these benefits, the performance is worse than in the previous carrier-phase-only based detector and it is used as a secondary test.

The Melbourne-Wübbena combination has a double benefit:

- The enlargement of the ambiguity spacing, thanks to the larger wavelength $\lambda_W = 86.2\text{cm}$.
- The noise is reduced by the narrow-lane combination of code measurement

Cycle-slip detection



Exercises:

- 1) Show that $\Delta N_1 = 9$ and $\Delta N_2 = 7$ produces jumps of few millimetres in the geometry-free combination.
- 2) Show that no jump happens in the geometry-free combination when $\Delta N_1 / \Delta N_2 = 77 / 60$. In particular when $\Delta N_1 = 77$ and $\Delta N_2 = 60$ the jump in the wide-lane combination is: $17\lambda_W = 15m$

Hint: Consider the following relationships (from [RD-1]):

The effect of a jump in the integer ambiguities in terms of ΔN_1 , ΔN_2 and N_W is given next:

$\Delta\Phi_w$, $\Delta\Phi_I$, $\Delta\Phi_C$ variations

$$\Delta\Phi_w = \lambda_W \Delta N_W = \lambda_W (\Delta N_1 - \Delta N_2) \quad (4.20)$$

$$\Delta\Phi_I = \lambda_1 \Delta N_1 - \lambda_2 \Delta N_2 = (\lambda_2 - \lambda_1) \Delta N_1 + \lambda_2 \Delta N_W$$

$$\Delta\Phi_C = \lambda_N \left(\frac{\lambda_W}{\lambda_1} \Delta N_1 - \frac{\lambda_W}{\lambda_2} \Delta N_2 \right) = \lambda_N \left(\Delta N_1 + \frac{\lambda_W}{\lambda_2} \Delta N_W \right)$$

Example of Single frequency Cycle-slip detector

Input data: Code pseudorange (P_1) and carrier phase (L_1) measurements.

Output: [satellite (PRN), time, cycle-slip flag]

For each epoch (k)

For each tracked satellite (s)

- Declare cycle-slip when data hole greater than $tol_{\Delta t}^{24}$.
- If no data hole larger than $tol_{\Delta t}$, thence:
- Update an array with the last N differences of

$$d(s; k) = L_1(s; k) - P_1(s; k)$$

That is: $[d(s; k - N), \dots, d(s; k - 1)]$

- Compute the mean and sigma discrepancy over the previous N samples $[k - N, \dots, k - 1]$:

$$\begin{aligned} m_d(s; k - 1) &= \frac{1}{N} \sum_{i=1}^N d(s; k - i) \\ m_{d^2}(s; k - 1) &= \frac{1}{N} \sum_{i=1}^N d^2(s; k - i) \\ S_d(s; k - 1) &= \sqrt{m_{d^2}(s; k - 1) - m_d^2(s; k - 1)} \end{aligned} \quad (4.27)$$

- Compare the difference at the epoch k with the mean value of differences computed over the previous N samples window. If the value is over a threshold $= n_T * S_d$ (e.g., $n_T = 5$), declare cycle-slip²⁵.

That is:

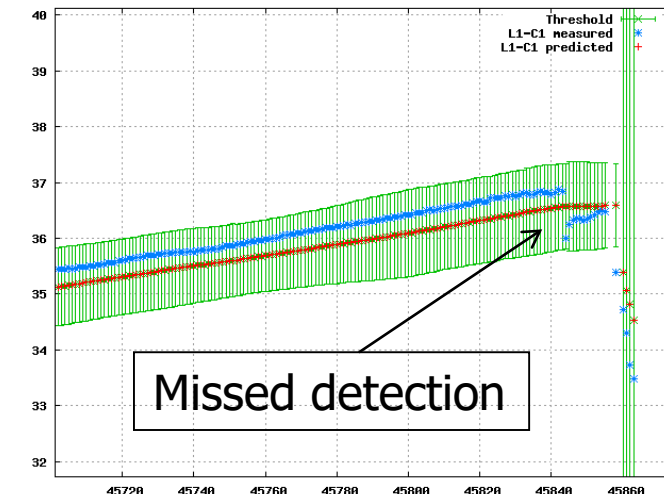
If $|d(s; k) - m_d(s; k - 1)| > n_T S_d(s; k - 1)$,
Thence, cycle-slip.

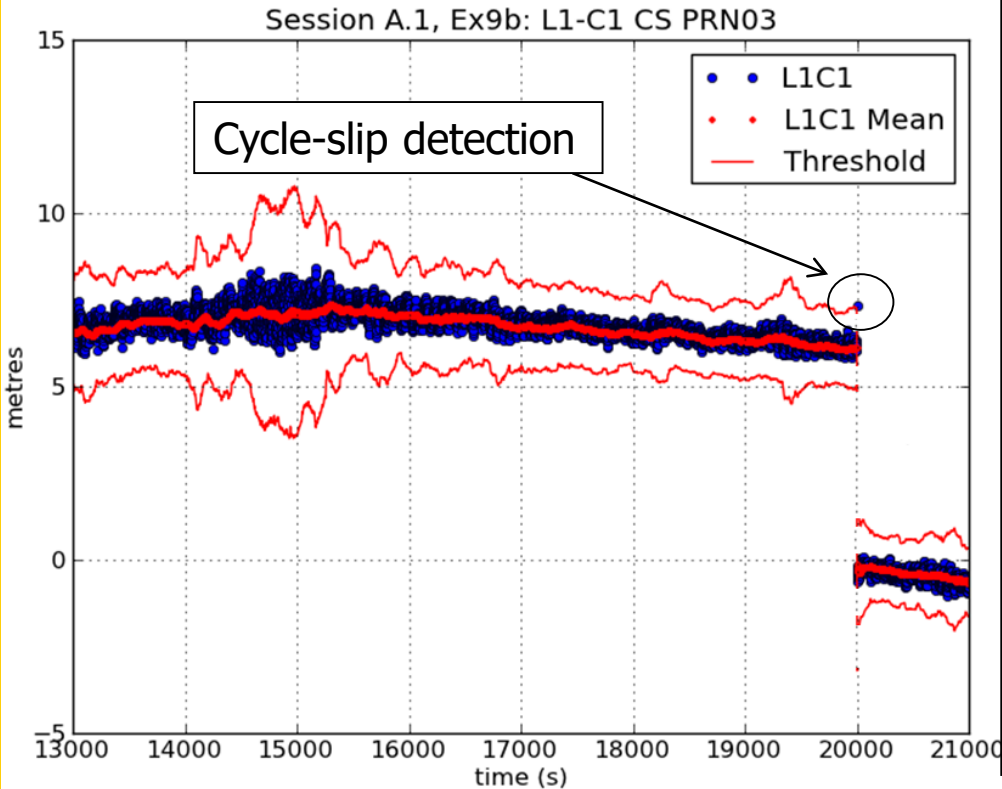
End

End

The detection is based on real-time computation of mean and sigma values of the differences ($d=L_1-P_1$) of the code pseudorange and carrier over a sliding window of N samples (e.g. $N=100$).

A cycle-slip is declared when a measurement differs from the mean bias value over a predefined threshold.



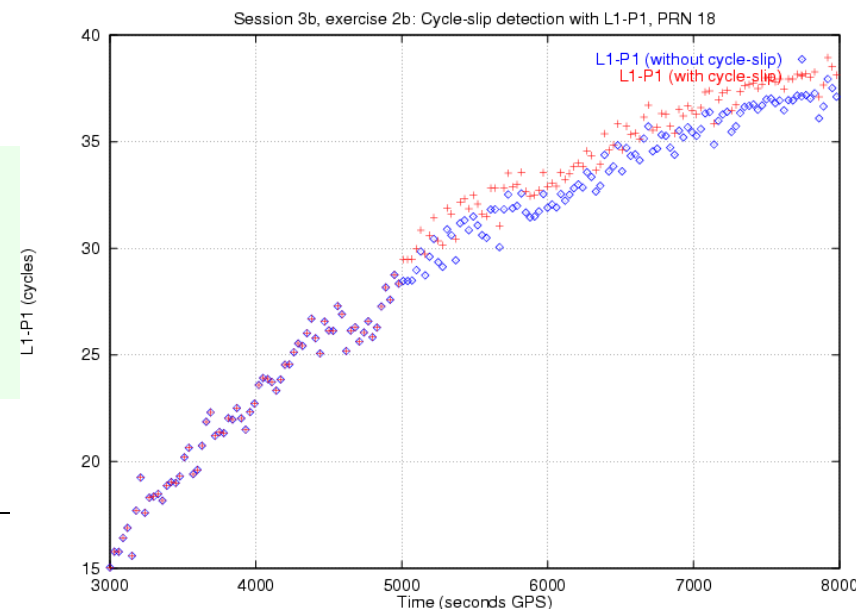


This detector is affected by the code pseudorange noise and multipath as well as the divergence of the ionosphere.

Higher sampling rate improves detection performance, but smalest jumps can still escape from this detector.

On the other hand, a minimum number of samples is needed for filter initialization in order to ensure a reliable value of sigma for the detection threshold

More details, exercises and examples of software code implementation of these detectors can be found in [RD-1] and [RD-2].



Contents

1. Review of GNSS measurements.
2. Linear combinations of measurements.
3. Carrier cycle-slips detection.
4. Carrier smoothing of code pseudorange.
5. Code Multipath.

Carrier smoothing of code pseudorange

The noisy (but unambiguous) code pseudorange can be smoothed with the precise (but ambiguous) carrier. A simple algorithm is given next:

Hatch filter:

$$\hat{P}(k) = \frac{1}{n} P(k) + \frac{n-1}{n} (\hat{P}(k-1) + L(k) - L(k-1))$$

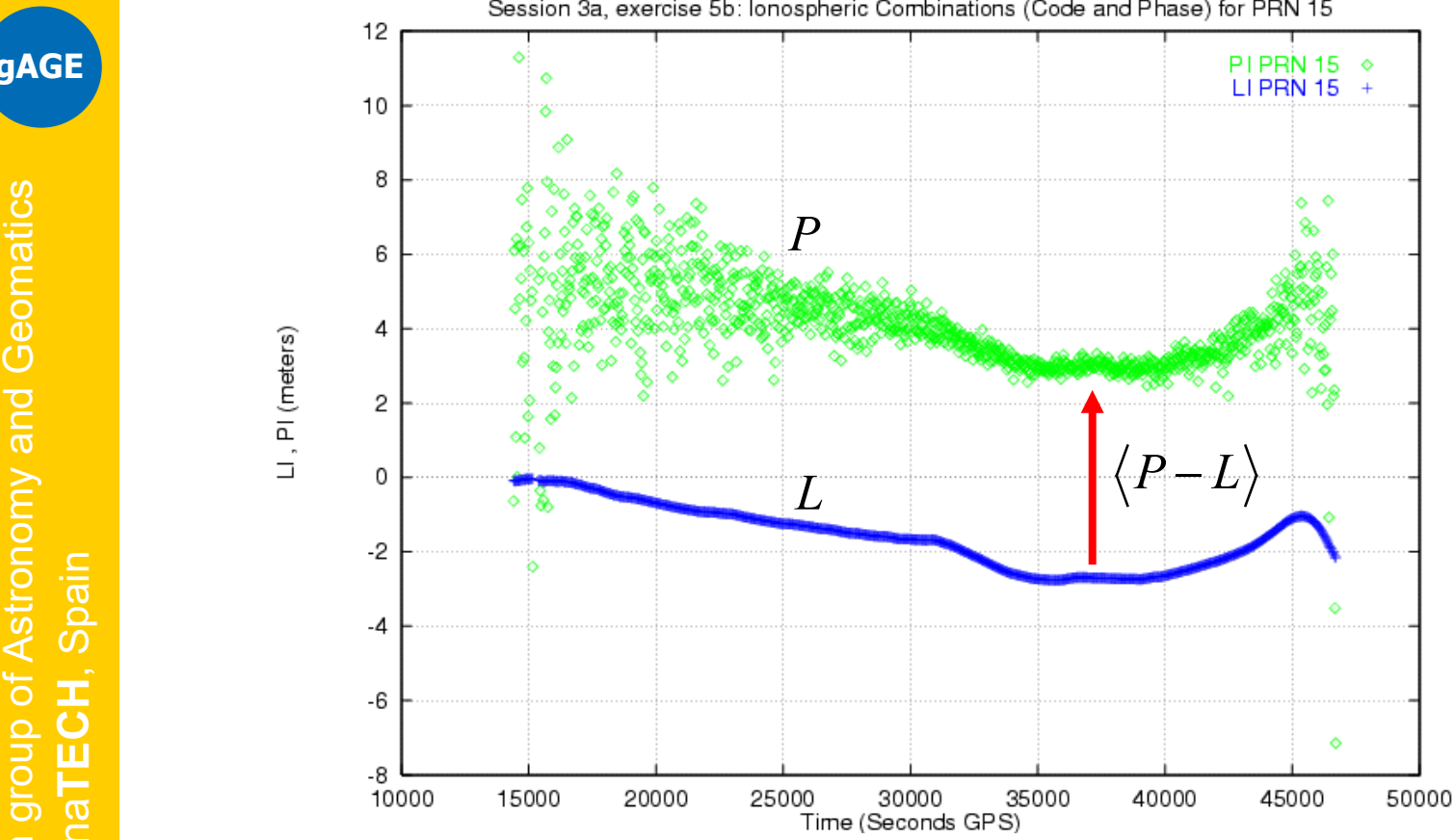
where $\hat{P}(1) = P(1)$ and

$$n = k; \quad k < N$$

$$n = N; \quad k \geq N$$

This algorithm can be interpreted as a real-time alignment of the carrier phase with the code measurement:

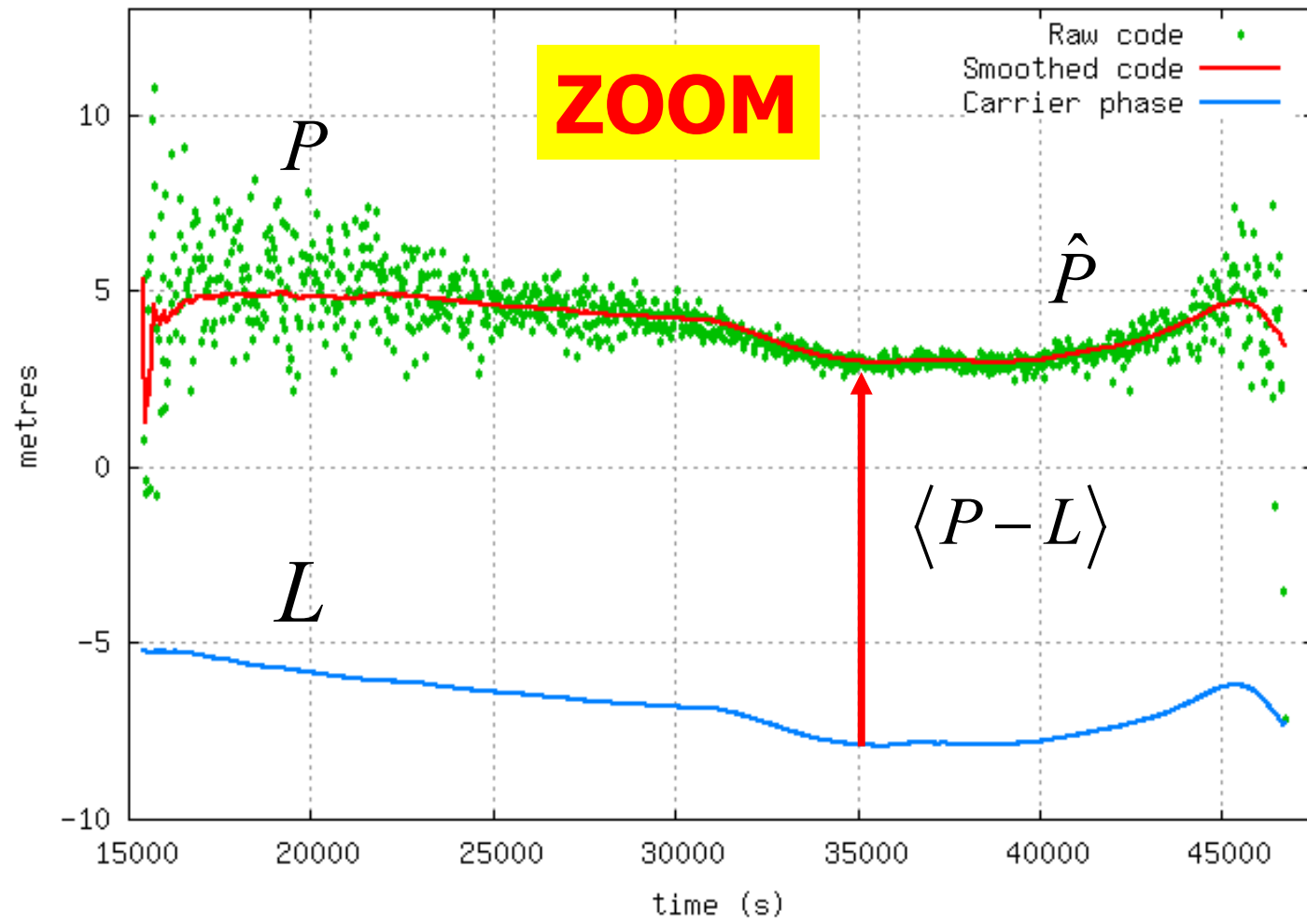
$$\hat{P}(k) = \frac{1}{n} P(k) + \frac{n-1}{n} (\hat{P}(k-1) + L(k) - L(k-1)) = L(k) + \langle P - L \rangle_{(k)}$$



This algorithm can be interpreted as a real-time alignment of the carrier phase with the code measurement:

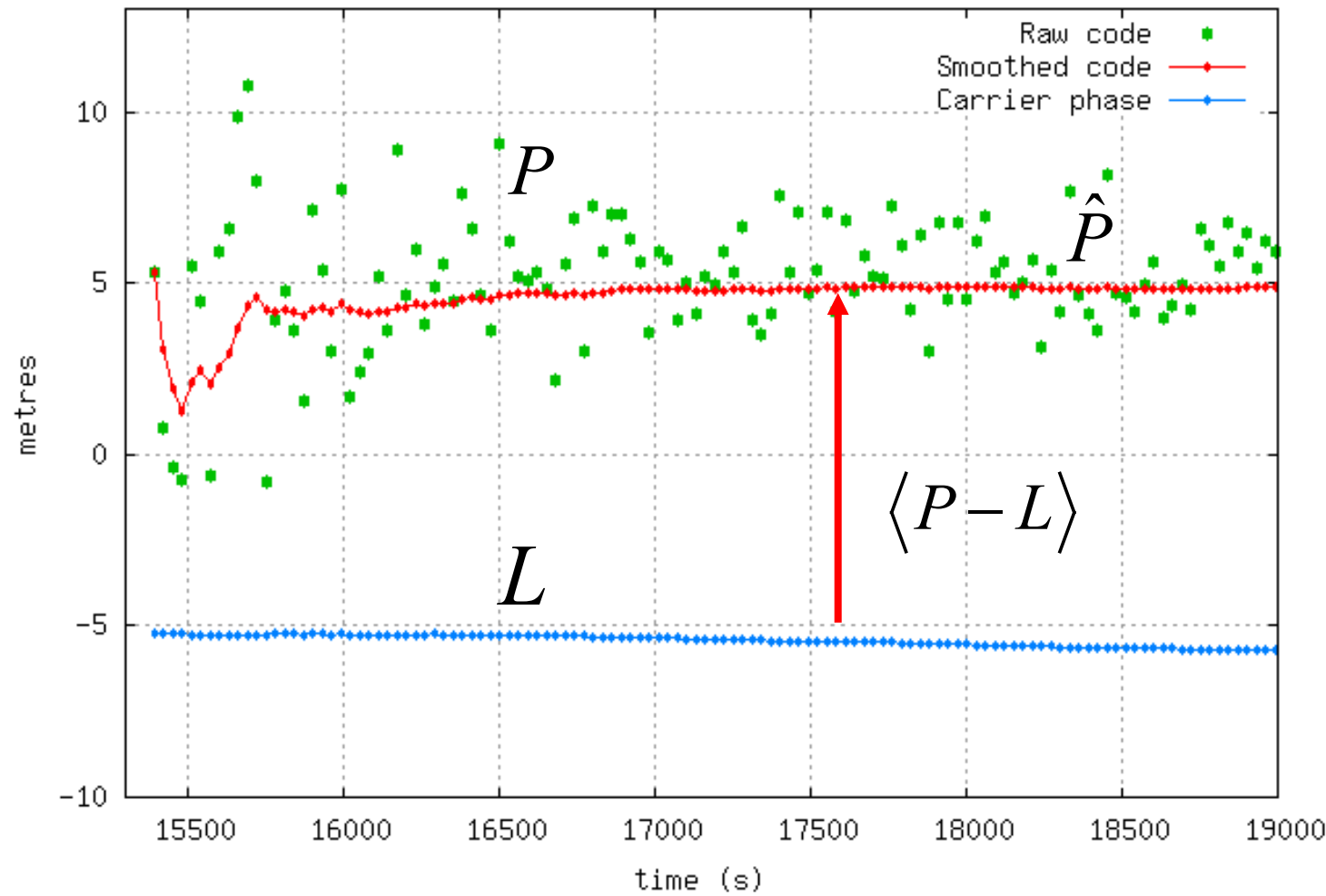
$$\hat{P}(k) = \frac{1}{n} P(k) + \frac{n-1}{n} (\hat{P}(k-1) + L(k) - L(k-1)) = L(k) + \boxed{\langle P - L \rangle_{(k)}}$$

Hatch filter: Carrier-smoothed code. N=100 epochs



$$\hat{P}(k) = \frac{1}{n} P(k) + \frac{n-1}{n} (\hat{P}(k-1) + L(k) - L(k-1)) = L(k) + \langle P - L \rangle_{(k)}$$

Hatch filter: Carrier-smoothed code. N=100 epochs



$$\hat{P}(k) = \frac{1}{n} P(k) + \frac{n-1}{n} (\hat{P}(k-1) + L(k) - L(k-1)) = L(k) + \boxed{\langle P - L \rangle_{(k)}}$$

Code-carrier divergence: SF smoother

Time varying ionosphere induces a bias in the single frequency (SF) smoothed code when it is averaged in the smoothing filter (Hatch filter).

Let:

$$P_1 = \rho + I_1 + \varepsilon_1$$

$$L_1 = \rho - I_1 + B_1 + \zeta_1$$

thence,

$$P_1 - L_1 = 2I_1 - B_1 + \varepsilon_1 \Rightarrow 2I_1 : \text{Code-carrier divergence}$$

Substituting $P_1 - L_1$ in Hatch filter equation

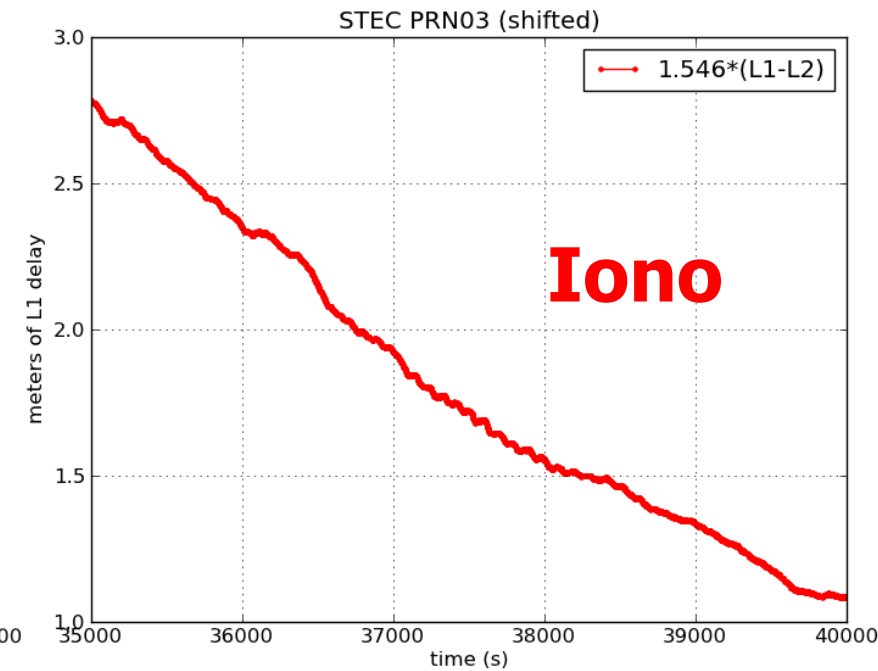
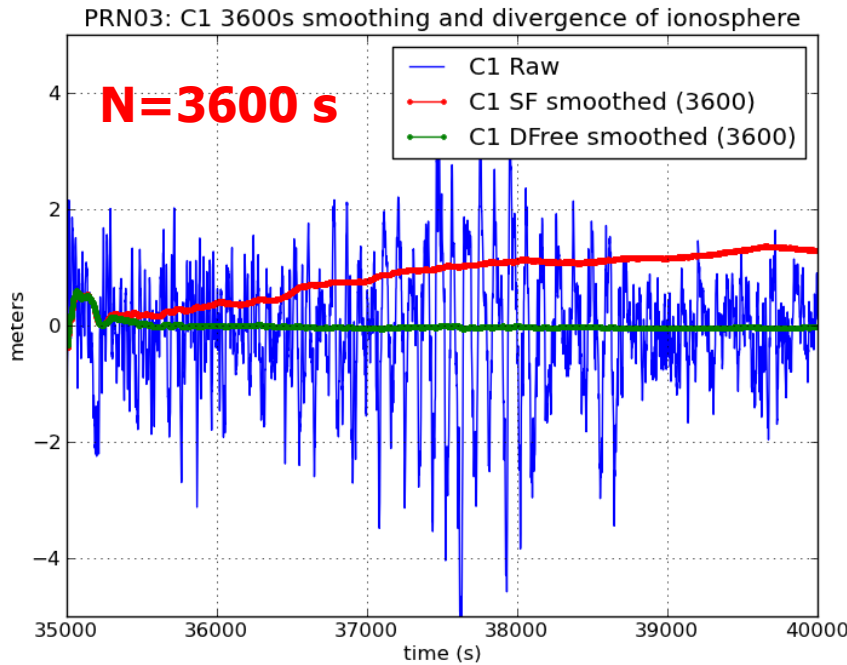
$$\begin{aligned} \hat{P}(k) &= L(k) + \langle P - L \rangle_{(k)} = \rho(k) - I_1(k) + B_1 + \langle 2I_1 - B_1 \rangle_{(k)} = \\ &= \rho(k) + I_1(k) + 2\left(\langle I_1 \rangle_{(k)} - I_1(k)\right) \end{aligned}$$

bias_I

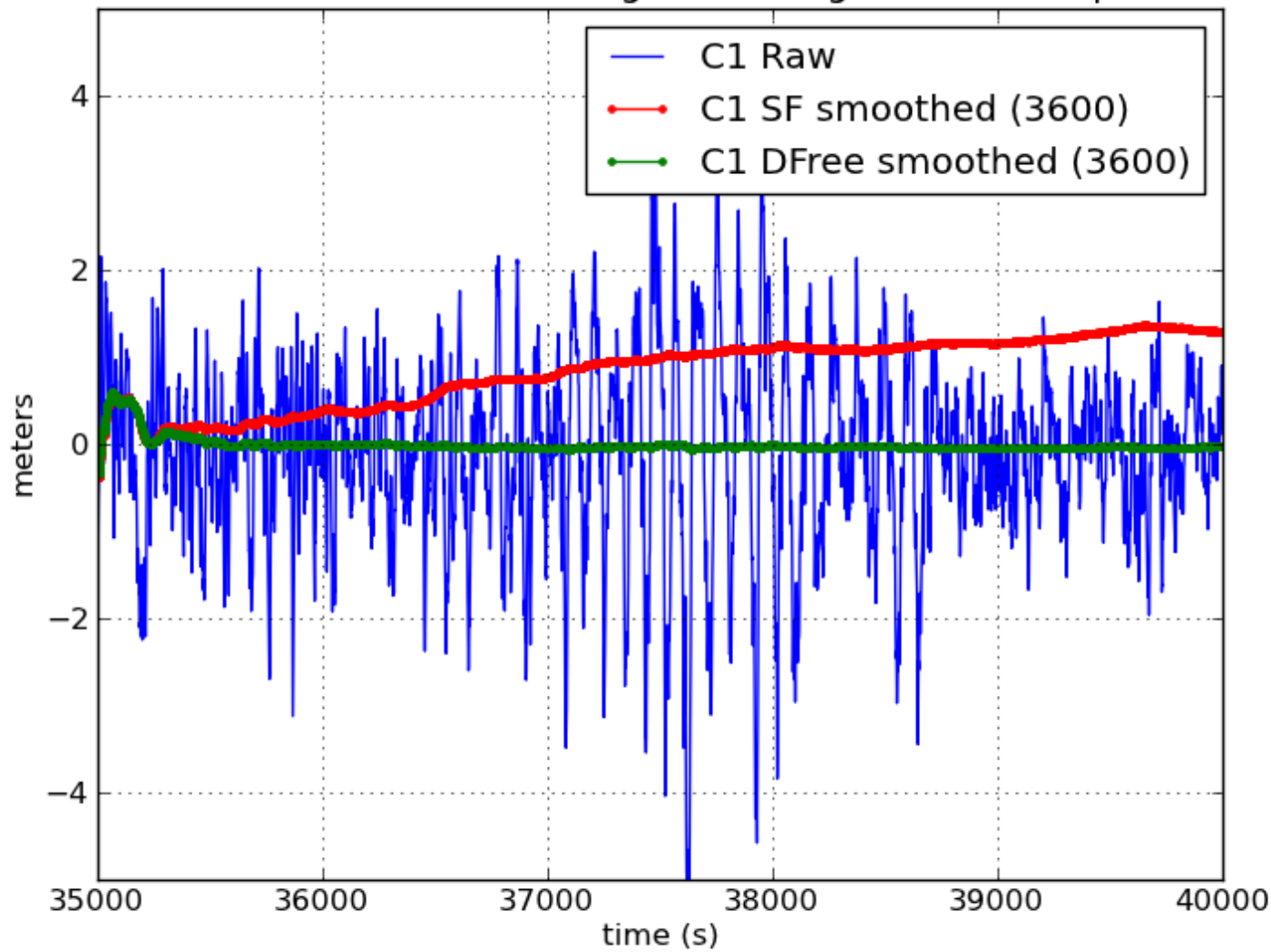
$$\Rightarrow \hat{P}_1 = \rho + I_1 + \text{bias}_I + v_1$$

where, being the ambiguity term B_1 a constant bias, thence $\langle B_1 \rangle_{(k)} \approx B_1$, and cancels in the previous expression.

where v_1 is the noise term after smoothing.

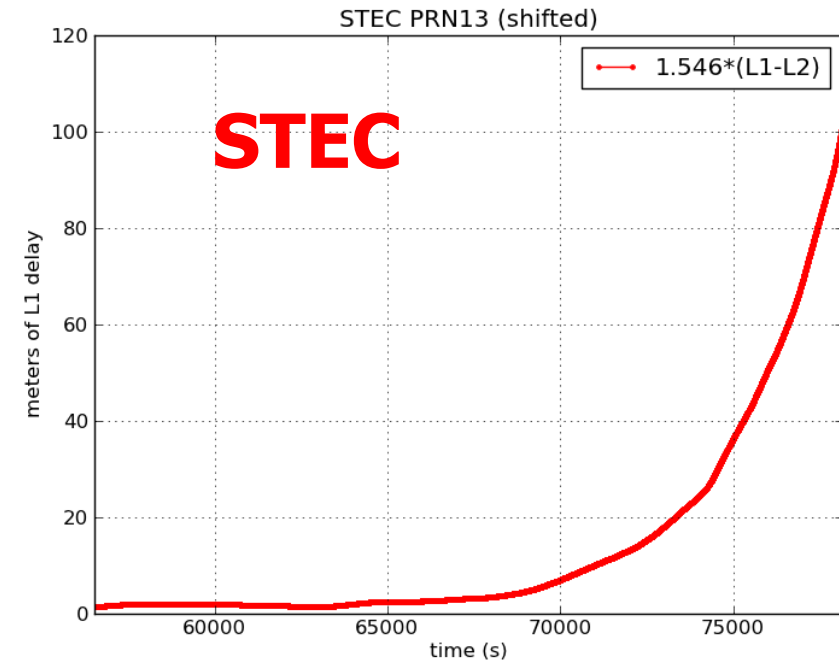
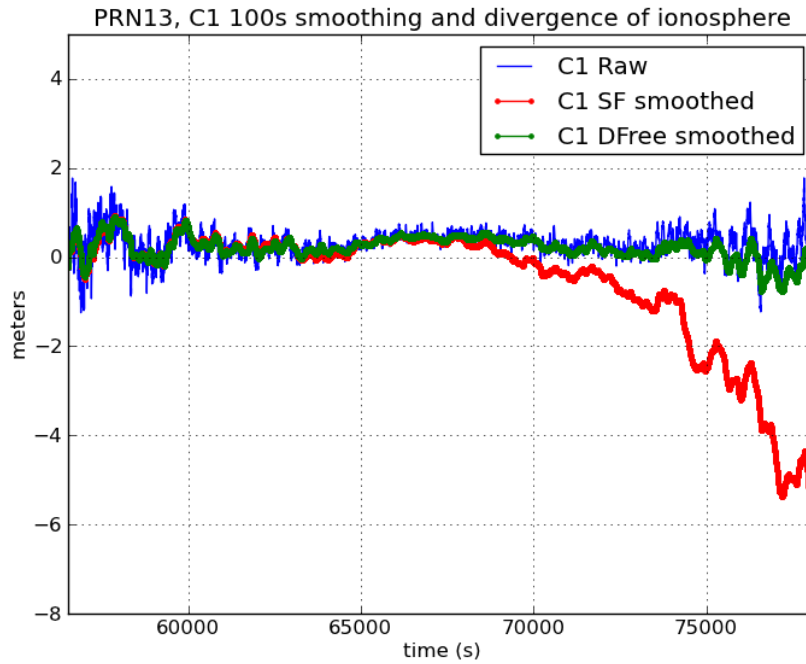


PRN03: C1 3600s smoothing and divergence of ionosphere



Halloween storm

Data File: amc23030.03o_1Hz



$N=100$ (i.e. filter smoothing time constant $\tau=100$ sec).

Halloween storm

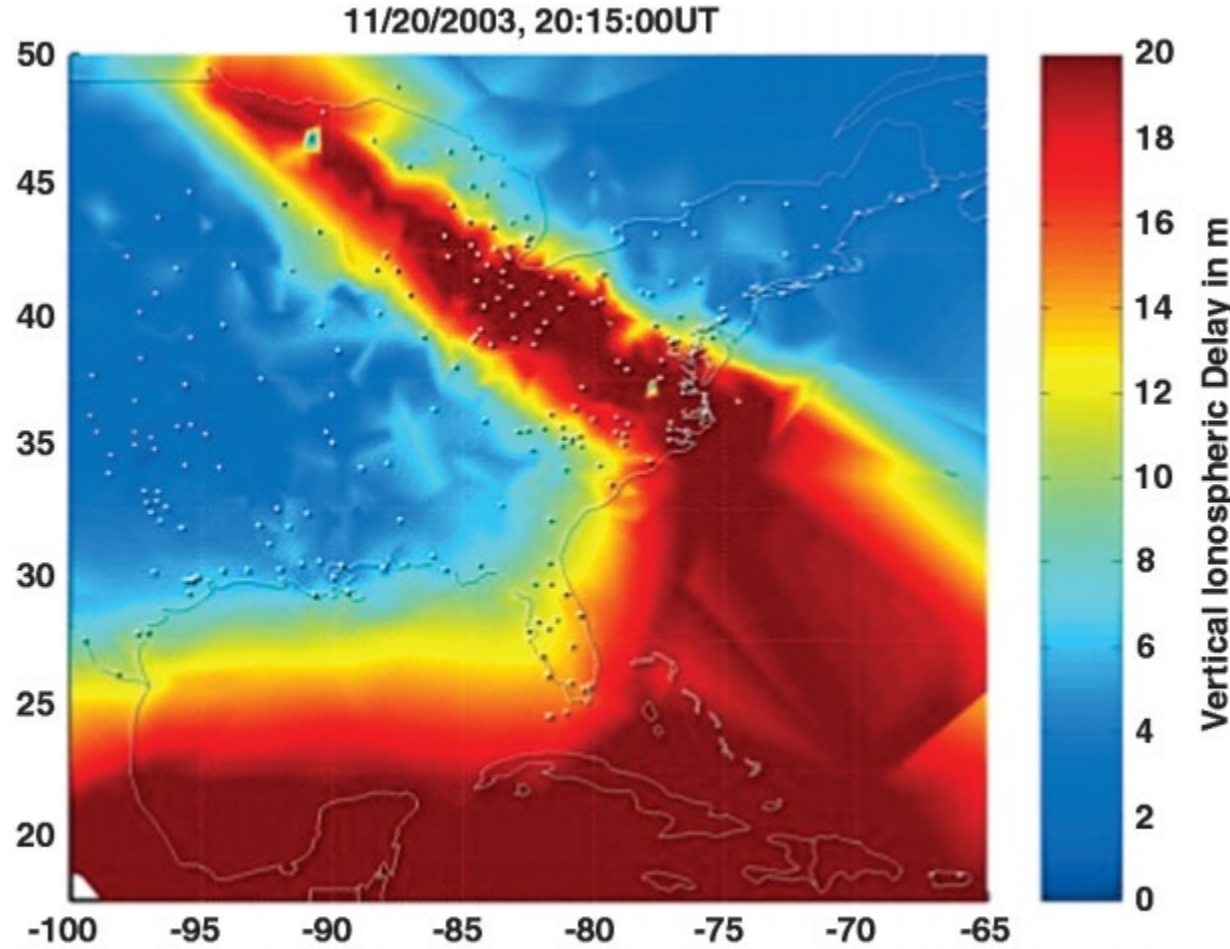


Fig. 2 Map of equivalent vertical ionospheric delay over eastern United States on 20 Nov. 2003 at 20:15 UT.

[*] **Ionospheric Threat Parameterization for Local Area Global-Positioning-System-Based Aircraft Landing Systems, Datta-Barua et al, Journal of Aircraft Vol. 47, No. 4, July–August 2010, DOI: 10.2514/1.46719**

Carrier-smoothed pseudorange: DFree

Divergence-Free (Dfree) smoother:

With two frequency **carrier** measurements **a combination of carriers** with the same ionospheric delay (the same sign) as the code can be generated:

$$L_{1,DF} = L_1 + 2\bar{\alpha}_1(L_1 - L_2) = \rho + I_1 + B_{1,DF} + \zeta_{1,DF}$$

$$\bar{\alpha}_1 = \frac{f_2^2}{f_1^2 - f_2^2} = \frac{1}{\gamma - 1} = 1.545$$
$$\gamma = \left(\frac{77}{60}\right)^2$$

With this new combination we have:

$$P_1 = \rho + I_1 + \varepsilon_1$$

$$L_{1,DF} = \rho + I_1 + B_{1,DF} + \zeta_{1,DF}$$

Thence,

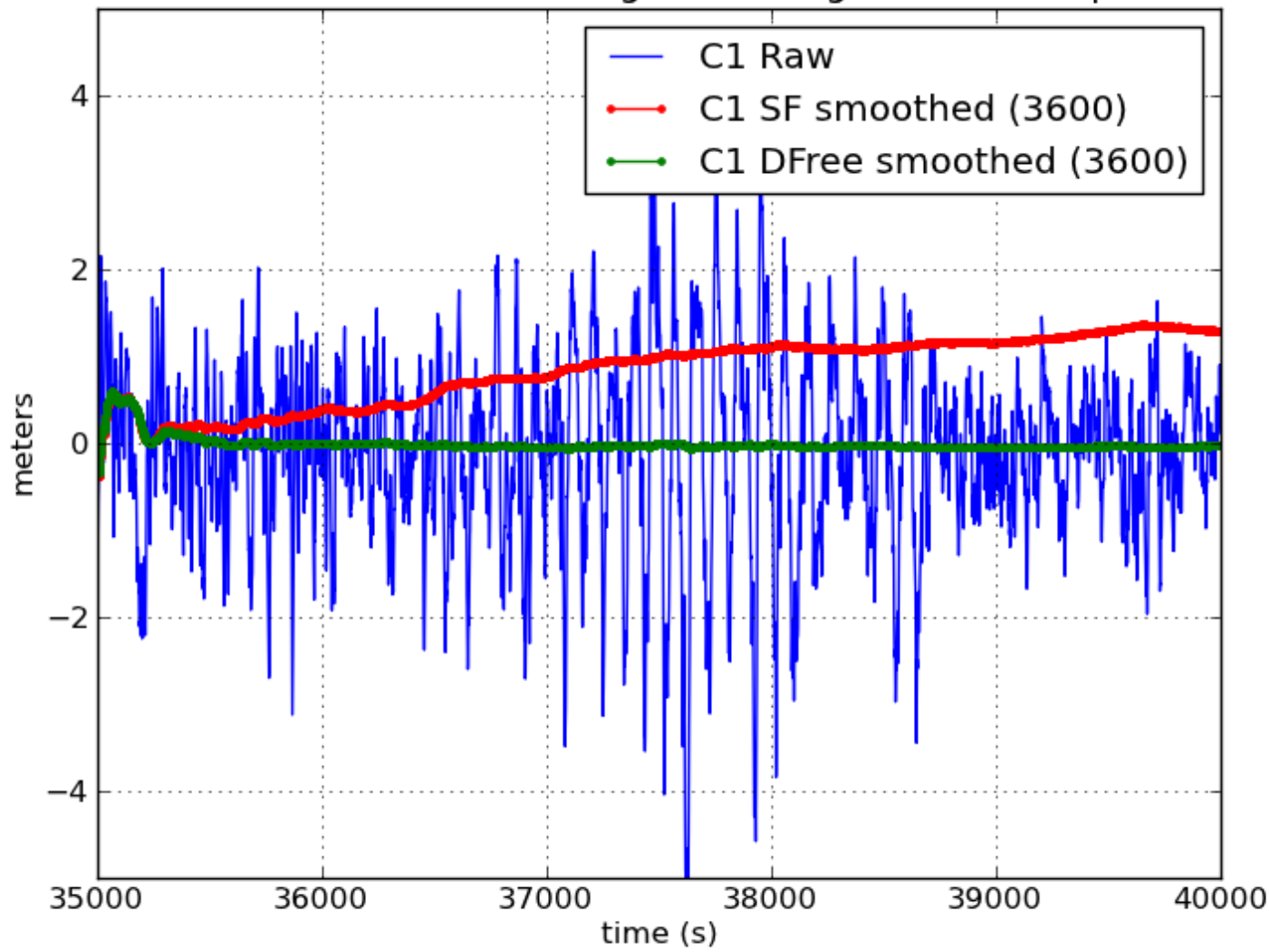
$$P_1 - L_{1,DF} = B_{1,DF} + \varepsilon_1$$

\Rightarrow No Code-carrier divergence!

This smoothed code is **immune to temporal gradients** (unlike the SF smoother), being the same ionospheric delay as in the original raw code (i.e. I_1). Nevertheless, as it is still affected by the ionosphere, its **spatial decorrelation** must be taken into account in differential positioning.

$$\Rightarrow \hat{P}_{1,DF} = \rho + I_1 + v_{12}$$

PRN03: C1 3600s smoothing and divergence of ionosphere



Carrier-smoothed pseudorange: IFree

Ionosphere-Free (Ifree) smoother:

Using both code and carrier dual-frequency measurements, it is possible to remove the frequency dependent effects using the ionosphere-free combination of code and carriers (PC and LC). Thence:

$$P_C = \rho + \varepsilon_{P_C}$$

$$L_C = \rho + B_{L_C} + v_{L_C}$$

$$P_{IFree} \equiv P_C = \frac{\gamma P_1 - P_2}{\gamma - 1} ; \quad L_{IFree} \equiv L_C = \frac{\gamma L_1 - L_2}{\gamma - 1} \quad \gamma = \left(\frac{77}{60} \right)^2$$

Thence,

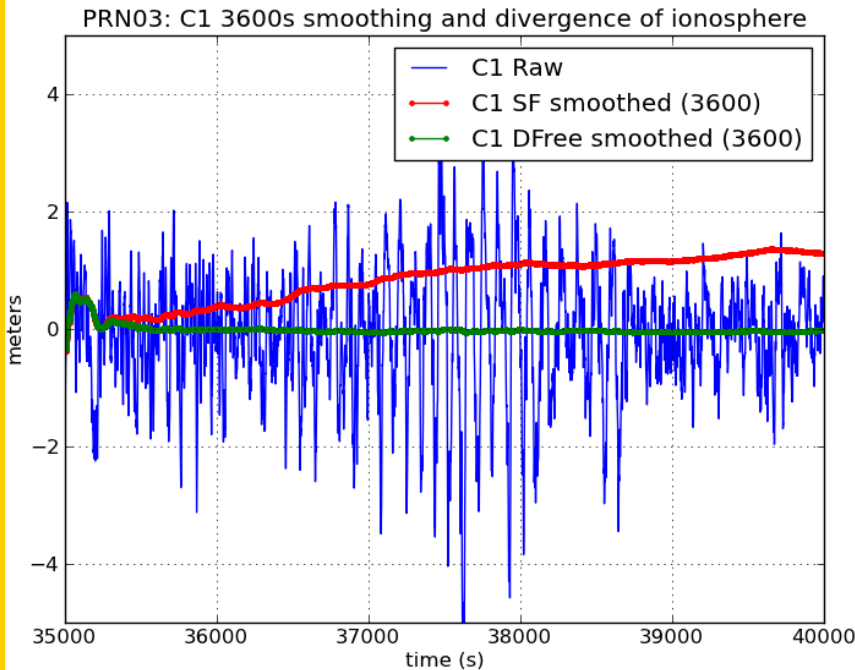
$$P_C - L_C = B_C + \varepsilon_{P_C}$$

$$\Rightarrow \hat{P}_{IFree} \equiv \hat{P}_C = \rho + v_{IFree}$$

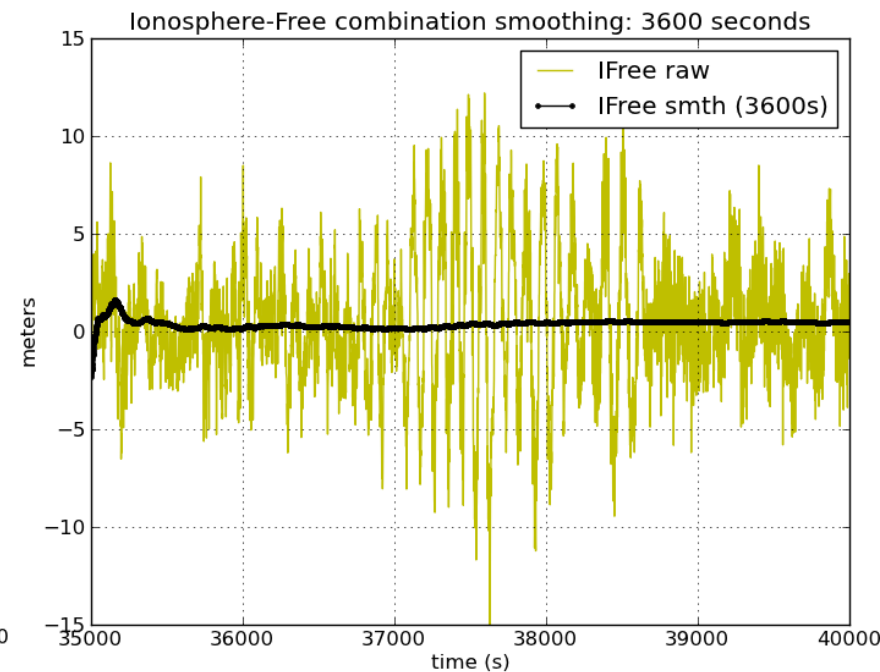
$$\sigma_{P_C} = \frac{\sqrt{\gamma^2 + 1}}{\gamma - 1} \sigma_{P_1} \approx 3 \sigma_{P_1}$$

This smoothed is based on the ionosphere-free combination of measurements, and therefore it is unaffected by either the spatial and temporal ionospheric gradients, but has the disadvantage that **the noise is amplified by a factor 3** (using the legacy GPS signals).

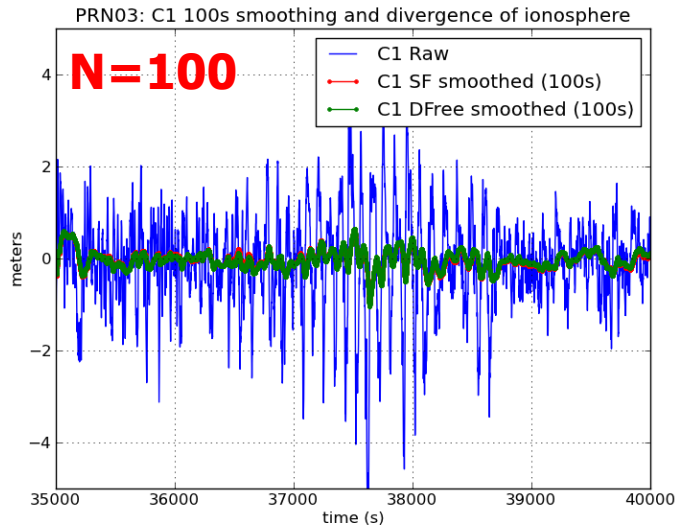
Vertical range: [-5 : 5]



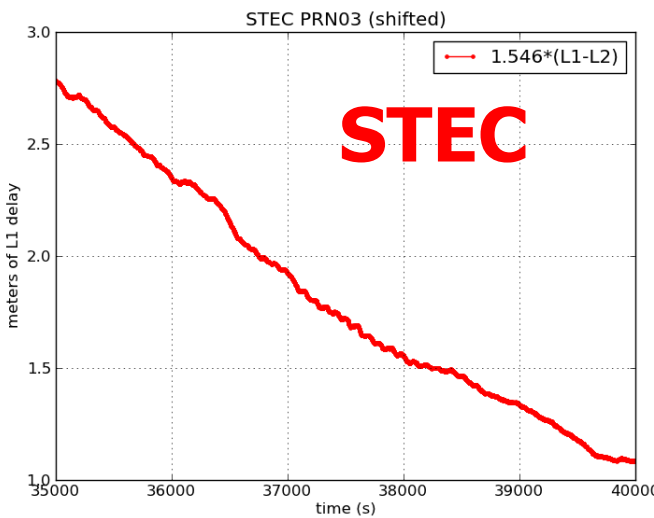
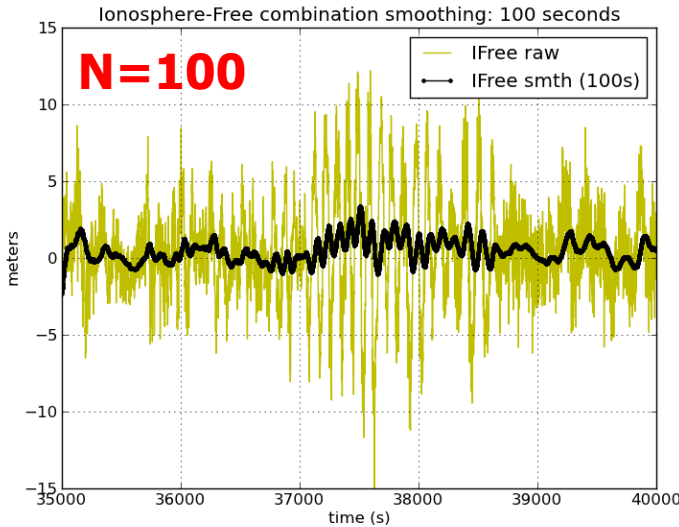
Vertical range: [-15:15]



C1, L1



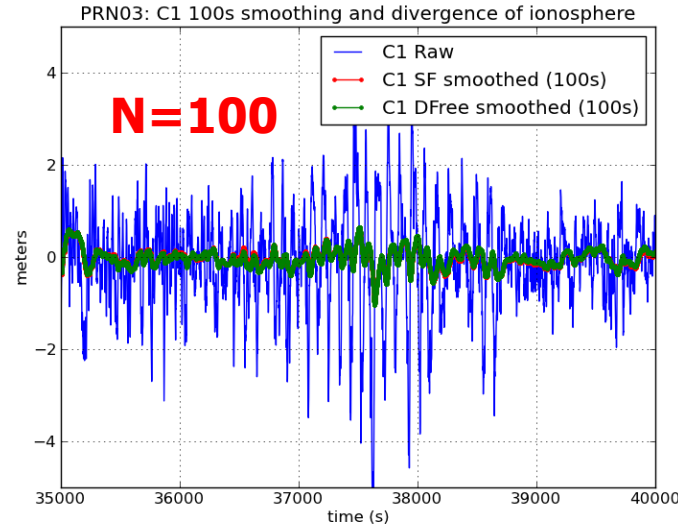
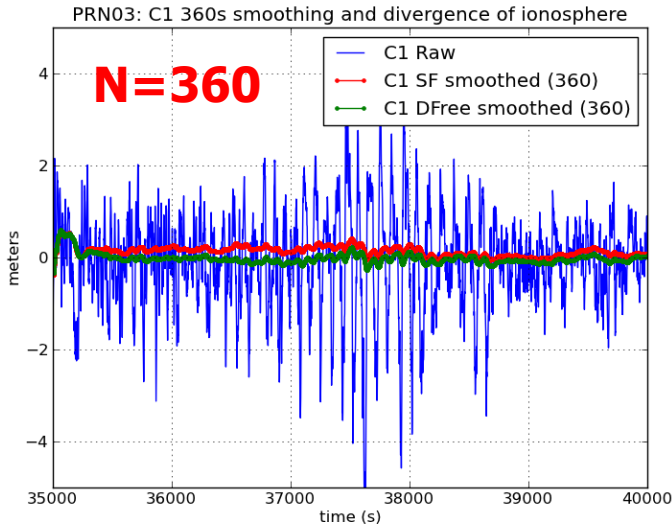
PC, LC



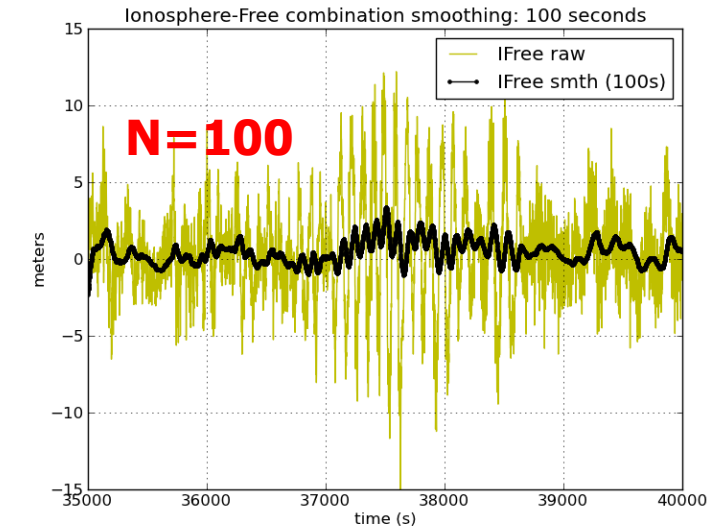
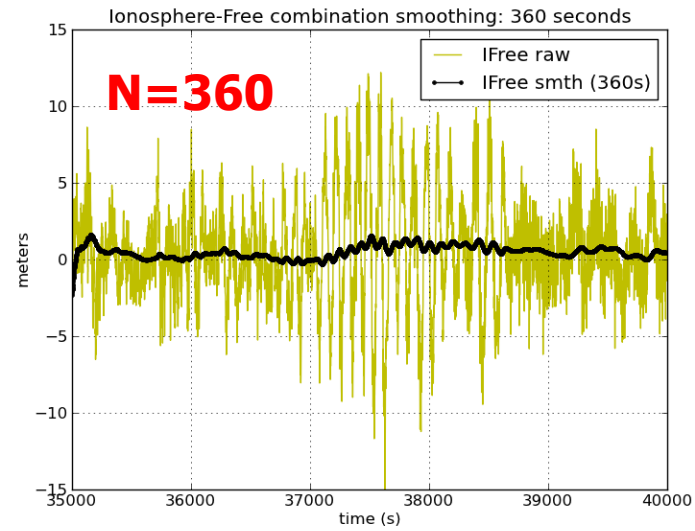
Exercise:

Justify that the ionosphere-free combination (**PC**) is (obviously) not affected by the code-carrier divergence, but it is 3 times noisier.

C1, L1

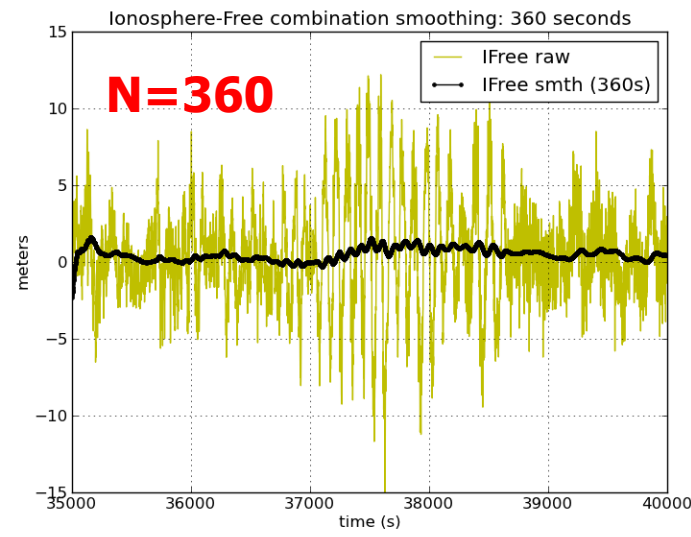
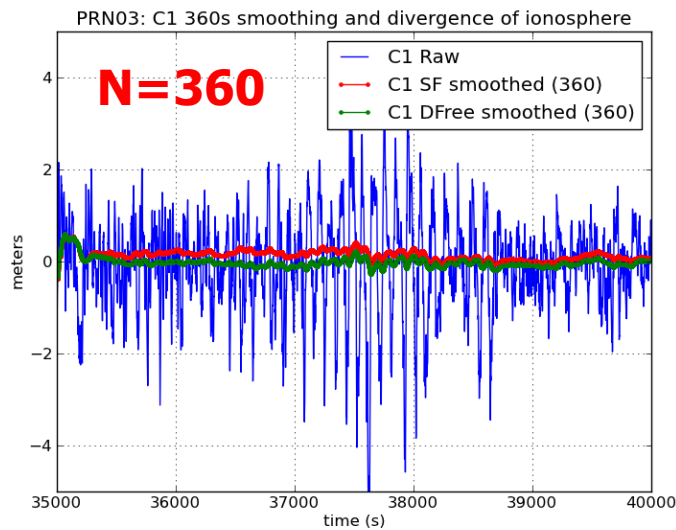
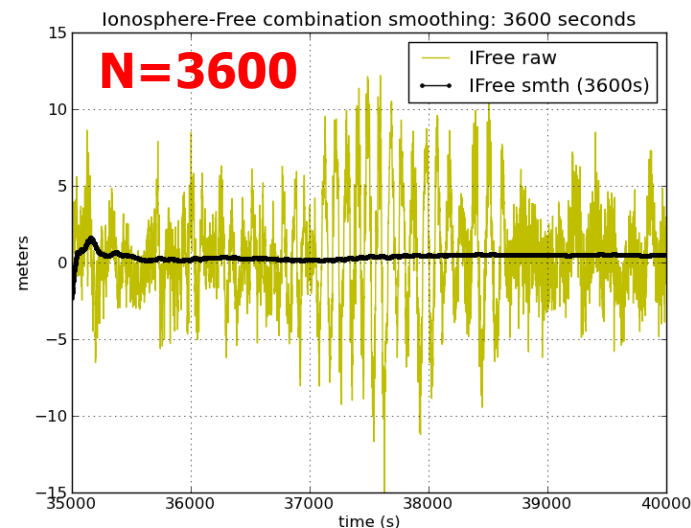
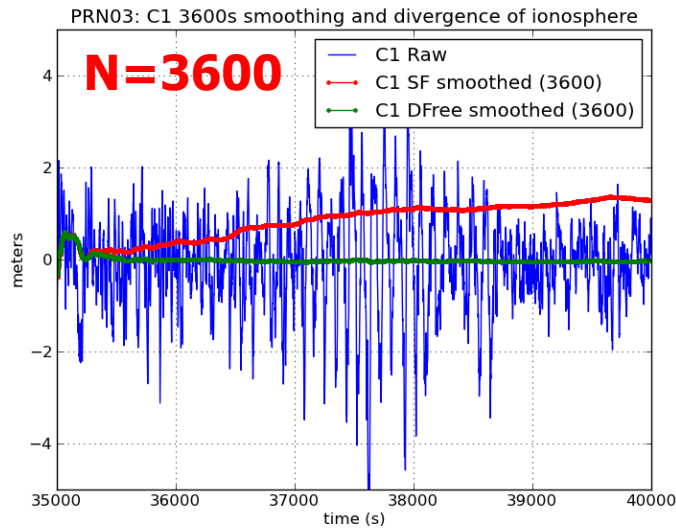


PC, LC



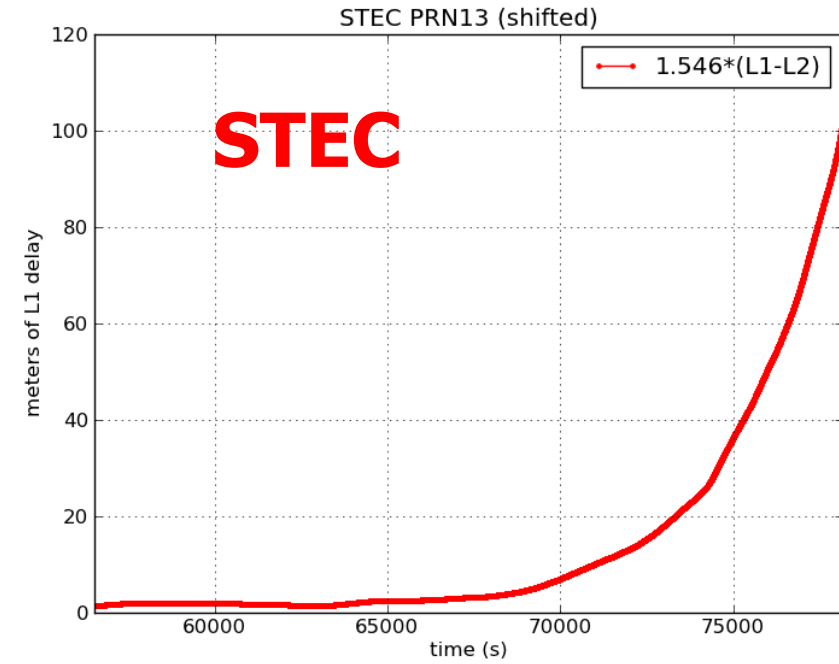
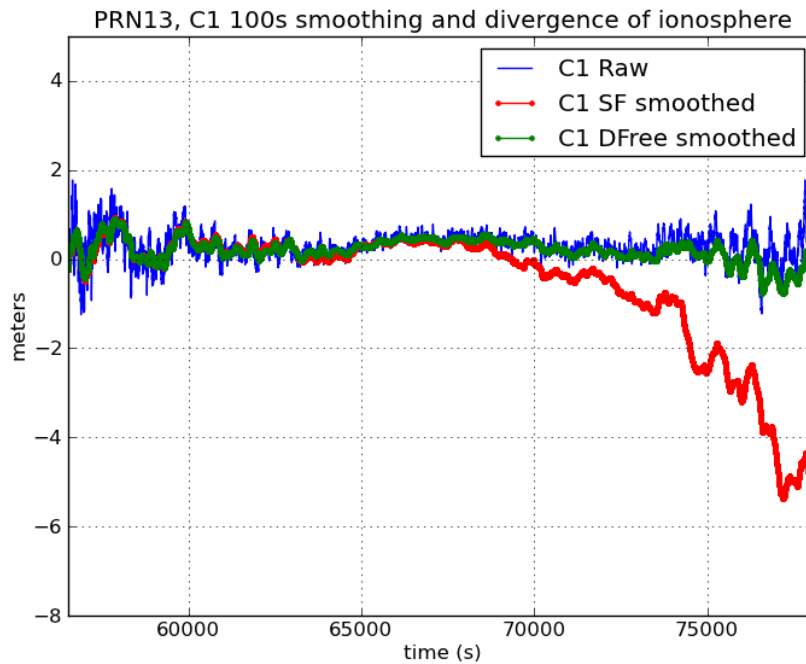
C1, L1

PC, LC



Halloween storm

Data File: amc23030.03o_1Hz



$N=100$ (i.e. filter smoothing time constant $\tau=100$ sec).

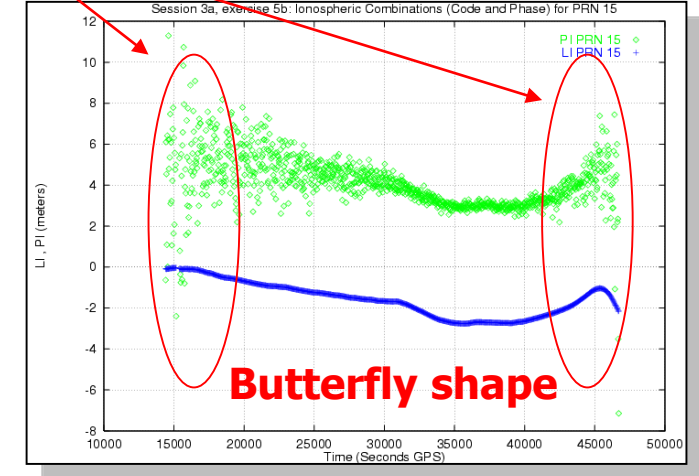
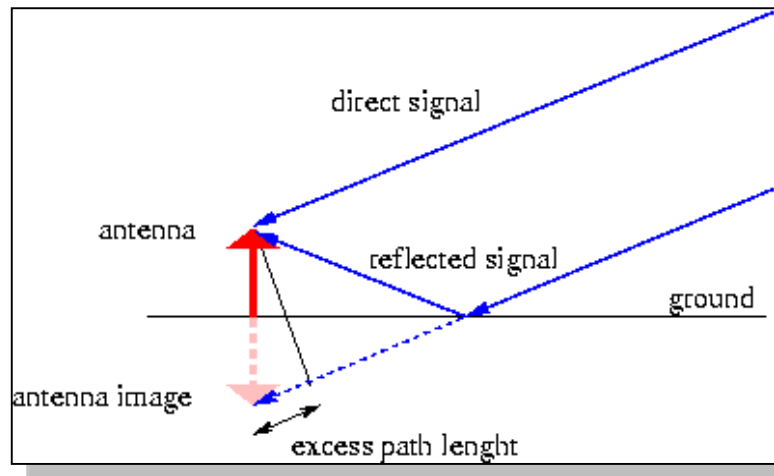
Contents

1. Review of GNSS measurements.
2. Linear combinations of measurements.
3. Carrier cycle-slips detection.
4. Carrier smoothing of code pseudorange.
5. Code Multipath.

Multipath

One or more reflected signals reach the antenna in addition to the direct signal. Reflective objects can be earth surface (ground and water), buildings, trees, hills, etc.

It affects both code and carrier phase measurements, and it is more important at low elevation angles.

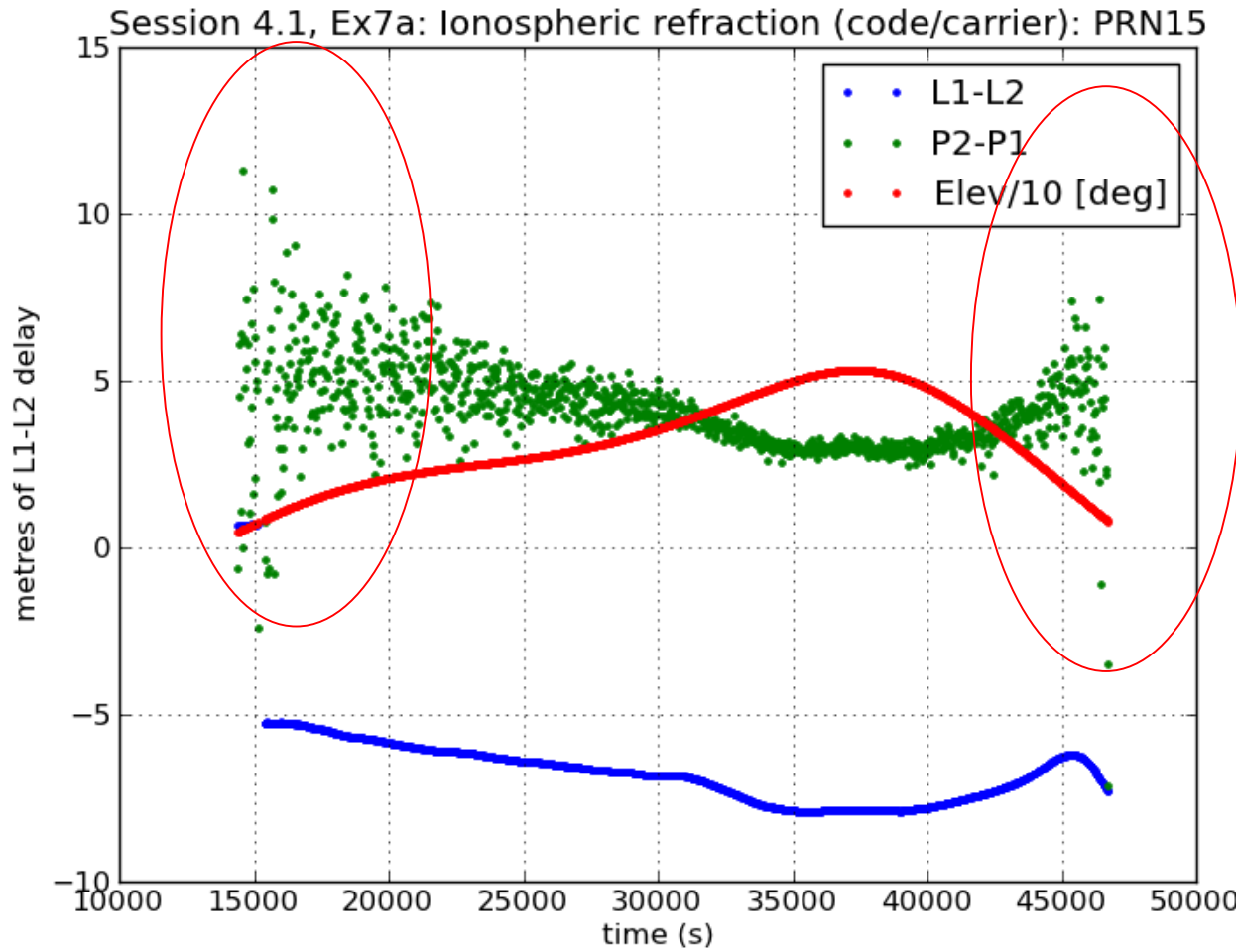


Code: up to 1.5 chip-length → up to 450m for C1 [theoretically]
Typically: less than 2-3 m.

Phase: up to $\lambda/4$ → up to 5 cm for L1 and L2 [theoretically]
Typically: less than 1 cm

Exercise

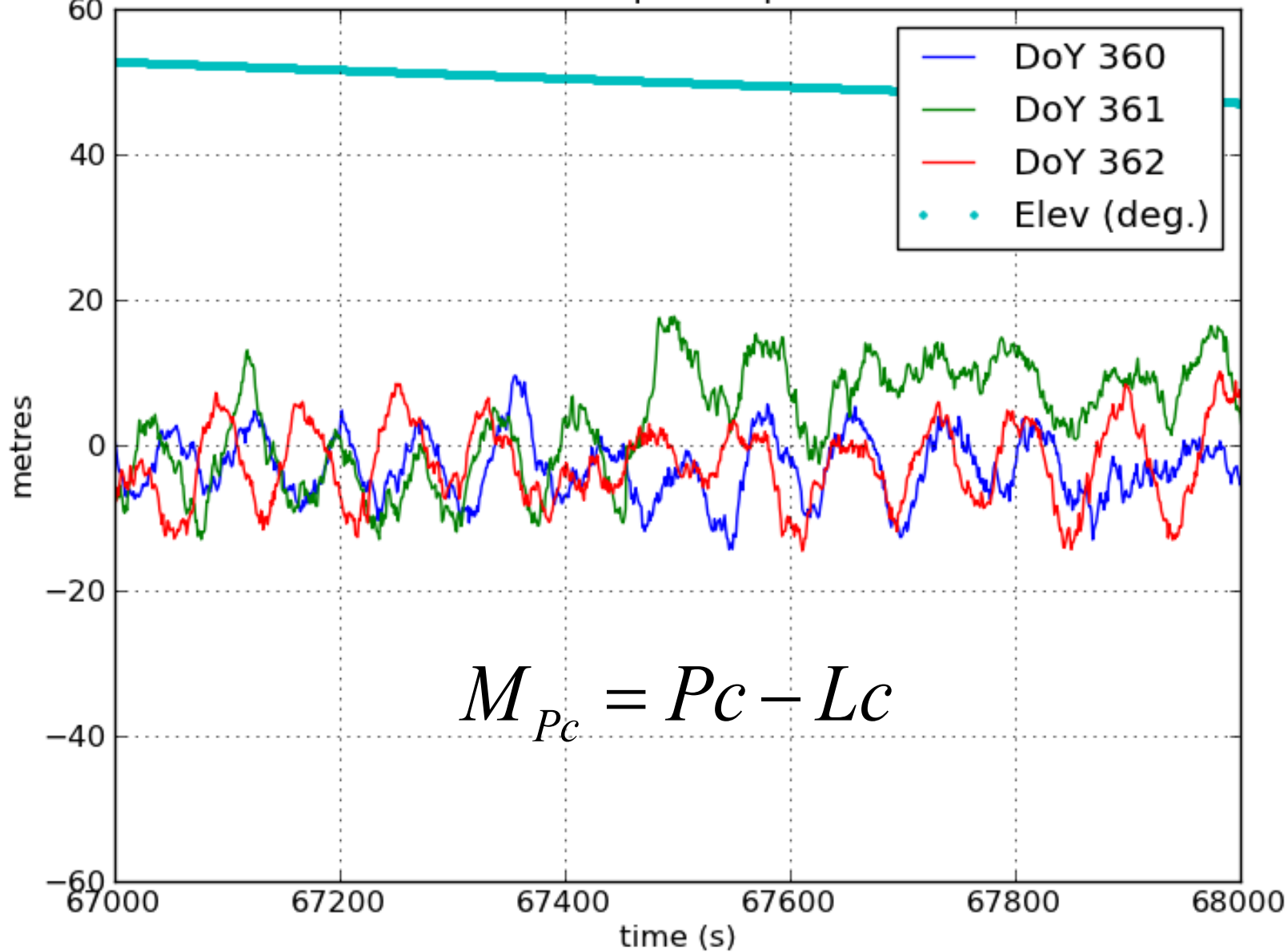
Plot code and phase geometry-free combination for satellite PRN 15 of file 97jan09coco_r0.rnx and discuss the results.



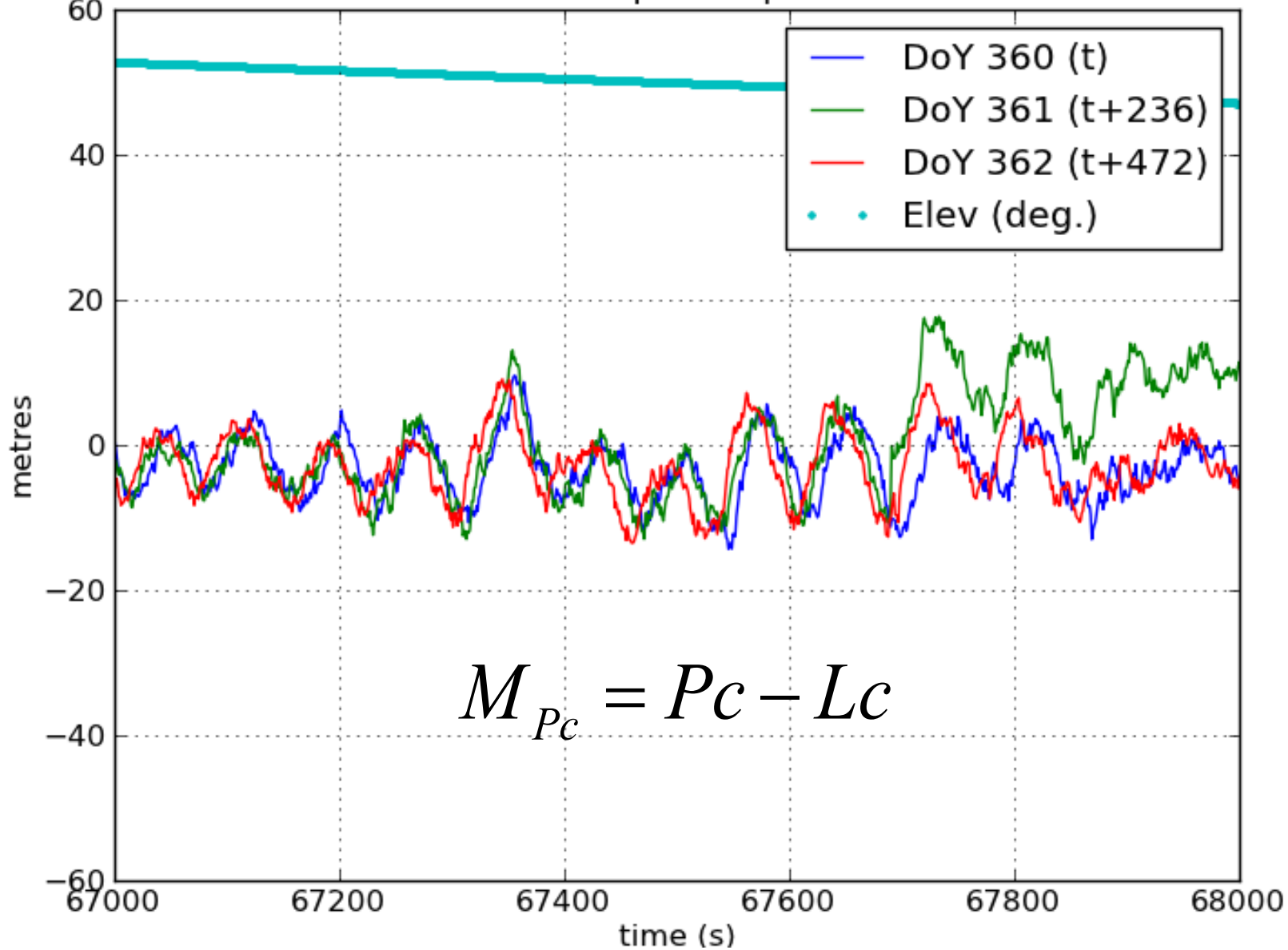
Butterfly shape:

High multipath for low elevation rays (when satellite rises and sets)

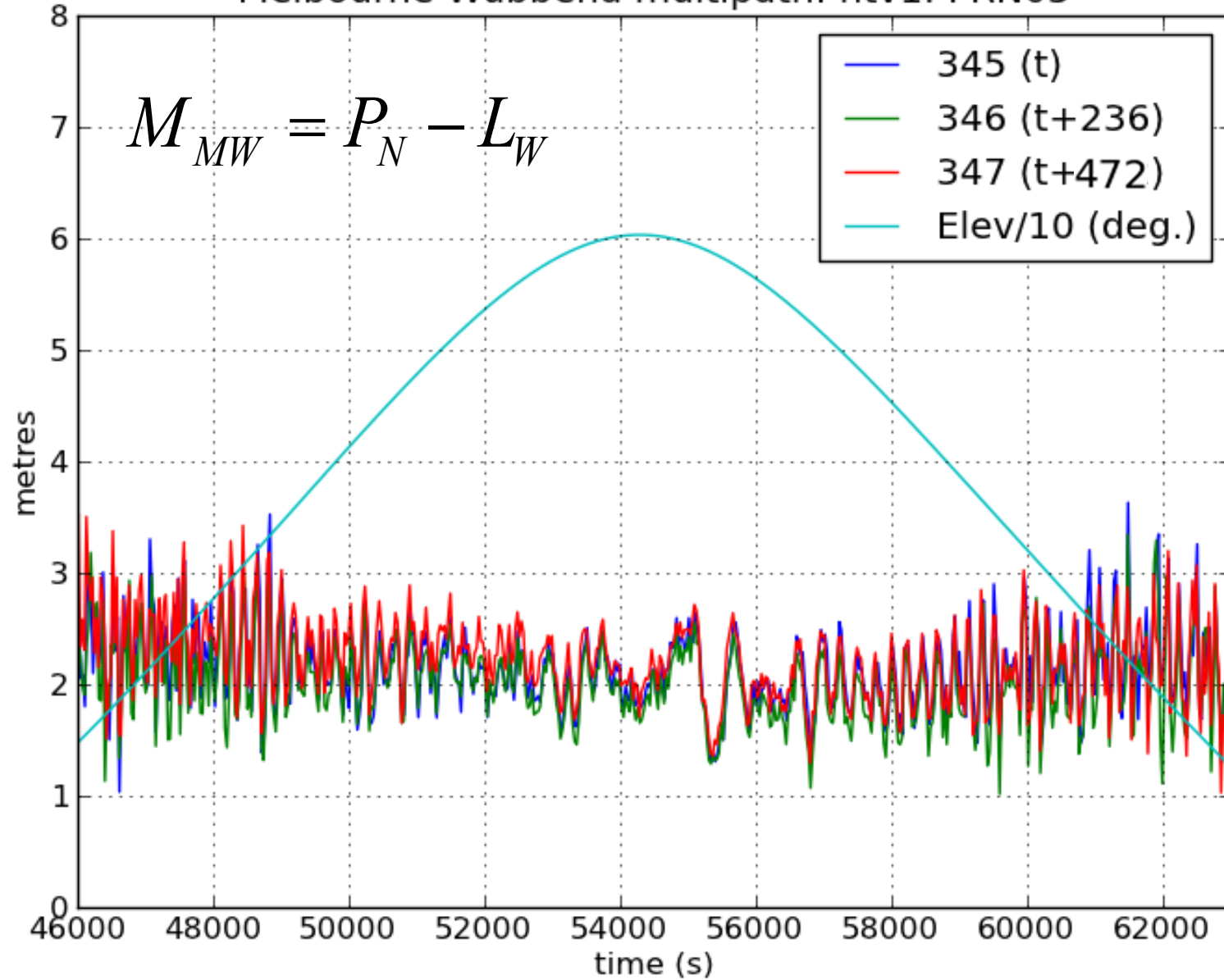
PC code multipath: upc3: PRN20

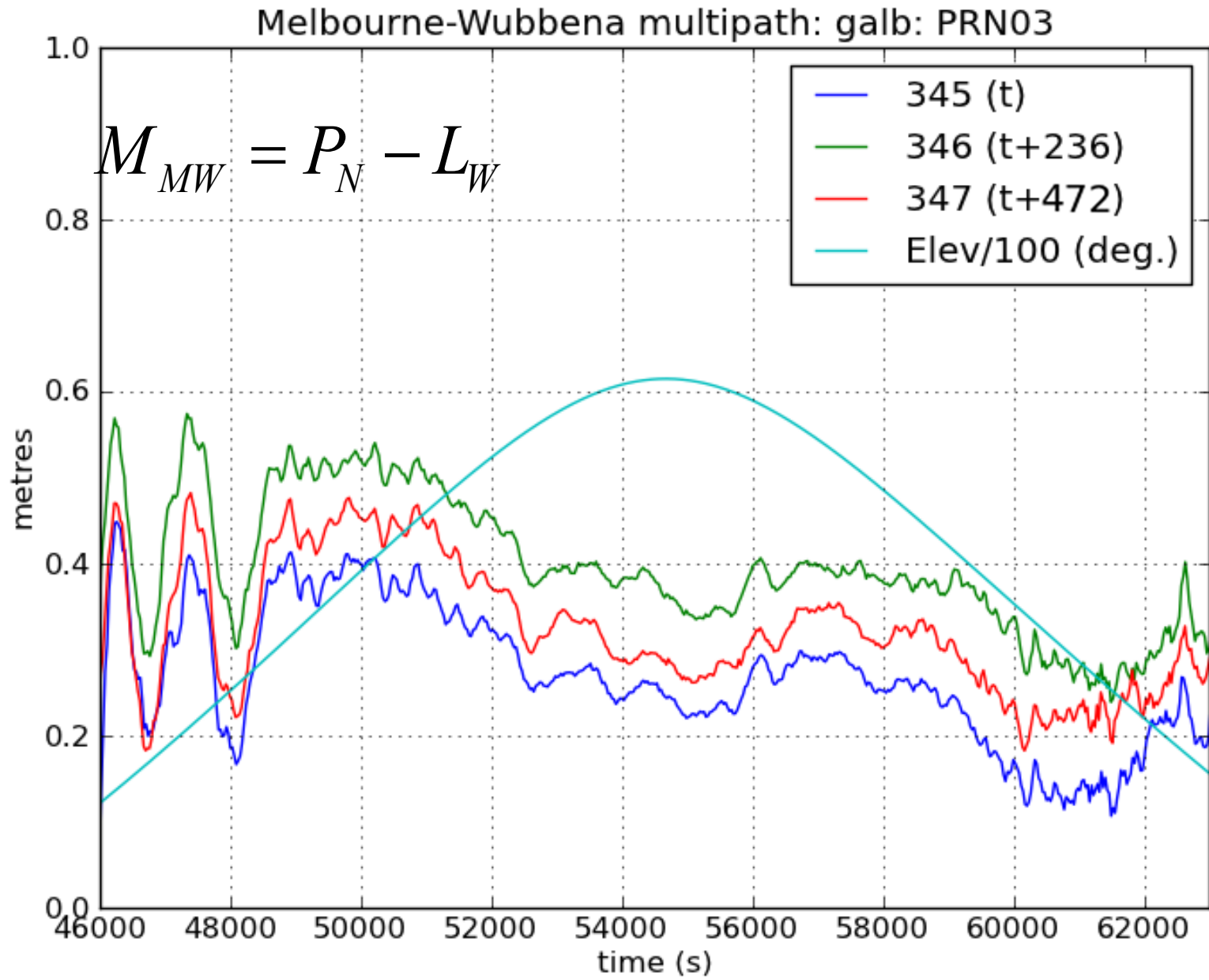


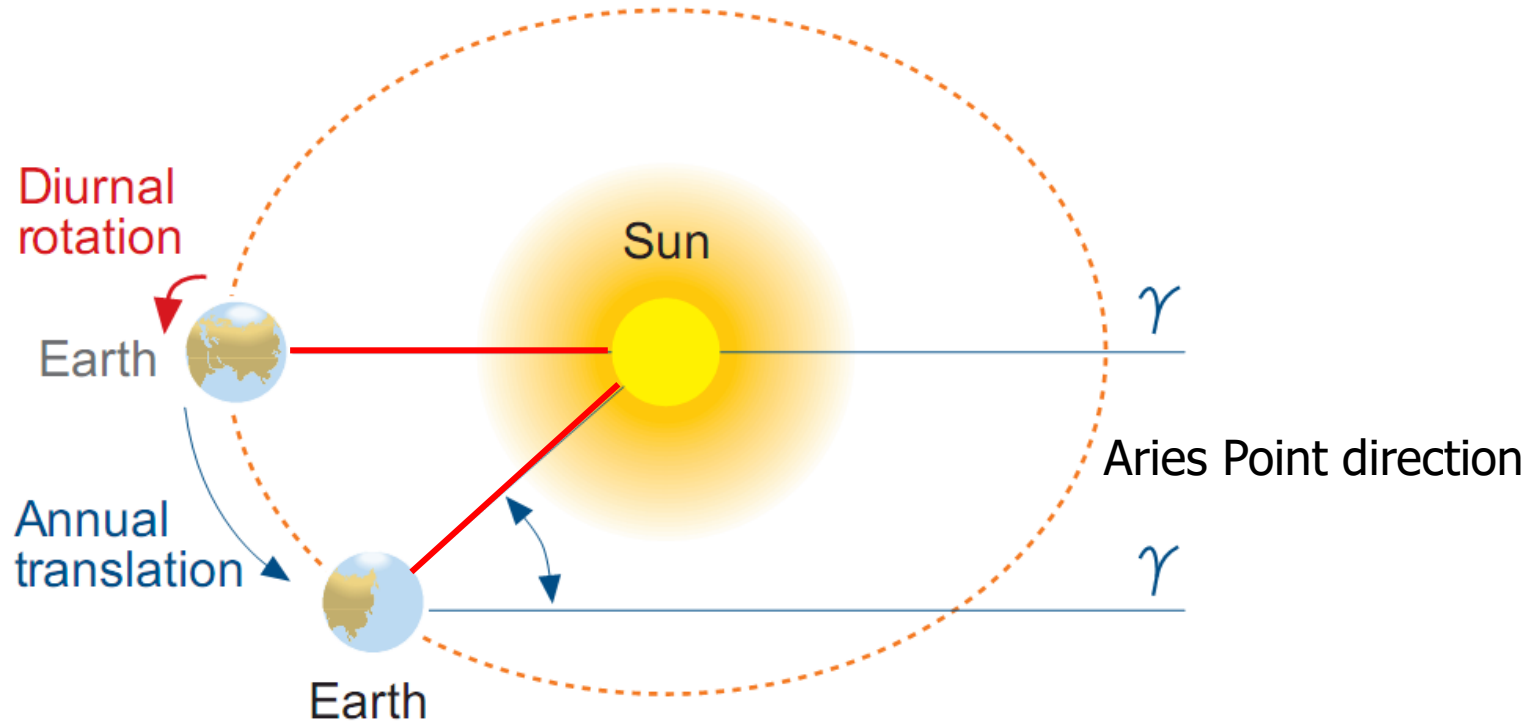
PC code multipath: upc3: PRN20



Melbourne-Wubbena multipath: htv1: PRN03





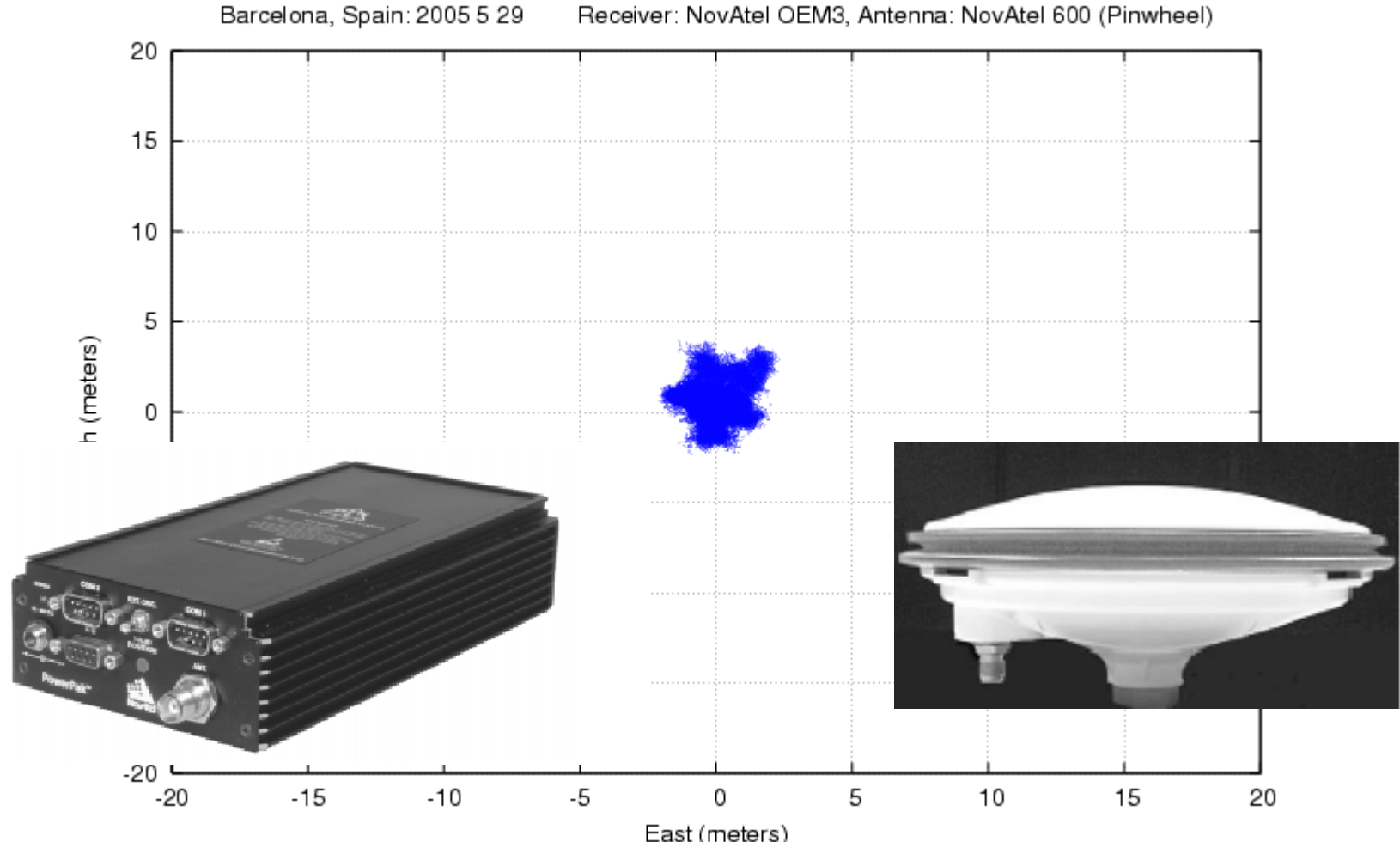


After one year, the directions of the Sun and Aries coincide again, but the **number of laps** relative to the Sun (solar days) is **one less** than those relative to Aries (sidereal days).

$$\frac{24\text{h}}{365.2422} = 3^{\text{m}} 56^{\text{s}}$$

Thus, a **sidereal day is shorter** than a solar day for about $3^{\text{m}} 56^{\text{s}}$

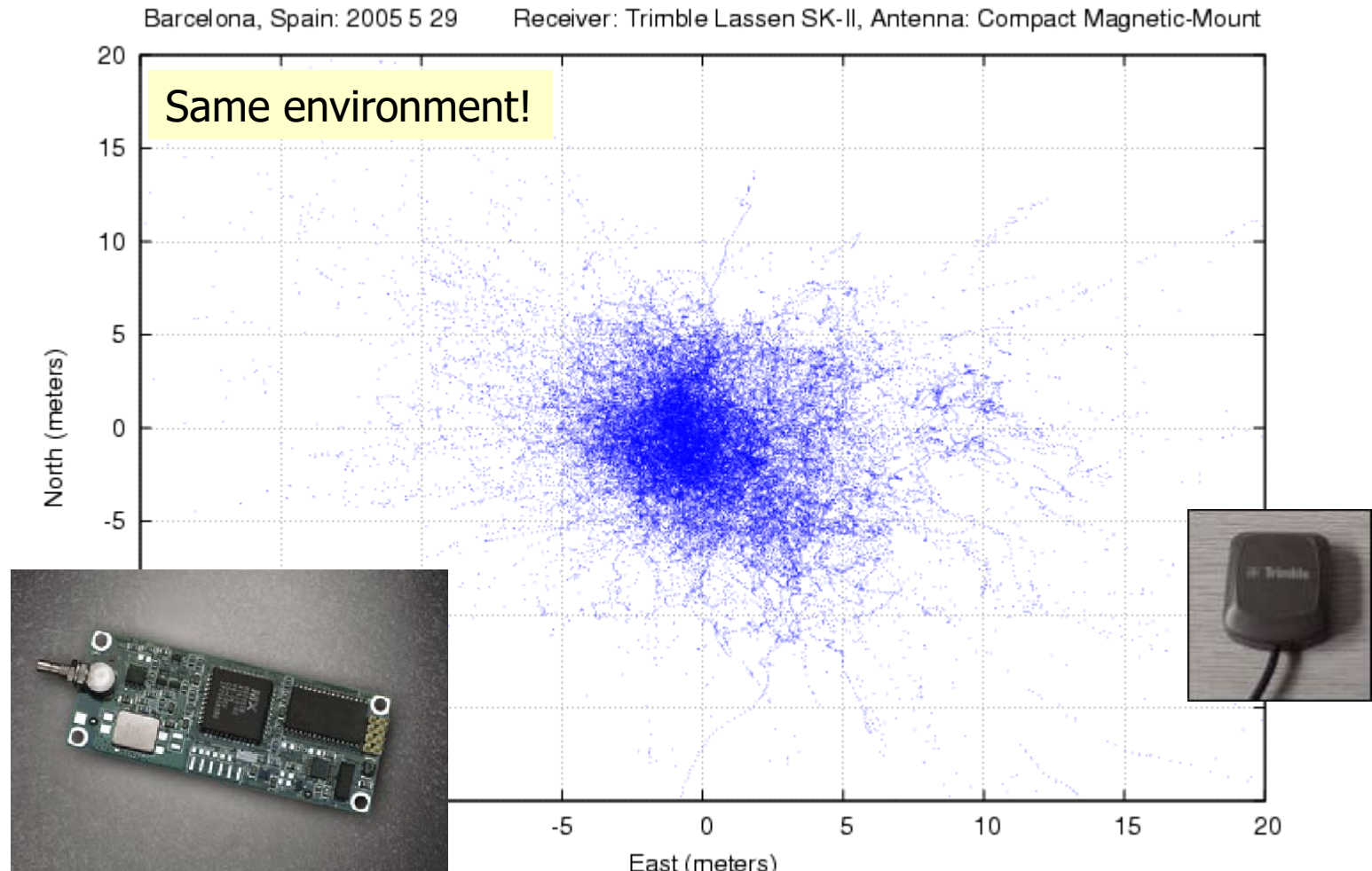
Receiver noise and multipath



GPS standalone (C1 code)

10,000 €

Receiver noise and multipath



GPS standalone (C1 code)

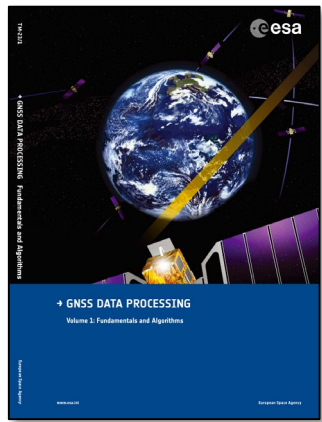
100 €

References

- [RD-1] J. Sanz Subirana, J.M. Juan Zornoza, M. Hernández-Pajares, GNSS Data processing. Volume 1: Fundamentals and Algorithms. ESA TM-23/1. ESA Communications, 2013.
- [RD-2] J. Sanz Subirana, J.M. Juan Zornoza, M. Hernández-Pajares, GNSS Data processing. Volume 2: Laboratory Exercises. ESA TM-23/2. ESA Communications, 2013.
- [RD-3] Pratap Misra, Per Enge. Global Positioning System. Signals, Measurements, and Performance. Ganga-Jamuna Press, 2004.
- [RD-4] B. Hofmann-Wellenhof et al. GPS, Theory and Practice. Springer-Verlag. Wien, New York, 1994.

Thank you

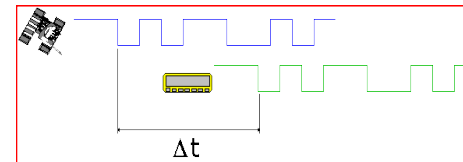
Backup



Rewriting GNSS equations: Combinations of Measurements Written in a Closed Form

See more details in
J. Sanz Subirana, J.M. Juan Zornoza, M. Hernández-Pajares, GNSS Data processing.
Volume 1: Fundamentals and Algorithms. ESA TM-23/1. ESA Communications, 2013.

$$R_{P_f} = c [t_{rcv}(T_2) - t^{sat}(T_1)]$$



Notation in book
P → R_{P_f} or R
L → Φ_{L_f} or Φ

$$R_{P_f} = \rho + c(dt_{rcv} - dt^{sat}) + Tr + \alpha_f STEC + K_{P_f,rcv} - K_{P_f}^{sat} + \mathcal{M}_{P_f} + \varepsilon_{P_f}$$

$$\Phi_{L_f} = \rho + c(dt_{rcv} - dt^{sat}) + Tr - \alpha_f STEC + k_{L_f,rcv} - k_{L_f}^{sat} + \lambda_{L_f} N_{L_f} + \lambda_{L_f} w + m_{L_f} + \epsilon_{L_f}$$

4.1.1.1 Clock Redefinition and Differential Code Biases

By defining a new clock δt as

$$c\delta t = cdt + K_{C_{12}}, \quad \text{where } K_{C_{12}} = \frac{f_1^2 K_1 - f_2^2 K_2}{f_1^2 - f_2^2}$$

it is not difficult to find that

$$cdt + K_1 = c\delta t + \tilde{\alpha}_1(K_2 - K_1)$$

$$cdt + K_2 = c\delta t + \tilde{\alpha}_2(K_2 - K_1)$$

with

$$1 \text{ TECU} = 10^{16} e^-/\text{m}^2$$

$$\tilde{\alpha}_i \equiv \frac{\alpha_i}{\alpha_2 - \alpha_1} \quad (i = 1, 2) \quad \text{and} \quad \alpha_i = \frac{40.3}{f_i^2} 10^{16} \text{ m}_{\text{delay(signal } \Phi_{f_i})}/\text{TECU}$$

Ionosphere-free comb.

$$R_C = \frac{f_1^2 R_1 - f_2^2 R_2}{f_1^2 - f_2^2}$$

$$\Phi_C = \frac{f_1^2 \Phi_1 - f_2^2 \Phi_2}{f_1^2 - f_2^2}$$

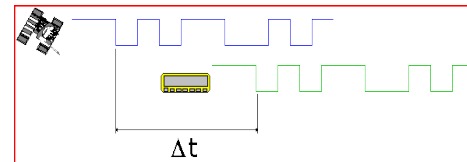
$$K_i \equiv K_{i,rcv} - K_i^{sat}$$

$$k_i \equiv k_{i,rcv} - k_i^{sat}$$

$$K_{21} = K_2 - K_1$$

Both, Ionosphere and Code-Instrumental-Delay, will cancel in the Iono.-Free combination!

$$R_{P_f} = c [t_{rcv}(T_2) - t^{sat}(T_1)]$$



Notation in book

P → R_{P_f} or R
L → Φ_{Lf} or Φ

$$R_{P_f} = \rho + c(dt_{rcv} - dt^{sat}) + Tr + \alpha_f STEC + K_{P_f,rcv} - K_{P_f}^{sat} + \mathcal{M}_{P_f} + \varepsilon_{P_f}$$

$$\Phi_{L_f} = \rho + c(dt_{rcv} - dt^{sat}) + Tr - \alpha_f STEC + k_{L_f,rcv} - k_{L_f}^{sat} + \lambda_{L_f} N_{L_f} + \lambda_{L_f} w + m_{L_f} + \epsilon_{L_f}$$

$$I \equiv (\alpha_2 - \alpha_1) STEC = \frac{40.3(f_1^2 - f_2^2)}{f_1^2 f_2^2} 10^{16} STEC$$

$$STEC = \int N_e dl$$

$$R_i = \rho + c(\delta t_{rcv} - \delta t^{sat}) + Tr + \tilde{\alpha}_i(I + K_{21}) + \mathcal{M}_i + \varepsilon_i$$

$$\Phi_i = \rho + c(\delta t_{rcv} - \delta t^{sat}) + Tr - \tilde{\alpha}_i(I + K_{21}) + b_i + \lambda_i N_i + \lambda_i w + m_i + \epsilon_i$$

with

$$\tilde{\alpha}_i \equiv \frac{\alpha_i}{\alpha_2 - \alpha_1} \quad (i = 1, 2) \quad \text{and} \quad \alpha_i = \frac{40.3}{f_i^2} 10^{16} \text{ m}_{\text{delay(signal } \Phi_{f_i})} / \text{TECU}$$

$$K_i \equiv K_{i,rcv} - K_i^{sat}$$

$$k_i \equiv k_{i,rcv} - k_i^{sat}$$

$$K_{21} = K_2 - K_1$$

Input measurements R_i and Φ_i ($i = 1, 2$):

$$R_i = \rho + c(\delta t_{rcv} - \delta t^{sat}) + Tr + \tilde{\alpha}_i(I + K_{21}) + \mathcal{M}_i + \varepsilon_i$$

$$\Phi_i = \rho + c(\delta t_{rcv} - \delta t^{sat}) + Tr - \tilde{\alpha}_i(I + K_{21}) + B_i + \lambda_i w + m_i + \epsilon_i$$

where the ambiguity B_i is given by

$$B_i = b_i + \lambda_i N_i, \quad \lambda_i = c/f_i, \quad \tilde{\alpha}_1 = 1/(\gamma_{12} - 1), \quad \tilde{\alpha}_2 = \gamma_{12} \tilde{\alpha}_1 = 1 + \tilde{\alpha}_1, \\ \gamma_{12} = (f_1/f_2)^2$$

with the bias b_i a real number and N_i an integer ambiguity.

Note that $K_{21} = K_{21,rcv} - K_{21}^{sat}$, $b_i = b_{i,rcv} - b_i^{sat}$.

Ionosphere-free combination:

Both, Iono. and Code-Instrum.-delay, cancel in the Iono-Free combination.

$$R_C = \rho + c(\delta t_{rcv} - \delta t^{sat}) + Tr + \mathcal{M}_C + \varepsilon_C$$

$$\Phi_C = \rho + c(\delta t_{rcv} - \delta t^{sat}) + Tr + B_C + \lambda_N w + m_C + \epsilon_C$$

where the bias B_C is given by

$$B_C = b_C + \lambda_N (N_1 + (\lambda_W/\lambda_2)N_W)$$

- - - - -

The frequency dependent terms Iono. and Code-Instrum.-Delay $I + K_{21}$ appear always together with a frequency dependent coef.

Geometry-free combination:

$$R_I = I + K_{21} + \mathcal{M}_I + \varepsilon_I$$

$$\Phi_I = I + K_{21} + B_I + (\lambda_1 - \lambda_2)w + m_I + \epsilon_I$$

The frequency dependent terms Iono. and Code-Instrum.-Delay $I + K_{21}$ appear always together with a frequency dependent coef.

where the bias B_I is given by

$$B_I = b_I + \lambda_1 N_1 - \lambda_2 N_2$$

Wide-lane (phase) and narrow-lane (code) combinations:

$$R_N = \rho + c(\delta t_{rcv} - \delta t^{sat}) + Tr + \tilde{\alpha}_W(I + K_{21}) + \mathcal{M}_N + \varepsilon_N$$

$$\Phi_W = \rho + c(\delta t_{rcv} - \delta t^{sat}) + Tr + \tilde{\alpha}_W(I + K_{21}) + B_W + m_W + \epsilon_W$$

where the bias B_W is given by

$$B_W = b_W + \lambda_W N_W$$

$$\begin{aligned} N_W &\equiv N_1 - N_2, \\ \lambda_W &\equiv c/(f_1 - f_2), \quad \lambda_N \equiv c/(f_1 + f_2), \\ \tilde{\alpha}_W &\equiv \sqrt{\tilde{\alpha}_1 \tilde{\alpha}_2} = f_1 f_2 / (f_1^2 - f_2^2) = \sqrt{\gamma_{12}} / (\gamma_{12} - 1), \quad \gamma_{12} = (f_1/f_2)^2, \\ b_W &\equiv (f_1 b_1 - f_2 b_2) / (f_1 - f_2), \quad b_C \equiv (f_1^2 b_1 - f_2^2 b_2) / (f_1^2 - f_2^2), \\ b_I &\equiv b_1 - b_2, \quad b_W - b_C = \tilde{\alpha}_W b_I, \end{aligned}$$

Other combinations involving code and phase measurements:

The Melbourne–Wübbena combination

$$\Phi_W - R_N = b_W + \lambda_W N_W + \mathcal{M}_{MW} + \varepsilon_{MW}$$

The GRAPHIC (Group and Phase Ionospheric Calibration) combination

$$\frac{1}{2}(R_i + \Phi_i) = \rho + c(\delta t_{rcv} - \delta t^{sat}) + Tr + \frac{1}{2}B_i + \frac{1}{2}\lambda_i w + \mathcal{M}_G + \varepsilon_G$$

Definitions and relationships (where $(\cdot)_X \equiv (\cdot)_{X_{12}}$) :

$$N_W \equiv N_1 - N_2,$$

$$\lambda_W \equiv c/(f_1 - f_2), \quad \lambda_N \equiv c/(f_1 + f_2),$$

$$\tilde{\alpha}_W \equiv \sqrt{\tilde{\alpha}_1 \tilde{\alpha}_2} = f_1 f_2 / (f_1^2 - f_2^2) = \sqrt{\gamma_{12}} / (\gamma_{12} - 1), \quad \gamma_{12} = (f_1/f_2)^2,$$

$$b_W \equiv (f_1 b_1 - f_2 b_2) / (f_1 - f_2), \quad b_C \equiv (f_1^2 b_1 - f_2^2 b_2) / (f_1^2 - f_2^2),$$

$$b_I \equiv b_1 - b_2, \quad b_W - b_C = \tilde{\alpha}_W b_I,$$

the same expressions for B_X as for b_X .

(4.19)

GNSS_Data_processing_course1.png | gAGE : Advanced GNSS Research and Innovative Applications - Mozilla Firefox

File Edit View History Bookmarks Tools Help

GNSS_Data_processing_course1.png | gA... +

www.gage.es/drupal6/content/gnssdataprocessingcourse1png Bing

About gAGE/UPC About gAGE-NAV, S.L. Contact Us

gAGE : Advanced GNSS Research and Innovative Applications

Home

Personnel

- Permanent Staff
- Researchers
- Former Researchers

Publications

- Peer Reviewed Papers
- Meeting proceedings
- Posters
- PhD Dissertations

Learning Material

- Library
- Software Tools

Projects

- gAGE/UPC
- gAGE-NAV, S.L.

Patents

- Topics and description

GNSS_Data_processing_course1.png

Tue, 09/03/2013 - 15:39 — jaume.sanz

GNSS Data Processing Theory Slides
<http://www.gage.edu>

GNSS Data Processing Laboratory Slides
<http://www.gage.edu>

The Learning material is composed by a collection of slides for Theory & Laboratory exercises.

A book on GNSS Data Processing is given as complementary material.

>Login to post comments Original Thumbnail

About us

gAGE is a Consortium of the gAGE/UPC Research group of UPC and the Spin-off Company gAGE-NAV, S.L.

gAGE Brochure

Shortcuts

- gLAB Tool Suite
- gAGE Products
- Useful GNSS links
- GNSS Course and associated Tutorials
- MasterMast
- gAGE upload file facility

User login

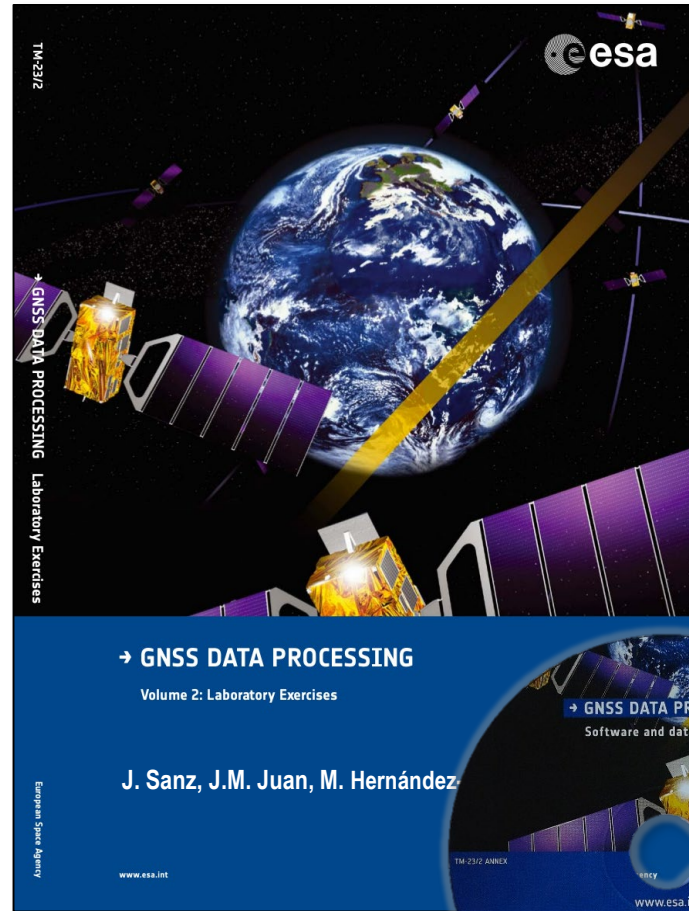
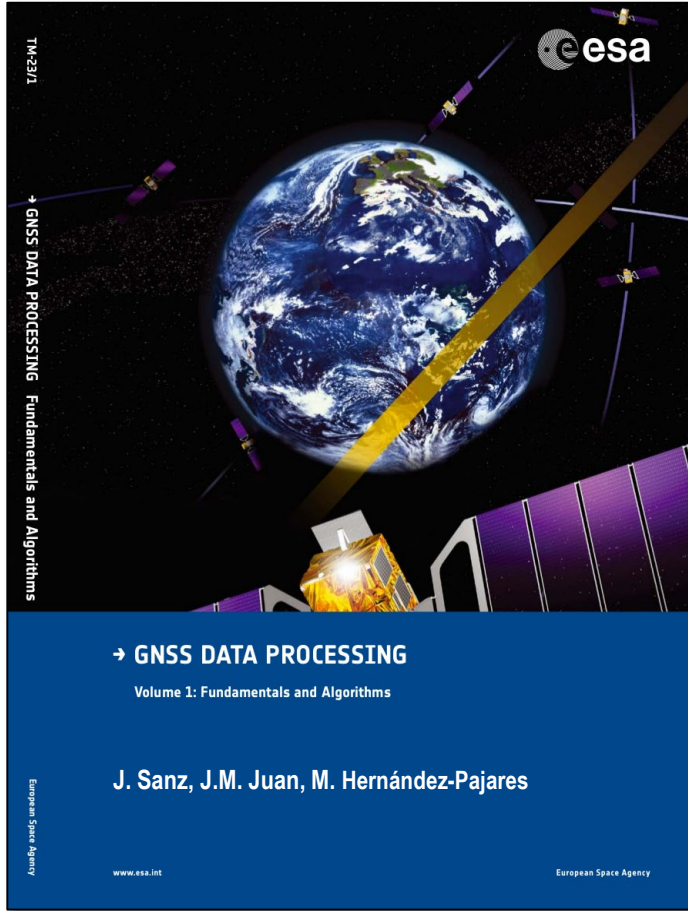
Username: * jaume.sanz

Password: *

Log in using OpenID
 Request new password

Who's online





GNSS Data Processing, Vol. 1: Fundamentals and Algorithms. GNSS Data Processing, Vol. 2: Laboratory exercises.